THE HONG KONG
POLYTECHNIC UNIVERSITY
香港理工大學
Pao Yue-kong Library
包玉剛圖書館

Copyright Undertaking

This thesis is protected by copyright, with all rights reserved.

By reading and using the thesis, the reader understands and agrees to the following terms:

1. The reader will abide by the rules and legal ordinances governing copyright regarding the use of the thesis.
2. The reader will use the thesis for the purpose of research or private study only and not for distribution or further reproduction or any other purpose.
3. The reader agrees to indemnify and hold the University harmless from and against any loss, damage, cost, liability or expenses arising from copyright infringement or unauthorized usage.

IMPORTANT

If you have reasons to believe that any materials in this thesis are deemed not suitable to be distributed in this form, or a copyright owner having difficulty with the material being included in our database, please contact lbsys@polyu.edu.hk providing details. The Library will look into your claim and consider taking remedial action upon receipt of the written requests.

Pao Yue-kong Library, The Hong Kong Polytechnic University, Hung Hom, Kowloon, Hong Kong

http://www.lib.polyu.edu.hk

This thesis in electronic version is provided to the Library by the author. In the case where its contents is different from the printed version, the printed version shall prevail.

AUTOMATIC INCIDENT DETECTION UNDER NO-RAIN AND RAIN CONDITIONS

LI XIANGMIN

M.Phil

The Hong Kong
Polytechnic University

2014

The Hong Kong Polytechnic University
Department of Civil and Environmental Engineering

Automatic Incident Detection under No-Rain and Rain Conditions

LI Xiangmin

A thesis submitted in partial fulfillment of the requirements for the degree of Master of Philosophy

February 2014

Certificate of Originality

I hereby declare that this thesis is my own work and that, to the best of my knowledge and belief, it produces no material previously published or written, nor material that has been accepted for the award of any other degree or diploma, except where due acknowledgment has been made in the text.

Signature: _____

Name: LI Xiangmin

Abstract

This research presented in this thesis focuses on the development of automatic incident detection (AID) algorithms for use under no-rain and rain conditions. A new extended standard normal deviate (ESND) algorithm is proposed by extending the widely used standard normal deviate (SND) algorithm.

The previous SND algorithm is modified with two extensions. In the first extension, the weighting method is adopted to enhance the reliability of detection results. In the second extension, the variation of input data within sampling periods is restricted to reduce false alarms for incident detection.

The algorithm development is on the basis of the available data collected originally for journey time estimation purpose in Hong Kong. These data have been collected by both video traffic detectors and automatic vehicle identification readers. Instead of installing more expensive traffic detectors, the proposed ESND algorithm has proved feasible in effective traffic incident detection, with the use of the available data collected originally for journey time estimation purpose.

In addition to the widely used traffic stream parameters such as traffic speed, flow and occupancy for incident detection, two new traffic stream parameters are proposed as incident indicators. They are (1) the coefficient of variation of speed at the upstream detector and (2) the correlation coefficient of speeds of two adjacent detectors. Traffic data collected from both single detector stations and dual detector stations are selected as the inputs for the proposed ESND algorithm.

The proposed ESND algorithm is firstly extended to be a flow-dependent ESND algorithm for incident detection under no-rain conditions. The preincident traffic flow condition is considered explicitly in the detection logic to improve the detection performance under various traffic flow conditions. Historical traffic and incident data on a selected urban road section in Hong Kong are used for calibration and validation of the proposed flow-dependent ESND algorithm. Five existing AID algorithms are selected and calibrated for comparison with the proposed flow-dependent ESND algorithm with the use of the available data collected for journey time estimation purpose on the previously selected urban

road section under no-rain conditions. The comparison results show that the proposed algorithm outperforms the five selected AID algorithms in terms of the detection rate, false alarm rate and mean time to detect.

The proposed ESND algorithm is then extended to be a more generalized flow-rain-dependent ESND algorithm for incident detection under both no-rain and rain conditions. The rain condition together with the preincident traffic condition are considered explicitly in detection threshold determination. Instead of the traffic flow, the volume/capacity ratio is adopted to indicate the preincident traffic condition. Compared to the discrete detection thresholds in the previous flow-dependent AID algorithms, continuous detection thresholds are adopted in the proposed flow-rain-dependent ESND algorithm. These continuous detection thresholds are generated by a generalized detection threshold function in which both preincident volume/capacity ratio and rainfall intensity are modeled. The proposed flow-rain-dependent ESND algorithm is applied to the urban road network under the Hong Kong Journey Time Indication System (JTIS) in order to examine the detection performance of the proposed algorithm on a territory-wide basis.

In this research, the proposed flow-rain-dependent ESND algorithm is calibrated on the basis of available Hong Kong historical traffic, incident and rainfall intensity data collected on the urban road network under the JTIS. The detection performance of the proposed flow-rain-dependent ESND algorithm outperforms the flow-dependent ESND algorithm and the five selected AID algorithms on a territory-wide basis.

It is shown in this research that the proposed flow-dependent ESND algorithm performed satisfactorily for incident detection in urban areas even when data are collected for journey time estimation purpose only. The proposed flow-rain-dependent ESND algorithm could be used for incident detection under both no-rain and rain conditions. This is of importance to cities with substantial rainfalls similar to Hong Kong.

Publications Arising from the Thesis

Journal Papers:

1. **Li, X.**, Lam, W. H. K., and Tam, M. L., 2013, New Automatic Incident Detection Algorithm Based on Traffic Data Collected for Journey Time Estimation. *ASCE Journal of Transportation Engineering*, 139(8), pp. 840-847.
2. Lam, W. H. K., Tam, M. L., Cao, X., and **Li, X.**, 2013, Modeling the Effects of Rainfall Intensity on Traffic Speed, Flow, and Density Relationships for Urban Roads. *ASCE Journal of Transportation Engineering*, 139(7), pp. 758-770.

Conference Papers:

1. **Li, X.**, Lam, W. H. K., and Tam, M. L., 2013, Automatic Incident Detection under Various Rain Conditions. *Proceeding of Asia Symposium on Engineering and Information*, Asia-Pacific Education & Research Association Bangkok, Thailand, pp.125-135.
2. Li, D. P., **Li, X.**, and Lam, W. H. K., 2012. Temporal and Spatial Impacts of Rainfall Intensity on Traffic Accidents in Hong Kong. *Proceeding of the 17th Hong Kong Society for Transportation Studies International Conference*, Hong Kong Society for Transportation Studies, Hong Kong, pp. 333-340.

Acknowledgements

I would like to express my deepest thanks and appreciation to my chief supervisor, Professor William H. K. Lam, for his supervision, guidance and encouragement during the past two years of my study. This thesis could not be completed without his motivation, patient instruction and insightful comments. The knowledge and the strict self-disciplined attitude towards research, which I learned from him, will guide and benefit my future career.

I am grateful to the government of Hong Kong Special Administration Region (HKSAR) and The Hong Kong Polytechnic University for providing me a postgraduate stipend, a competitive earmarked research grant from the Research Grant Council of the HKSAR (Project No. PolyU 5196/10E). With the stipend, I could focus on my study in Hong Kong without the financial burden. This research is also supported by an internal research project funded by Research Institute for Sustainable Urban Development (RISUD) of the Hong Kong Polytechnic University (1-ZVBZ). I would also like to appreciate the supports of the Transport Department of the HKSAR for provision of traffic and incident data for this research.

I would like to express my gratitude to my co-supervisor, Dr. Agachai Sumalee, for his constructive suggestions and comments. Special thanks also must be given to Dr. Mei Lam Tam, who spent much of her precious time in discussing with me and reviewing my working papers. Special thanks also should be given to Dr. Zhen Leng, Dr. Hu Shao, Dr. Xingang Li and Mr. Daojun Ye for their helpful suggestions and sharing of experience in transportation studies.

I must express my acknowledgement to Mrs. Elaine Anson, who devoted her efforts in teaching me the academic English writing and improving the quality of my working papers. I learned a lot every time when she sent me the revised pieces of work.

Thanks should be given to the following individuals for their help and cooperation during my study: Ms. Zixin Chen, Ms. Xinqing Cao, Mr. Junlong

Zhang, Mr. Depeng Li, Mrs. Yanyan Chen, Dr. Mable Chan, Mrs. Elizabeth Dean Luther and Mrs. Connie F. Y. Lam. Many thanks are also given to anonymous reviewers of my journal papers arising from this thesis for their valuable comments and suggestions in improving the paper quality.

I sincerely appreciate the supports from my mother, Mrs. Qingmei Li, and other family members for their consideration, encouragement and endless love over the years. I would also like to deeply cherish the memory of my passed father, Mr. Guowen Li.

Table of Contents

List of Tables

List of Figures

List of Notations

t	Time interval
i	Traffic detector reference
j	Time interval reference
λ	Traffic stream parameter reference
T	Detection threshold
n	The number of time intervals over the sampling period prior to the current time interval t
n'	The number of time intervals in which the traffic data are not equal to zero over the sampling period
v	Traffic speed
q	Traffic flow (or traffic volume)
d	Traffic density
O	Traffic occupancy
C	Traffic capacity
r	Rainfall intensity
l	Speed limit
ds	Detector spacing
λ_t	Traffic stream parameter λ at time t
$\overline{\lambda}_t$	The average of λ_j over the sampling period prior to time t
σ_t	The standard deviate of λ_j over the sampling period prior to time t
p	The number of time intervals for raw data smoothing for the current time period
u	The number of time intervals for raw data smoothing for the past time period
τ	The journey time between two adjacent detectors;
τ_t	The journey time at time interval t
$\overline{\tau}_t$	The mean of all journey time within the comparison window at time interval t

var_t	The variance of all journey times within the comparison window at time interval *t*
$\hat{\mu}_t$	The log-normal mean of all journey time within the comparison window at time *t*;
$\hat{\sigma}_t^2$	The log-normal variance of all journey time within the comparison window at time *t*;
z	The z value corresponding to the level of confidence
UL_t	The upper confidence limit at time *t*
v_c	Speed at capacity
v_f	Free-flow speed
w_j	The weight of λ_j
$\overline{\lambda}_t^w$	The weighted average of λ_j over the sampling period prior to time *t*
σ_t^w	The weighted standard deviate of λ_j over the sampling period prior to time *t*
CV_t	The coefficient of variation of λ_j over the sampling period prior to time *t*
θ	The predetermined threshold for CV_t
CCS_t	The correlation coefficient of speeds of two adjacent detectors at time *t*
$v_{u,j}$	The traffic speed at upstream detectors at time *j*
$v_{d,j}$	The traffic speed at downstream detectors at time *j*
$\overline{v}_{u,t}$	The sample average speeds at the upstream detectors, over a sampling period of m intervals prior to and including *t*
$\overline{v}_{d,t}$	The sample average speeds at the downstream detectors, over a sampling period of m intervals prior to and including *t*
$\sigma_{u,t}$	The sample standard deviates at the upstream detectors, over a sampling period of *n* intervals prior to and including *t*.
$\sigma_{d,t}$	The sample standard deviates at the downstream detectors, over a sampling period of m intervals prior to and including *t*.
v_u	The traffic speed at the upstream detector

CVS_u	The coefficient of variation of speed at the upstream detector
CCS	The correlation coefficient of speeds of two adjacent detectors;
d_u	The density at the upstream detector
d_d	The density at the downstream detector
$SND_t^{'}$	The modified standard normal deviate at time *t*
$SND_{t-1}^{'}$	The modified standard normal deviate at time *t-1*
$SND_t^{'}(\lambda)$	The modified standard normal deviate value of traffic stream parameter λ at time *t*
$SND_{t-1}^{'}(\lambda)$	The modified standard normal deviate value of traffic stream parameter λ at time *t-1*
T_λ	The corresponding detection thresholds of traffic stream parameter λ
$Y(t+1)$	The range of forecasted difference in traffic stream parameters at time $(t+1)$
$\hat{z}_1(\lambda_t)$	Single exponential smoothing forecast with a smoothing constant α;
$\hat{z}_2(\lambda_t)$	Double exponential smoothing forecast with a smoothing constant α;
$e(\lambda_t)$	Prediction error
$y(\lambda_t)$	Cumulative predication error
$\mathrm{m}(\lambda_t)$	Mean absolute deviation
$TS(\lambda_t)$	Tracking signal
α	Smoothing constant to be calibrated
γ	Parameter to be calibrated
φ	Parameter to be calibrated
η	Parameter to be calibrated
ψ	Parameter to be calibrated
$O_i(t)$	Traffic occupancies at the upstream detector stations at time *t*
$O_{i+1}(t)$	Traffic occupancies at the downstream detector stations at time *t*

$O_i(t+1)$	Traffic occupancies at the upstream detector stations at time *t+1*
$O_{i+1}(t+1)$	Traffic occupancies at the downstream detector stations at time *t+1*
$O_i(t+p)$	The smoothed occupancy at the upstream detector station for time period $(t+p)$
$O_{i+1}(t+p)$	The smoothed occupancy at the downstream detector station for time period $(t+p)$
$O_i(t-q)$	The smoothed occupancy at the upstream detector station for time period $(t-q)$
$O_{i+1}(t-q)$	The smoothed occupancy at the downstream detector station for time period $(t-q)$
$\Delta O(t+p)$	The difference in smoothed occupancies at upstream and downstream detector stations for current time period
$\Delta O(t-q)$	The difference in smoothed occupancies at upstream and downstream detector stations for past time period

List of Abbreviations

AID	Automatic incident detection
ANN	Artificial neural network
APID	All-purpose incident detection
ARMA	Auto-regression integrated moving average
AVI	Automatic vehicle identification
CCS	Correlation coefficient of speeds
CODE	Combined detector evaluation
CRS	Congested regime shifts
CVS	Coefficient of variation of speed
DES	Double exponential smoothing
DR	Detection rate
ESND	Extended standard normal deviate
ETC	Electronic toll collection
FAR	False alarm rate
FD	Fundamental diagram
HKSAR	Hong Kong Special Administration Region
ITS	Intelligent transportation system
ILD	Inductive loop detector
JTIS	Journey time indication system
MLF	Multi-layer feed-forward
MTTD	Mean time to detect
PNN	Probabilistic neural network
RFID	Radio frequency identification device
SND	Standard normal deviate
URS	Uncongested regime shifts
VIP	Video image processing

Chapter 1. Introduction and Objectives

1.1 Background

Non-recurrent congestion caused by unexpected traffic incidents has become a severe problem over past decades. Unexpected traffic incidents such as accidents, vehicle breakdowns and spilled loads may lead to congestion, traffic delays, air pollution, and secondary accidents. The unexpected traffic incidents have been found to account for approximately 60% of the total congestion on freeways (Lindley, 1987). About 1.2 million deaths have been reported yearly around the world as a result of unexpected traffic incidents (Dinh-Zarr, 2008). It is felt that early detection and timely disposition of unexpected traffic incidents can largely reduce traffic delays and alleviate traffic congestion (Dia and Thomas, 2011; Luk et al., 2001).

Incident management, one of the main functions provided by the automatic traffic management systems, involves four steps: (1) incident detection, (2) verification, (3) response, and (4) clearance. Incident detection is critical because its subsequent three steps are largely affected by the accuracy and reliability of the incident detection results (Parkaney and Xie, 2005). Information about the detected incidents can be used to assist traffic operators in (1) implementing emergency responses and (2) enabling travelers to avoid road sections impeded by those incidents. This research focuses on the incident detection.

Traditional incident detection relies on manual methods such as reports from patrol vehicles, calls from passing drivers and video surveillance. These traditional incident detection methods are labor-intensive, not necessarily effective, and sometimes unreliable.

Over the past few decades, incident detection has realized automation through the development of automatic incident detection (AID) algorithms. Mathematical models are used in AID algorithms to determine the presence of traffic incidents on the basis of traffic data obtained from traffic detectors. Compared with other traditional incident detection methods, AID algorithms provide continuous,

round-the-clock, and timely incident detection.

Automatic incident detection is based on capturing the sudden disturbances or changes in traffic stream parameters. When a traffic incident occurs, the road capacity on the incident spot is reduced. The reduced capacity tends to create congestion in the upstream of the incident spot. This upstream congestion is likely to decrease the traffic speed and increase the traffic occupancy. Fewer vehicles are able to pass the incident spot due to the upstream congestion, hence the downstream traffic flow decreases. This decrease in flow is likely to increase downstream traffic speed. Incident-induced traffic disturbance and its ensuing effects on traffic stream parameters form the assumptions upon which the AID algorithms are based.

Researchers have proposed several AID algorithms over the past decades. Some of these AID algorithms have been applied to road systems in many cities. These existing AID algorithms can be categorized into several types based on the input data, applied mathematical model, number of traffic detectors, and complexity of detection logic.

A Journey Time Indication System (JTIS), operated by the Hong Kong Transport Department, however, was launched in mid-2003 to provide the average instantaneous journey time on some major routes every 2 minutes (Tam and Lam, 2011). A few video traffic detectors (Autoscope) and automatic vehicle identification (AVI) readers, installed at 31 strategic locations, are used to collect traffic data on major routes (Fig. 1.1).

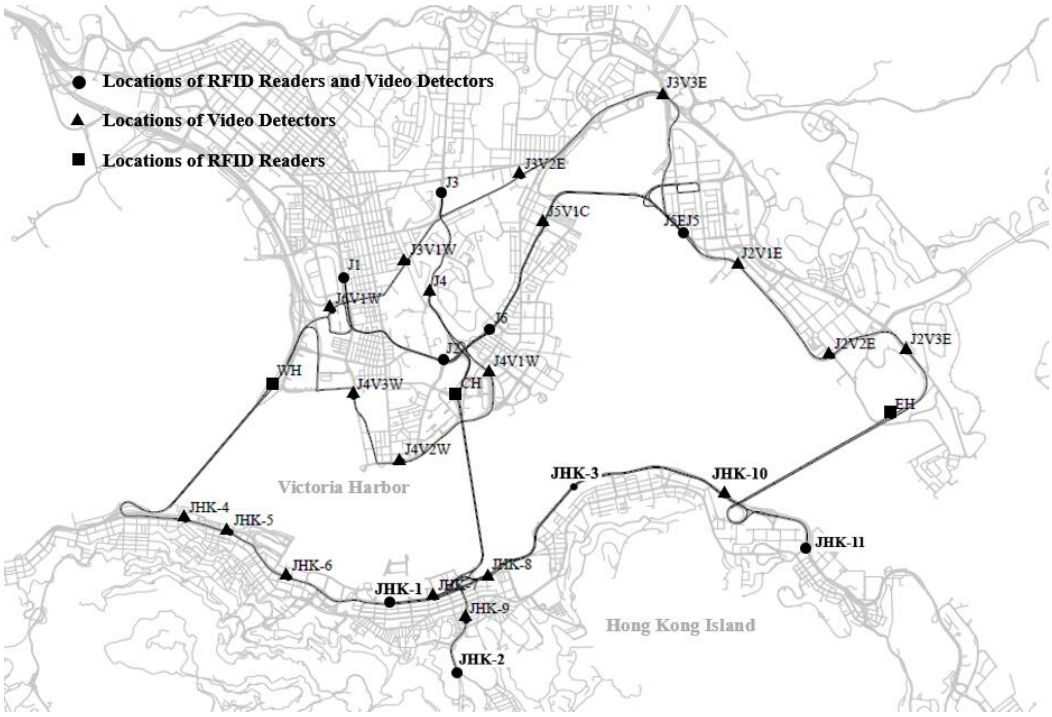

Fig. 1.1 Road network under the Journey Time Indication System (JTIS) and locations of traffic detectors

At each detector location, one or two video traffic detectors are installed to collect unidirectional or bidirectional traffic data on selected lanes. In addition, AVI readers are also installed at some detector locations to collect the time stamps of the passing vehicles. The video traffic detector spacing ranges from 0.56 to 2.14 km and the average is 1.34 km. The AVI reader spacing ranges from 0.28 to 9.85 km and the average is 3.98 km. The detailed detector spacing are listed in the tables in Appendix G and Appendix H. The collected traffic data are archived in the JTIS database.

The traffic data aggregate time interval is 2 minutes, a value longer than the commonly used 20-60 seconds in previous studies (Mak and Fan, 2006a). This long traffic data aggregate time interval may result in a longer time to detect traffic incidents. In addition, the video traffic detector spacing varies greatly, ranging from about 0.56 to 2.14 km. The detector spacing is also larger than the 0.25-1.5 km in previous studies (Martin et al., 2001; Mak and Fan, 2007). The unevenly spaced detectors and some large detector spacing may largely affect the effectiveness of existing AID algorithms. A new AID algorithm, with the use of the available traffic data collected for journey time estimation purposed only, is

needed for incident detection rather than the installation of a greater number of expensive traffic detectors. A nationwide survey in the United States also addressed the need to develop AID algorithms using the existing data collection infrastructures (Williams and Guin, 2007).

AID algorithms detect incidents by capturing incident-induced disturbances or changes in traffic stream parameters. The performance of AID algorithms is affected by many factors such as the preincident traffic condition (e.g. traffic flow condition), speed limit, detector spacing, the distance between the incident spot and its upstream/downstream traffic detectors, and adverse weather conditions such as rainfalls.

The effects of the preincident traffic flow condition on incident detection have been investigated in the development of some existing flow-dependent AID algorithms (Mak and Fan, 2007). These flow-dependent AID algorithms adopt different detection logic or detection thresholds under different preincident traffic flow conditions (i.e. low, medium and heavy flow).

The effects of rainfalls on incident detection performance have not been investigated. However, it has been found that different degrees of rainfall intensity have different effects on key traffic stream parameters (e.g. free-flow speed and capacity) and traffic speed-flow-density relationships (Lam et al., 2013). The changes of key traffic stream parameters and traffic speed-flow-density relationship under various rainfall intensities may affect traffic conditions, and then the overall detection performances of AID algorithms. Thus, it would be of value to develop new AID algorithms which can adapt to various preincident traffic and rainfall conditions.

A recent paper (Li et al. 2012) has found that the first hour of rain and the first hour after rain are shown to be the periods with the highest number of traffic accidents based on the accident and rainfall data in Hong Kong.

It is seen from Table 1.1, based on the rainfall data (annual averages for the 30-year period from 1981 to 2010) from the World Weather Information Services (http://www.worldweather.org/), Hong Kong has the highest average annual

rainfall (2383 mm) among all the major Pacific Rim cities. About 80% of yearly rainfall occurs between May and September. The yearly average of rainy days in Hog Kong is approximately 137.4 days.

Table 1.1 Average Annual Rainfall (mm) for the 30-year Period from 1981 to 2010 in Major Pacific Rim Cities

City	Average annual rainfall (mm)
Hong Kong	2383
Manila	2201
Singapore	2150
Jakarta	1655
Bangkok	1497
Tokyo	1467
Seoul	1344
Sydney	1222
Vancouver	1199
Beijing	578
San Francisco	500
Santiago	313

In such a densely populated city, traffic incidents and congestion problems increase particularly under rain conditions. Given such conditions, the development of AID algorithms, which can adapt to various rain conditions are of value and would likewise be of benefit to all well populated cities with substantial rainfalls.

1.2 Research Scope and Objectives

It is essential to develop AID algorithms, specifically for Hong Kong, in an effort to increase traffic safety and mobility. Instead of installing more expensive traffic detectors specifically for the use of incident detection, the development of AID algorithms on the basis of the existing data collection infrastructures is also necessary. Specific to the development of new algorithms is the consideration of rain conditions in order to accommodate Hong Kong's substantial rainfall and thus more effectively detect incidents under rain conditions. Hence the study presented in this thesis focuses on the development of AID algorithms for incident detection under both no-rain and rain conditions.

The traffic data originally collected for journey time estimation purpose on the Hong Kong road network are available for use to develop AID algorithms. Traffic data collected by both video traffic detectors and AVI readers will be fused for use as traffic inputs for the proposed AID algorithms. The rainfall intensity data collected by the Hong Kong Observatory also makes it possible to investigate the effects of rainfalls on incident detection. The traffic accident database provided by the Hong Kong Police and the Transport Department will be used to calibrate and validate the proposed AID algorithms in this research.

The main objectives of this research are as follows:

(1) To develop a new AID algorithm with the use of the available traffic data originally collected for journey time estimation purpose only;

(2) To develop an AID algorithm for use under no-rain conditions;

(3) To develop a generalized AID algorithm for use under both no-rain and rain conditions.

The interrelationship of the research objectives and chapters in the study of the thesis are illustrated in Fig. 1.2.

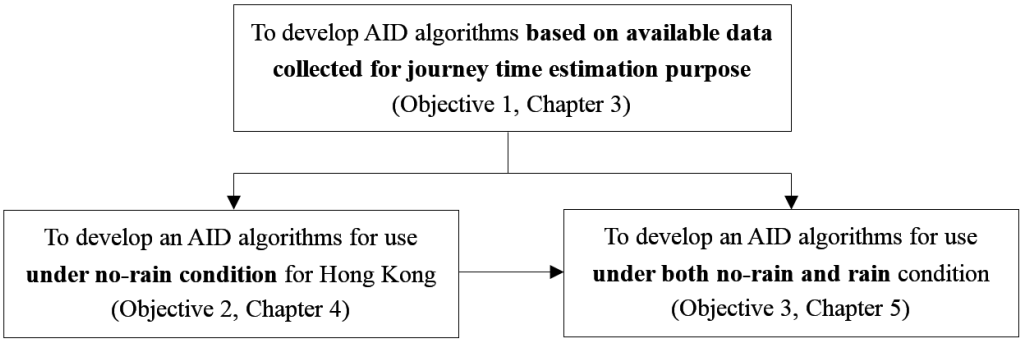

Fig. 1.2 Interrelationship of the research objectives and chapters of the thesis

As shown in Fig. 1.2, an AID algorithm with the use of the available traffic data originally collected for journey time estimation purpose is firstly developed (Objective 1 in Chapter 3). The developed algorithm is then extended to be an AID algorithm for incident detection under no rain conditions(Objective 2 in Chapter 4). With consideration of the effects of rainfalls, a generalized AID algorithm is developed for incident detection under both no-rain and rain

conditions (Objective 3 in Chapter 5).

1.3 Thesis Structure

The remainder of this thesis consists of five more chapters as follows:

In Chapter 2, a comprehensive literature review of the related studies in automatic incident detection (AID) is conducted. Traffic data collection technologies are firstly introduced, followed by a review of existing AID algorithms. Strengths and weaknesses of these existing AID algorithms are discussed. The performance measurements of AID algorithms and the influencing factors on performance of AID algorithms are then described. Finally, the experience in the deployments of existing AID algorithms are summarized.

Chapter 3 presents the development of the extended standard normal deviate (ESND) algorithm. A traffic incident on the Hong Kong road network is used as an example to illustrate the improvements of the proposed ESND algorithm. Two new traffic stream parameters are also proposed for use as traffic inputs to the proposed ESND algorithm.

In Chapter 4, the proposed ESND algorithm is further extended to be a flow-dependent ESND algorithm for incident detection under no-rain conditions. The selection of input traffic data for the proposed ESND algorithm is also presented. The proposed flow-dependent ESND algorithm is calibrated and validated with the collected traffic data on a selected road section in Hong Kong. The proposed flow-dependent ESND algorithm is finally compared with five selected AID algorithms when applied to the selected road section in Hong Kong.

Chapter 5 describes the development of a flow-rain-dependent ESND algorithm for incident detection under both no-rain and rain conditions. Both preincident traffic and rain conditions are considered explicitly for the detection threshold determination. The proposed flow-rain-dependent ESND algorithm is calibrated and validated on the basis of the collected data on the Hong Kong road network to exam its performance on a network wide basis. The proposed flow-rain-dependent ESND algorithm is also compared with the five selected AID algorithms on the basis of the traffic and rainfall data collected on the Hong

Kong road network. Additionally, the estimation method of the generalized detection threshold functions for roads with various speed limits is demonstrated.

In Chapter 6, conclusions are drawn and further research recommendations given.

1.4 Contributions

In this research, the following contributions are made:

(1) The proposed AID algorithms are developed based on the traffic data originally collected for journey time estimation only. Thus, there is no need to install more expensive traffic detectors specifically for the use of incident detection.

(2) The proposed flow-rain-dependent AID algorithm adopts continuous detection thresholds other than discrete ones. The continuous detection thresholds which are generated by the generated detection threshold function are more sensitive and reasonable in practice.

(3) Apart from the preincident traffic flow, rainfall intensity is also considered in the determination of the detection thresholds. The consideration of the preincident rainfall intensity in incident detection improved the detection performance especially under rain condition.

(4) The previous standard normal deviate algorithm (Dudek et al., 1974) has been extended to be the extended standard normal deviate algorithm. The weighting method is used to increase the reliability of detection results. The restriction to the input data within the comparison window is used to reduce the false alarms.

(5) Two new traffic stream parameters are proposed as the input of the developed AID algorithms. These two new traffic stream parameters are (1) the coefficient of variation of speeds (CVS) at upstream detectors and (2) the correlation coefficient of speeds (CCS) of two adjacent detectors. These two traffic stream parameters have proved feasible in indicating the incidents.

Chapter 2. Literature Review

2.1 Introduction

Researchers have proposed several automatic incident detection (AID) algorithms over the past decades. These AID algorithms are composed of various input data, mathematical models and forms of detection logic. Performance measurements are essential to evaluate the effectiveness of AID algorithms. The detection performance of AID algorithms is affected by many factors such as traffic and weather conditions.

In this Chapter, traffic data collection technologies are firstly summarized. The principles, strengths and weaknesses of existing AID algorithms are then fully reviewed. The performance measurements are also introduced. In addition, factors influencing the AID performance are summarized and discussed.

2.2 Traffic Data Collection Technologies

Automatic incident detection is based on the use of traffic data collected by various traffic data collection technologies as inputs. The traffic data quality may largely affect the detection performance of AID algorithms. The most widely used traffic data collection technologies, fixed-location detectors and probe vehicle technologies, are introduced in this Section.

2.2.1 Fixed-location Detectors

Fixed-location detectors, such as inductive loop detectors and video detectors, are embedded in the road pavements or installed beside or above the roads. Fixed-location detectors are used to provide point traffic data at a specific site. The point traffic data such as traffic speed, flow and occupancy reflect the sectional traffic conditions near traffic detectors. Most previous AID algorithms are developed on the basis of traffic data collected by fixed-location detectors. These fixed-location detector based AID algorithms are reviewed in Section 2.5.

Inductive loop detectors (ILD) work by detecting the change of inductance caused by the passing vehicles. There are many types of inductive loop detectors based on the different loop shapes (e.g. circular and rectangular), number of loops (e.g. single-loop and dual-loop), installation locations (e.g. stop-line and far-upstream) and installation forms (e.g. saw cut and the preformed). Video traffic detectors take advantage of the Video Image Processing technology to extract information from images. Video traffic detectors adopt virtual tripwires to emulate the function of inductive loop detectors.

Table 2.1 summarizes the strengths and weaknesses of both inductive loop detectors and video detectors (Klein, 2001; Parkany and Xie, 2005).

Table 2.1 Comparison between Inductive Loop Detectors and Video Detectors

Type	Strength	Weakness
Inductive loop detector	1. Low per unit cost 2. Acceptable performance 3. Rich experience base 4. Insensitive to adverse weather	1. Pavement cut and lane closure are required during installation and maintenance
Video detector	1. Live visual images are provided 2. Provide more detailed information 3. No traffic interruption during installation and maintenance	1. High per unit cost 2. Performance is affected by adverse weather, vehicle shadows, lightning and other factors

In general, ILDs can provide acceptable detection performance with low per unit cost. The detection performance of the ILDs is insensitive to the adverse weather conditions such as rainfalls and fogs. Rich experience has been accumulated and can be provided in application. However, pavement cut and lane closure are required during the installation and maintenance. ILDs are also susceptible to damages by heavy traffic loads.

Compared to ILDs, video detectors can visually provide information regarding traffic incidents to traffic operators. This enables easier incident verification and problem identification. In addition to the traffic speed, flow, occupancy, queue lengths and delays, more information is provided. The installation and maintenance have no interruption on the traffic. The performance of video detectors may be affected by weather, vehicle shadows, lightning and other factors.

2.2.2 Probe Vehicle Technologies

Probe vehicle technologies such as automatic vehicle identification (AVI) are used to provide point-to-point traffic data over a road section. The point-to-point traffic data such as journey time better describes the traffic condition over a road section (Hellinga and Knapp, 2000; Khoury et al., 2003).

Probe vehicle technologies collect information from sensors installed in vehicles operating in the road traffic flow. The data collected from probe vehicles is then used to estimate the road traffic condition. The accuracy and reliability of the estimation, however, is largely affected by the market penetration rate of vehicles with sensors installed.

AVI technology, one of the probe vehicle technologies, is designed to identify the vehicle at a specific time and at a specific location. With the temporal and spatial vehicle information collected by the AVI technology, the journey time experienced by vehicles can be estimated. The matching of the same vehicle identified at two AVI reader locations can also be used in toll collection and vehicle fleet management.

With the development of automatic toll collection systems and route guiding systems, more and more vehicles are installed with GPS equipment and AVI tags. The increasing market penetration of probe vehicles makes it possible to detect incidents on the basis of the probe vehicle based traffic data. Several existing probe vehicle based AID algorithms are reviewed in Section 2.6.

2.3 Automatic Incident Detection (AID) Algorithms

Compared to manual incident detection methods, AID algorithms automatically trigger incident alarms when traffic data obtained from traffic detectors satisfy certain preset conditions (Parkany and Xie, 2005).

AID algorithms can be categorized into several types according to data collection technologies used, number of detectors adopted and mathematical models applied.

Based on the technologies used for data collection, the existing AID algorithms are categorized into fixed-location detector based algorithms and probe vehicle based algorithms as shown in Table 2.2.

Table 2.2 Existing AID Algorithms Based on Traffic Data Collected by Different Data Collection Technologies

Data collection technology	Category	Algorithm
Fixed-location detector	Pattern recognition algorithm	1. California algorithm 2. All-purpose incident detection algorithm etc.
	Statistical algorithm	1. Standard normal deviate algorithm 2. Bayesian algorithm 3. Flow-dependent combined detector evaluation algorithm etc.
	Time series algorithm	1. Auto-regressive integrated moving average algorithm 2. Double exponential smoothing algorithm 3. Minnesota algorithm etc.
	Traffic modelling algorithm	1. McMaster algorithm 2. Fundamental diagram based algorithm etc.
	Artificial intelligence algorithm	1. Artificial neural network model based algorithms 2. Fuzzy logic based algorithms etc.
Probe vehicle technology	Statistical time series model	1. Texas algorithm 2. Confidence limit algorithm 3. Speed and confidence limit algorithm 4. Dual confidence limit algorithm etc.

Most AID algorithms are developed with the use of traffic data obtained from fixed-location detectors. As shown in Table 2.2, these fixed-location detector based algorithms can be categorized into four groups based on the mathematical models applied. The first group is pattern recognition algorithms such as the California algorithm (Payne et al., 1978) which have been extended to 10 types of improved algorithms and the all-purpose incident detection (APID) algorithm (Masters et al., 1991). The second group is statistical algorithms, which includes: standard normal deviate (SND) algorithm (Dudek et al., 1974), Bayesian algorithm (Zhang and Taylor, 2006), and flow-dependent combined detector

evaluation (CODE) algorithm (Mak and Fan, 2007). The third group is time series algorithms such as auto-regressive integrated moving average (ARMA) algorithm (Ahmed and Cook, 1982), double exponential smoothing (DES) algorithm (Cook and Cleveland, 1974), and Minnesota algorithm (Stephanedes and Chassiakos, 1993). The fourth group includes traffic model algorithms such as the McMaster algorithm (Persaud et al., 1990) and fundamental diagram (FD) based algorithm (Jin and Ran, 2009). The last group consists of some artificial intelligence algorithms such as artificial neural network (ANN) based algorithms (Cheu and Ritchie, 1995; Dia and Thomas, 2011) and fuzzy logic based algorithms (Chang and Wang, 1994).

Some other AID algorithms are developed based on the use of journey time data collected by the AVI technology. These AVI-based AID algorithms include Texas algorithm (Balke et al., 1996), upper confidence limit algorithm, speed and confidence limit algorithm, and dual confidence limit algorithm (Hellinga and Knapp, 2000). Most AVI-based AID algorithms adopt statistical time series models.

Much efforts have also been made to integrate traffic data collected by both fixed-location detectors and probe vehicle technologies in order to improve the detection performances of AID algorithms (Westerman et al., 1996; Ivan and Sethi, 1998; Dia and Thomas, 2011).

Based on the numbers of traffic detectors used, the existing AID algorithms can be categorized into single-station algorithms and dual-station algorithms as shown in Table 2.3.

Table 2.3 Existing Single-Station and Dual-Station AID Algorithms

Category	Algorithm
Single-station AID algorithm	1. Standard normal deviate algorithm 2. Double exponential smoothing algorithm 3. Auto-regression integrated moving average algorithm …
Dual-station AID algorithm	1. California algorithm 2. All-purpose incident detection algorithm 3. Bayesian algorithm 4. Minnesota algorithm 5. Flow-dependent combined detector evaluation algorithm …

Single-station AID algorithms adopt traffic data obtained from only one traffic detector located either upstream or downstream of a traffic incident. Dual-station AID algorithms adopt traffic data obtained from detectors located at both upstream and downstream of the traffic incident.

At the same study site, dual-station AID algorithms tend to be more effective in detecting incidents with more information from both upstream and downstream traffic detectors. Single-station AID algorithms, however, may be more adaptive because they are less dependent on variations in road geometry, detector spacing, the presence of on/off ramps and the prevailing traffic flow condition (Mak and Fan, 2006a; Karim and Adeli, 2002). It is thus a challenging and worthwhile aim to develop AID algorithms that can combine the strengths of both single-station and dual-station algorithms.

2.4 Performance Measurements

The incident detection performance can be measured by the detection rate (DR), false alarm rate (FAR) and mean time to detect (MTTD) (Ishak and Al-Deek, 1999; Mussa and Upchurch, 2000). An effective AID algorithm needs to have a high DR, low FAR, and short MTTD. Incident detection performance curve is used to measure the overall performance of AID algorithms (Chung and Rosalion, 1999; Mak and Fan, 2006b).

2.4.1 Detection Rate

The detection rate (DR) is defined as the number of traffic incidents correctly detected by AID algorithms divided by the total number of traffic incidents as shown in Eq. (2.1). If the AID algorithm gives an alarm during the incident period, the incident is regarded as correctly detected.

$$\text{DR} = \frac{\text{Number of detected incidents}}{\text{Total number of incidents}} \times 100\% \tag{2.1}$$

2.4.2 False Alarm Rate

AID algorithms are usually applied once every time interval to the incoming traffic data in practice. The time interval between two successive algorithm applications is usually the same as the data aggregation time interval. If an alarm is triggered by the AID algorithms when no incidents have taken place, it is regarded as a false alarm. The false alarm rate (FAR) has two different definitions for different applications (Parkany and Xie, 2005). The most commonly used FAR is defined as the ratio of the number of false alarms to the total number of algorithm applications as shown in Eq. (2.2).

$$\text{FAR} = \frac{\text{Number of false alarms}}{\text{Total number of applications of the algorithm}} \times 100\% \tag{2.2}$$

For instance, when the FAR is 1.8%, it means that the AID algorithm may trigger 1.8 false alarms in average when applied every 100 times. Given the time interval between two algorithm applications, the FAR in Eq. (2.2) can be easily transferred into the hourly or daily number of false alarms. The hourly or daily false alarms can be used to measure the workloads of traffic operators. For instance, assuming that the AID algorithm is applied once every 30 seconds (i.e. 120 times per hour), the 1.8% FAR is equivalent to 2.16 false alarms per hour or 51.84 false alarms per day. The information of hourly or daily false alarms can also help in designing patrol routes or arranging rescue vehicles for possible incidents in advance.

The other definition of the FAR is the ratio of the number of false alarms to the total number of declared alarms. However, this type of FAR is not usually used in the development of most previous AID algorithms. In this research, the

performances of the proposed algorithms are intended to compare with other existing AID algorithms whose FAR is measured by Eq. (2.2). Therefore, the first definition of the FAR in Eq. (2.2) is used in this research.

When the time interval is small (e.g. 30 seconds), both hourly and daily false alarms can be used in practice. However, when the time interval is too large, the hourly false alarm would be too small to be used as the workload measure. For instance, assuming that the algorithm is applied every 5 minutes, the 1.8% FAR is equivalent to only 0.09 false alarm per hour. The 0.09 false alarm per hour is too small to be used to measure the workload in practice. However, the corresponding daily false alarms (i.e.5.18) are more reasonable to be used. Therefore, the daily false alarms are recommended for use when the time interval between two algorithm applications is large.

2.4.3 Mean Time to Detect

The mean time to detect (MTTD) is defined as the average difference between the actual occurring time of incidents and the detection time by AID algorithms as shown in Eq. (2.3).

$$\mathrm{TTD} = \frac{1}{n}\sum_{i=1}^{n}\left(T_{i,\,start} - T_{i,\,\mathrm{det}ected}\right) \tag{2.3}$$

Because it takes time for AID algorithms to detect traffic incidents, the detection time is the period from the occurring time of an incident ($T_{i,\,start}$) to the time it is detected ($T_{i,\,\mathrm{det}ected}$).

2.4.4 Performance Envelope Curve

The performance envelope curve is defined as the curve on which the DR versus the FAR are plotted. The performance of the AID algorithm in a related paper (Li et al., 2013) is plotted as an example in Fig. 2.1.

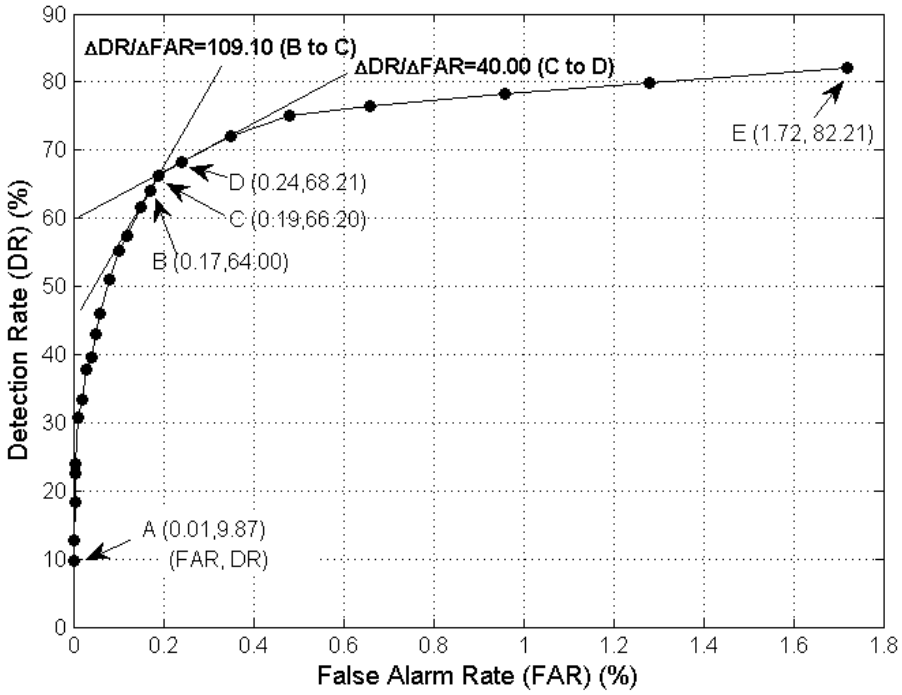

Fig. 2.1 A example of the performance envelope curve (Li et al., 2013)

It can be seen from Fig. 2.1 that a trade-off between the DR and FAR exists. The DR increases with the increasing FAR. For instance, the DR of point A on the performance curve in Fig. 2.1 increases from 9.87% to the 82.21% of point E when the corresponding FAR increases from 0.01% to 1.72%.

It is worth noting that the increasing rate ($\Delta DR / \Delta FAR$) of the DR decreases with the increasing FAR. This indicates that the increase of the DR will be less significant when the FAR increases. For instance, when the DR-FAR pair moves from point B to point C in Fig. 2.1, the increasing rate of the DR is 109.10, meaning the DR increases 10.91% at the cost of a 0.1% increase in the FAR. The increasing rate of the DR is 40.00 when the DR-FAR pair moves from point C to point D in Fig. 2.1. This means that the DR increases 4.00% at the cost of a 0.1% increase in the FAR. Thus, the increase of the DR at the cost of a same increase in FAR becomes less efficient when the FAR increases.

2.4.5 Average Mean Time to Detect

The average mean time to detect (MTTD) is the mean of MTTDs within certain

ranges of FAR or DR. The average MTTD is used to indicate the overall incident detection performance within a range of FAR or DR values (Mak and Fan, 2006b).

2.4.6 The Relationship between Performance Measurements

A trade-off exists between the DR, FAR, and MTTD. The relationship between the three measurements of the AID algorithm in the related paper (Li et al., 2013) are showed in Fig. 2.2 as an example.

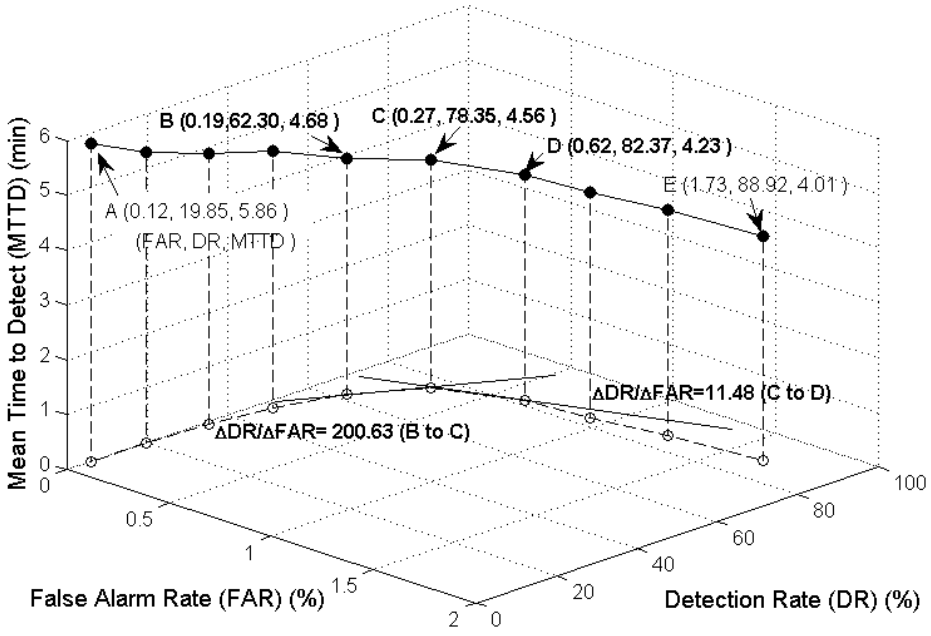

Fig. 2.2 An example of the relationship between the detection rate (DR), false alarm rate (FAR) and mean time to detect (MTTD) (Li et al., 2013)

It can be seen from Fig. 2.2 that a trade-off between the DR, FAR and MTTD exists. For instance, the DR increases from 19.85% to 88.92% when the FAR increases from 0.12% to 1.73% (from point A to E in Fig. 2.2). Meanwhile, the MTTD decreases from the 5.86 to 4.01 minutes. Additionally, it is shown in Fig. 2.2 that the increasing rate ($\Delta DR / \Delta FAR$) of the DR decreases with the increasing FAR. For instance, the increase of the DR at the same cost of a 1% increase in the FAR at point B and C in Fig. 2.2 are 200.63% and 11.48% respectively. This indicates that increase of the DR at the cost of the FAR tends to be less efficient

when the FAR increases.

The trade-off between the DR, FAR and MTTD is relates to the detection threshold. As the detection threshold of the AID algorithm increases, false alarms caused by non-incident-induced traffic disturbances can be reduced. However, some small incident-induced traffic disturbances may not be detected by the AID algorithm with a small detection threshold. Thus, the DR decreases with the decrease of the FAR. In addition, time is taken before any traffic disturbances change significantly enough to be detected by the predetermined detection threshold. More time is necessary before traffic stream parameters change significantly enough to be detected by the AID algorithm with a larger detection threshold. That means the MTTD increases with the decrease of both the DR and FAR.

Because of the trade-off between the DR, FAR and MTTD, it is not clear which of them is more important at the cost of the others. Even a "perfect" AID algorithm with 100% DR, 0% FAR and an acceptable short MTTD cannot achieve the perfect performance when applied to a different database. For different traffic management centers and operators, the acceptable combination of the DR, FAR and MTTD varies. The acceptable limits of the performance measurements were identified through a survey to several traffic management centers in the United States (Abdulhai, 1996). The survey results showed that the average acceptable DR is at least 88% and the acceptable FAR is at most 1.8%. These two performance limits can be used in algorithm calibration and evaluation.

The persistence test is usually adopted to reduce the FAR in previous AID algorithms such as the standard normal deviate (SND) algorithm (Dudek et al., 1974) and the flow-based dual-variable algorithm (Mak and Fan, 2006a). Traffic data of a second-time interval is often used to conduct a persistence test to confirm the preliminarily detected incidents through continuous warning. False alarms caused by random fluctuations of the traffic stream parameters can be largely reduced. However, the cost of the persistence test is longer MTTD.

2.5 Fixed-location Detector Based AID Algorithms

In fixed-location detector based AID algorithms, point traffic data such as traffic speed, flow and occupancy, collected by fixed-location detectors, are used to detect incidents. According to the mathematical model applied, the fixed-location detector based AID algorithms are categorized into: (1) pattern recognition algorithms, (2) statistical algorithms, (3) time series algorithms, (4) traffic modelling algorithms, and (5) artificial intelligence algorithms. Typical AID algorithms in the above categories are reviewed in the following Sections.

2.5.1 Typical Pattern Recognition AID Algorithms

Pattern recognition or comparative algorithms detect traffic incidents by comparing the values of the observed traffic stream parameters with predetermined detection thresholds. The California #7 algorithm (Payne et al., 1976) and all-purpose incident detection (APID) algorithm (Masters et al., 1991) are two typical pattern recognition AID algorithms.

2.5.1.1 The California #7 Algorithm

The California algorithm is a series of 11 sub-algorithms developed by Payne et al. (1976). The underlying principle of the California algorithm is that an incident may simultaneously lead to an increase in traffic occupancy at the upstream detector and a decrease in traffic occupancy at the downstream detector. The California algorithm is a dual-station AID algorithm which not only considers the variation of the upstream or downstream occupancy, but also considers the difference between them.

Among the 11 sub-algorithms, the California #7 algorithm proved to have the best incident detection performance and was most widely used (Payne and Tignor, 1978; Balke, 1993; Mak and Fan, 2006a). The California #7 algorithm is often used as a benchmark to be compared with newly developed AID algorithms. The detection logic of the California #7 algorithm includes three parallel tests and one persistence test as follows:

Test 1:

$$O_i(t) - O_{i+1}(t) \geq T_1 \tag{2.4}$$

Test 2:

$$\frac{O_i(t) - O_{i+1}(t)}{O_i(t)} \geq T_2 \tag{2.5}$$

Test 3:

$$O_{i+1}(t) < T_3 \tag{2.6}$$

Persistent test:

$$\frac{O_i(t+1) - O_{i+1}(t+1)}{O_i(t+1)} \geq T_2 \tag{2.7}$$

where $O_i(t)$, $O_{i+1}(t)$ = the respective traffic occupancies at the upstream and downstream detector stations at time *t*; $O_i(t+1), O_{i+1}(t+1)$ = the respective traffic occupancies at the upstream and downstream detector stations at time *t+1*; T_1, T_2, T_3 = the respective predetermined detection thresholds for (1) the absolute difference between the occupancies at the upstream and downstream detector stations, (2) the relative difference between occupancies at the upstream and downstream detector stations compared with the occupancy at the upstream detector station, and (3) temporal occupancy difference at the downstream detector station.

An incident alarm is triggered when the three tests and the persistent test are all satisfied. The persistent test takes a consecutive time interval to make the detection result more reliable and to reduce the false alarms of incident detection.

2.5.1.2 The All-purpose Incident Detection Algorithm

The all-purpose incident detection (APID) algorithm was developed as a part of the COMPASS advanced traffic management system in Toronto (Masters et al., 1991). This algorithm was designed to detect incidents under all traffic conditions. The APID algorithm is an extension to the California algorithms. This algorithm adopts different sub-algorithms under different preincident traffic flow conditions such as low, medium and high flow conditions. In addition, the detection framework of the APID algorithm also includes an incident termination routine, a compression wave test and a persistence test.

The primary strength of the APID algorithm is the capability to adapt to different traffic flow conditions by adopting different sub-algorithms. The detection results under low traffic flow conditions, however, is not as good as those under the medium and heavy traffic flow conditions. Under low traffic flow conditions, it is necessary to adopt other AID algorithms other than comparative algorithms.

2.5.2 Typical Statistical AID Algorithms

In statistical AID algorithms, the values of the observed traffic stream parameters are compared with the statistically estimated or predicted values to indicate traffic incidents. The standard normal deviate (SND) algorithm (Dudek et al., 1974) and Bayesian algorithm (Levin and Krause, 1978) are two typical statistical AID algorithms.

2.5.2.1 The Standard Normal Deviate Algorithm

The standard normal deviate (SND) algorithm (Dudek et al., 1974), a statistical algorithm, was developed by the Texas Transportation Institute and was used on Houston's Golf Freeway in the early 1970s. The SND algorithm, detects incidents by examining the difference between the observed traffic data and their corresponding statistically estimated or predicted values (Parkany and Xie, 2005).

The underlying working principle of the SND algorithm is that a sudden change in a particular traffic stream parameter indicates the occurrence of a traffic incident. The SND value of a particular traffic stream parameter is used as the incident

indicator. The SND value is calculated through dividing the difference between a particular traffic stream parameter and its mean by its standard deviate as shown in Eqs. (2.8) - (2.10).

$$\bar{\lambda}_t = \frac{\sum_{j=t-1}^{t-n} \lambda_j}{n} \tag{2.8}$$

$$\sigma_t = \sqrt{\frac{\sum_{j=t-1}^{t-n} \left(\lambda_j - \bar{\lambda}_t\right)^2}{n-1}} \tag{2.9}$$

$$SND_t = \frac{\lambda_t - \bar{\lambda}_t}{\sigma_t} \tag{2.10}$$

where n = number of time intervals over the sampling period prior to the current time interval t; λ_t = the input traffic stream parameter at time t; $\bar{\lambda}_t$ and σ_t = the respective average and standard deviate of λ_j over the sampling period prior to time t.

If the SND value of a particular traffic stream parameter, such as traffic occupancy, exceeds the predetermined detection threshold, a potential traffic incident is identified. A second-time interval is often used to conduct a persistence test to confirm the detected incidents in the previous time interval.

The weakness of the SND algorithm is the relatively high false alarms which are caused by traffic fluctuations.

2.5.2.2 The Bayesian Algorithm

Most existing AID algorithms give a binary detection result, i.e. incident or incident-free. Levin and Krause (1978), however, adopted Bayesian statistical techniques to give the probability of the lane-blocking incidents. The relative spatial occupancy difference in the California algorithm is used for comparison with the predetermined detection threshold to determine the incident probability. The detection threshold is determined by calculating the conditional

probabilities that the relative difference is caused by lane-blocking incidents, based on historical data.

In order to compute reliable conditional probabilities, the Bayesian algorithm needs a large database including: (1) traffic occupancy and flow data during incident conditions, (2) traffic occupancy and flow data during incident conditions, and (3) incident data such as type, location, and severity.

The calibration of the detection thresholds in the Bayesian algorithm is quite difficult and requires a large historical incident database. These drawbacks restrict the implementation of the Bayesian algorithm in practice.

2.5.2.3 The Flow-dependent Combined Detector Evaluation Algorithm

The flow-dependent combined detector evaluation (CODE) algorithm was developed for incident detection on expressways in Singapore (Mak and Fan, 2007). Unlike previous fixed-location detector based AID algorithms, the flow-dependent CODE algorithm adopts traffic stream parameters collected by video traffic detectors as inputs. The mathematical model of this algorithm is similar to that of the SND algorithm. The differences in traffic occupancy and speed at the upstream and downstream detector stations are used. The preincident traffic flow condition is also considered explicitly in determining the detection thresholds.

The flow-dependent CODE algorithm comprises two components, forecasting and determination. The forecasting component is used to obtain the expected traffic condition (i.e. the difference in traffic occupancy and speed at the upstream and downstream detector stations) as shown in Eq. (2.11).

$$Y(t+1) = \bar{\lambda}(t) \pm T\sigma(t) \tag{2.11}$$

where $Y(t+1)$ = the range of forecasted difference in traffic stream parameters at time $(t+1)$; $\bar{\lambda}(t)$, $\sigma(t)$ = the mean and standard deviate of traffic stream parameter λ at time (t) over a sampling period; T = the predetermined

detection threshold. Eq. (2.11) is a transformation of the SND algorithm. The input data of the flow-dependent CODE algorithm, however, is the occupancy or speed difference between the upstream and downstream detector stations instead of the occupancy at a single detector station in the SND algorithm.

Additionally, the preincident traffic flow condition is considered explicitly in detection threshold determination. Different detection thresholds are adopted under low, medium and heavy flow conditions. The flow-dependent CODE algorithm proved effective in improving the incident detection performance under different traffic flow conditions.

2.5.3 Typical Time Series Algorithms

Time series AID algorithms detect incidents by comparing short-time traffic stream parameter values forecasted by time series models with the recently observed traffic stream parameter values. These time serious AID algorithms include the ARIMA algorithm (Ahmed and Cook, 1980) and the exponential smoothing algorithm (Cook and Cleveland, 1974).

2.5.3.1 The Auto-regression Integrated Moving Average Algorithm

Ahmed and Cook (1982) applied the time series analysis techniques formulated by Box and Jenkins (1976) to incident detection. The auto-regressive integrated moving average (ARIMA) model was found to be able to describe the dynamic character of freeway traffic stream parameters. The assumption of the ARIMA model is that the difference in a traffic stream parameter at current time intervals and at the previous time intervals can be predicted by averaging the errors between predicated and observed traffic stream parameter values within the three previous time intervals. The short-term traffic occupancy forecasts and the corresponding confidence limits can be calculated by the ARIMA model. An incident alarm will be triggered if the observed occupancy value exceeds the confidence limit of the corresponding forecasted value.

2.5.3.2 The Double Exponential Smoothing Algorithm

In the double exponential smoothing (DES) algorithm (Cook and Cleveland, 1974), short-time traffic conditions are predicted by giving weights to the past and current traffic stream parameter values. The DES algorithm detects incidents based on the tracking signals. The calculation of the tracking signal is calculated by Eqs. (2.12) - (2.17).

$$\hat{z}_1(\lambda_t) = \alpha\lambda_t + (1-\alpha)\hat{z}_1(\lambda_{t-1}) \tag{2.12}$$

$$\hat{z}_2(\lambda_t) = \alpha\left(\hat{z}_1(\lambda_t)\right) + (1-\alpha)\hat{z}_2(\lambda_{t-1}) \tag{2.13}$$

$$e(\lambda_t) = \lambda_t - \hat{z}_2(\lambda_t) \tag{2.14}$$

$$y(\lambda_t) = y(\lambda_{t-1}) + e(\lambda_t) \tag{2.15}$$

$$\mathrm{m}(\lambda_t) = \gamma\left|e(\lambda_t)\right| + (1-\gamma)\mathrm{m}(\lambda_{t-1}) \tag{2.16}$$

$$TS(\lambda_t) = \frac{y(\lambda_t)}{m(\lambda_t)} \tag{2.17}$$

where λ_t = the traffic stream parameter λ at time *t*; $\hat{z}_1(\lambda_t)$ = single exponential smoothing forecast with a smoothing constant α; $\hat{z}_2(\lambda_t)$ = double exponential smoothing forecast with a smoothing constant α; $e(\lambda_t)$ = prediction error; $y(\lambda_t)$ = cumulative predication error; $\mathrm{m}(\lambda_t)$ = mean absolute deviation; $m(\lambda_0) = \left\{\sqrt{2/\pi}\sqrt{2/(2-\gamma)}\right\}\sigma_z$ = initial value obtained from a sample of standard deviations; $TS(\lambda_t)$ = tracking signal; and α, γ = parameters to be calibrated.

An incident is detected if the tracking signal exceeds the predetermined detection threshold.

2.5.3.3 The Minnesota Algorithm

The Minnesota algorithm is a smoothing or filtering algorithm (Stephanedes and

Chassiakos, 1993). Compared to other existing AID algorithms, the Minnesota algorithm is able to reduce the false alarms caused by temporal random fluctuations in traffic stream parameters. Sharp fluctuations are eliminated while wide or low fluctuations associated with traffic incidents remain for incident detection.

In the Minnesota algorithm, two types of smoothed occupancies are used to reflect the current and past traffic conditions. The smoothed occupancies can be obtained by three types of techniques: (1) moving average, (2) median filtering, and (3) exponential smoothing. The exponential smoothing is used to demonstrate the detection logic of the Minnesota algorithm.

The formulas of the Minnesota algorithm is as follows:

$$\Delta O(t+p) = O_i(t+p) - O_i(t+p) \tag{2.18}$$

$$\Delta O(t-u) = O_i(t-u) - O_{i+1}(t-u) \tag{2.19}$$

$$Max\, O(t) = Max\left[O_i(t-u), O_{i+1}(t-u)\right] \tag{2.20}$$

$$\frac{\Delta O(t+p)}{Max\, O(t)} > T_1 \tag{2.21}$$

$$\frac{\Delta O(t+p) - \Delta O(t)}{Max\, O(t)} > T_2 \tag{2.22}$$

where $\Delta O(t+p)$, $\Delta O(t-u)$ = the respective difference in smoothed occupancies at upstream and downstream detector stations for current time period and past time period; $O_i(t+p)$, $O_i(t-u)$ = the respective smoothed occupancy at the upstream detector station *i* for time period $(t+p)$ and $(t-u)$; $O_{i+1}(t+p)$, $O_{i+1}(t-u)$ = the respective smoothed occupancy at the downstream detector station *i+1* for time period $(t+p)$ and $(t-u)$; *p, q* = the respective number of time interval for raw data smoothing for current time period and past time period.

Eq. (2.18) and Eq. (2.19) are used to obtain the smoothed occupancy difference for

the current period and past time period. .The incident is detected by the following two tests: (1) whether the normalized value of spatial occupancy difference for the current period exceeds the predetermined detection threshold, and (2) whether the normalized value of spatial occupancy difference between the current and past time periods exceeds the predetermined detection threshold.

2.5.4 Typical Traffic Modelling AID Algorithms

Traffic modelling AID algorithms are developed on the basis of the knowledge of traffic flow theories. Incident condition is distinguished from incident-free condition by comparing the observed traffic condition with that predicted or estimated by traffic models. Typical traffic modelling AID algorithms include McMaster algorithm (Persaud and Hall, 1989) and fundamental diagram (FD) based AID algorithm (Jin and Ran, 2009).

2.5.4.1 McMaster Algorithm

The McMaster algorithm (Persaud and Hall, 1989) was developed based on the Catastrophe theory. It was assumed that when traffic changes from congested state to uncongested state, traffic flow and occupancy change smoothly, whereas speed changes sharply.

In the McMaster algorithm, a flow-occupancy template is firstly developed, based on the historical flow-occupancy relationship during changes from congested to uncongested traffic state. The flow-occupancy template is then divided into four areas which represent different traffic conditions. Historical data are used to calibrate the boundaries of these four areas. The traffic states at two adjacent detector stations are used to detect incidents on the road section between the two detectors. A decision tree is used to detect incidents based on the traffic states at upstream and downstream detector stations.

The boundaries of different traffic state areas in the McMaster algorithm need to be calibrated individually at each traffic detector station because the flow-occupancy template varies across traffic detector stations. The implementation of the McMaster algorithm is limited by such excessive

calibration.

2.5.4.2 Fundamental Diagram based AID Algorithm

In the fundamental diagram (FD) based AID algorithm (Jin and Ran, 2009), two new traffic variables, uncongested and congested regime shifts (URS and CRS) are generated by conducting coordinate transformation on the traffic flow and occupancy. In the coordinate transformation, the flow-occupancy coordinate of a traffic state is projected to the URS-CRS coordinate. The URS and CRS were used for incident detection in the FD based algorithm.

The two new proposed variables were proved more sensitive and stable in detecting incident-induced traffic condition changes. Compared to the McMaster algorithm, the FD algorithm detects incidents based on the changes of the URS and CRS.

2.5.5 Artificial Intelligence based AID Algorithms

Artificial intelligence such as artificial neural network (ANN) and fuzzy logic techniques have been used for incident detection since 1990s. Several ANN based AID algorithms (Ritchie and Cheu, 1993; Cheu and Ritchie, 1995; Stephanedes and Liu 1995; Dia and Rose, 1997; Abdulhai and Ritchie, 1999; Adeli and Samant, 2000) and fuzzy logic based AID algorithms (Chang and Wang, 1994; Lin and Chang, 1998) were developed.

2.5.5.1 Artificial Neural Network based AID Algorithms

The Artificial Neural Network technique, inspired by the property of biological neural systems, was developed to simulate the reasoning and determination process of the human brain. ANN technique is capable of dealing with massive amounts of multi-dimensional data and has good predictive ability (Karlaftis and Vlahogianni, 2011).

The ANN comprises several simple processing elements which are used to receive input information. The input information is weighted by associated connection values to generate the computation results by a transfer function. The computation

results are then communicated to other processing elements in the next layer.

The ANN technique was firstly used for incident detection on freeways by Ritchie and Cheu (1993). The neural network is trained to distinguish the recurring and nonrecurring congestions. The commonly used ANNs in incident detection are multi-layer feed-forward (MLF) neural network (Ritchie and Cheu 1993; Cheu and Ritchie, 1995; Stephanedes and Liu, 1995; Dia and Rose, 1997) and probabilistic neural network (PNN) (Abdulhai 1996; Abdulhai and Rithchie, 1999).

The structure of the MLF neural network includes three layers: input layer, hidden layer and output layer (Black, 1997). Traffic data such as traffic speed and occupancy are often used as the inputs. The output of the ANN based AID algorithm is incident or incident-free.

Unlike the MLF based ANN algorithms, the PNN based ANN algorithms is capable of integrating the prior probability of incident occurrence, road conditions and the cost of misclassifying an incident.

The ANN based AID algorithms are used like a black box to detect incidents without priori knowledge and interpretation of the results. Insights on the data, incident occurrence process and incident effects are not required in the ANN based AID algorithms. The drawbacks of ANN based AID algorithms are the need for extensive data and substantial training. In addition, compared with other rule-based AID algorithms, the ANN based AID algorithms need longer MTTD to detect incidents.

2.5.5.2 Fuzzy Logic based AID Algorithms

Fuzzy logic technique deals with approximate reasoning rather than exact or precise reasoning. The fuzzy logic based AID algorithms can be used to detect incidents even when input traffic data are inexact or missing. Compared to other existing AID algorithms with sharp decisions (i.e. incident or not), the fuzzy logic based AID algorithms provide the probability of the presence of an incident. Several studies (Chang and Wang, 1994; Ishak and Al-Deek, 1997) were conducted to apply the fuzzy logic techniques in incident detection. The strength

of the fuzzy logic based AID algorithms is their ability to detect incidents based on incomplete data with good performance.

2.6 Probe Vehicle Based AID Algorithms

Most existing AID algorithms are fixed-location detector based algorithms. The point traffic data collected by fixed-location detectors, however, cannot provide the whole picture of traffic conditions on the road section. The point-to-point traffic data collected by probe vehicle technologies such as automatic vehicle identification (AVI) is thus used for incident detection. The journey time between adjacent traffic detectors collected by AVI technologies is usually used as the typical input for probe vehicle based AID algorithms including Texas algorithm (Balke et al., 1996), upper confidence limit algorithm, speed and confidence limit algorithm, and dual confidence limit algorithm (Hellinga and Knapp, 2000). Most AVI-based algorithms are statistical time series models.

2.6.1 The Texas Algorithm

The Texas algorithm was developed to detect freeway incidents based on the probe vehicle journey time (Balke et al., 1996). The probe vehicle journey time were collected from the reports by hundreds of probe vehicles equipped with cellar telephones. The premise of this algorithm is that the journey time after the incident significantly increases over the journey time normally experienced at the same time of the day under incident-free conditions. The mathematical model of the Texas algorithm is similar to that of the SND algorithm, but with different input data and different comparison benchmarks. The SND algorithm usually adopts fixed-location detector based traffic stream parameters such as traffic occupancy as inputs while the Texas algorithm adopts the probe vehicle based journey time as inputs. In the SND algorithm, the traffic stream parameter value at the current time interval is compared with the mean of traffic stream parameter values within previous several time intervals. In the Texas algorithm, however, the current traffic stream parameter value is compared with the expected value derived from historical values on the same time of a day and day of a week.

2.6.2 Confidence Limit Related Algorithms

Hellinga and Knapp (2000) developed three confidence limit related algorithms with the use of the journey time collected by the AVI technology used for electronic toll collection (ETC). These three confidence limit related algorithms include: (1) confidence limit algorithm, (2) speed and confidence limit algorithm, and (3) dual confidence limit algorithms.

The underlying assumption of these three confidence limit related algorithms is that the journey time experienced by vehicles over a road section increases more rapidly as a result of capacity change than as a result of demand change (Hellinga and Knapp, 2000). The journey time of a road section will increase when the capacity is reduced by a traffic incident on the road section in question. It is believed that the journey time characterized by mean and variance belong to different population before and after incident occurrence. An incident is detected if the obtained journey time lies outside the confidence limit.

2.6.2.1 Confidence Limit Algorithm

The time-dependent stochastic traffic condition in the confidence limit algorithm is characterized by mean and variance of mean interval journey time based on recently acquired data in a comparison window. It is assumed that the mean interval journey time is log-normally distributed. The log-normal mean [Eq. (2.25)] and variance [Eq. (2.26)] of the mean interval journey time within the comparison window are used to calculate the upper confidence limit [Eq. (2.27)].

$$\bar{\tau}_t = \frac{1}{n}\sum_{j=1}^{n}\tau_j \tag{2.23}$$

$$\mathrm{var}_t = \frac{1}{n-1}\sum\left(\tau_j - \bar{\tau}_t\right)^2 \tag{2.24}$$

$$\hat{\mu}_t = \ln\left(\bar{\tau}_t\right) - 0.5\sigma_t^2 \tag{2.25}$$

$$\hat{\sigma}_t^2 = \ln\left(1 + \frac{\mathrm{var}_t}{\bar{\tau}_t^2}\right) \tag{2.26}$$

$$UL_t = e^{(\hat{\mu}_t + z\hat{\sigma}_t)} \tag{2.27}$$

where τ_t = the journey time at time interval *t*; n = the number of time interval within the comparison window; $\overline{\tau}_t$, var_t = the mean and variance of all journey times within the comparison window at time interval *t*; $\hat{\mu}_t, \hat{\sigma}_t^2$ = the log-normal mean and variance of all journey time within the comparison window; *z* = *z* value corresponding to the level of confidence; UL_t = the upper confidence limit at time *t*. In operation, an incident is detected if the collected journey time exceeds the upper confident limit.

The confidence limit algorithm detects incidents by capturing the abnormal journey time variation. The journey time variation, however, can be a result of incident or recurring congestion. Therefore, the confidence limit algorithm may not distinguish the incident-induced congestion from the recurring congestion, leading to more false alarms.

2.6.2.2 The Speed and Confidence Limit Algorithm

The speed and confidence limit algorithm (Hellinga and Knapp, 2000) is an extension of the confidence limit algorithm, but with an additional traffic speed test. As described in Section 1.1, the traffic speed downstream of the incident spot is likely to increase after an incident occurs. In the speed and confidence limit algorithm, an incident is detected if the following two conditions are simultaneously satisfied: (1) the established confidence limit being exceeded by the mean interval journey time, and (2) the mean of vehicle traffic speeds within the comparison window being exceeded by the mean interval traffic speed downstream of the incident spot. The traffic speed can be collected by either fixed-location detectors or probe vehicle technologies.

2.6.2.3 The Dual Confidence Limit Algorithm

The difference between the confidence limit algorithm and dual confidence limit algorithm is the use of the comparison window. In the confidence limit algorithm, the comparison window always includes a fixed number of previous time intervals

regardless of the detection results. The journey time data which exceed the confidence limit, however, are not statistically part of the comparison window population and thus should not be included in the following comparison window. In the dual confidence limit algorithm, two confidence limits are established: (1) window limit and (2) alarm limit. The comparison window moves forward by one time interval only if the calculated mean interval journey time at the forthcoming time interval, does not exceed the window limit. An alarm is triggered if the calculated mean interval journey time at the forthcoming time interval, exceeds the alarm limit.

2.6.3 The Mobile Sensor and Sample-based Algorithm

The mobile sensor and sample-based (MOSES) algorithm (Cheu et al., 2002) detects incidents by capturing the statistical difference between the mean section journey time from two sets of probe vehicle samples before and during an incident. The difference between the mean section journey time from two sets of samples is identified with a one tail hypnosis test in Eq. (2.28). If the condition in Eq. (2.28) is met, an incident alarm will be triggered.

$$\frac{\overline{T}_1 - \overline{T}_2}{\sqrt{\frac{(n_1-1)s_1^2+(n_2-1)s_2^2}{n_1+n_2-2}\left(\frac{1}{n_1}+\frac{1}{n_2}\right)}} > t_{\alpha,n_1+n_2-2} \tag{2.28}$$

where n_1 = the number of most recently observed probe vehicles; n_2 = the number of probe vehicles that has exited the section just before the n_1 probe vehicles; T_1, T_2 = the mean section journey time of two samples; s_1, s_2 = the standard deviates of the journey time of the two samples; t_{α,n_1+n_2-2} is the t-statistic with tail-end probability of α and n_1+n_2-2 degrees of freedom.

Cheu and Tay (2004) also investigated the performance of the MOSES algorithm under conditions of different probe vehicle penetration rates and three probe vehicle aggregation methods. These probe vehicle data aggregation methods include (1) fixed sample size, (2) fixed time interval, and (3) rolling interval. It was

found that different probe vehicle data aggregation methods have their own advantages within different probe vehicle penetration rate intervals. When the penetration rate exceeds 30%, the fixed time interval data aggregation methods would generate a high DR, lowest number of false alarms and fastest MTTD. The penetration rate of probe vehicles which equipped with AVI tags in Hong Kong is about 40%. Therefore, the fixed time interval data aggregation method is used in this research.

2.7 Sensor Fusion Based AID Algorithms

Point traffic data collected by fixed-location detectors and point-to-point data collected by probe vehicle technologies both have strengths and weaknesses. However, the development of AID algorithms based on integrated data collected is expected to be more reliable and effective. Several AID algorithms have been developed to detect incidents with the use of integrated data from multiple data sources (Westerman et al., 1996; Ivan and Sethi, 1998; Dia and Thomas, 2011).

Westerman et al. (1996) integrated the traffic data collected by both fixed-location detectors and probe vehicle technologies to estimate the journey time and detect incidents. This sensor fusion based algorithm adopts a parallel structure in which probe vehicle based algorithms and fixed-location detector based algorithms perform independently. The detection results in terms of incident probability of these two types of sub-algorithms (a probe vehicle based algorithm and a fixed-location detector based algorithm). They are then integrated through the weighting method to make a final decision on the incident occurrence.

Ivan and Sethi (1998) attempted to combine fixed-location detector based and probe vehicle based data for incident detection on urban arterial roads. Two fusion approaches were proposed, in order to combine the two types of traffic data: (1) to directly process input data from multiple data sources, and (2) to process the outputs of single algorithms designed to detect incidents based on a single data source. The processing method can be based on a neural network or statistical methods.

Dia and Thomas (2011) developed an ANN based AID algorithm for incident

detection on urban arterial roads, based on simulated data from inductive loop detectors and probe vehicles. Several data fusion neural network structures were analyzed and their incident detection performances compared. The optimal probe vehicle penetration rate and loop detector configuration which resulted in the best incident detection performance are identified.

2.8 Factors Influencing the Detection Performance of AID Algorithms

The incident detection performance of AID algorithms is influenced by many factors. Weil et al. (1998) summarized these influencing factors as: (1) operating traffic conditions such as preincident traffic flow conditions, (2) road configurations such as on/off ramps, (3) environmental factors such as rainfalls, (4) incident duration, (5) incident severity, (6) detector spacing, (7) incident location, (8) topography features such as slope and other factors.

Because the incident detection performance relies on the adopted detection thresholds, thus detection thresholds are affected by the factors given above. The detection threshold (T) can be formulated by a generalized model as shown in Eq. (2.28). It should be noted that some factors can be easily quantified such as the preincident traffic flow, traffic speed and rainfall intensity, whereas others such as road configurations, are difficult to quantify.

$$T = f\left(v, q, r.....\right) \tag{2.29}$$

where v = the traffic speed (km/h); q = the traffic flow (or traffic volume) (veh/h/lane); r = the rainfall intensity (mm/h).

Although the generalized detection threshold function is of great use in the threshold determination, it is not easy to calibrate the exact numerical function because of many reasons such as those given below:

(1) Some factors interact and are self-correlated. For instance, rainfall intensity which affects the detection threshold, also has an influence on the preincident traffic flow condition.

(2) Some factors lack observed data for analysis. For instance, incident duration is sometimes not recorded in the incident database. It is not easy to fully consider the effects of incident duration on detection thresholds with no incident duration data.

(3) Some factors are too complex to be included in the generalized detection threshold function. For instance, road configurations include numerous aspects such as on/off ramps, number of lanes and lane width. It is not easy to consider exactly all aspects of road configurations for detection threshold determination.

These influencing factors cannot be all considered in the development of one single AID algorithm because the impact mechanism of these factors on detection thresholds is complicated. A sophisticated AID algorithm that can be adapted to all of these influencing factors remains difficult to develop.

2.8.1 Preincident Traffic Flow Condition

The magnitude of incident-induced traffic disturbance obviously varies under different traffic flow conditions. The variation of incident-induced traffic disturbance may lead to different vehicle maneuverable flexibilities during an incident (Mak and Fan, 2006a). It is thus sensible for the preincident traffic flow condition to be incorporated into the detection framework. The AID algorithms with consideration of the preincident traffic flow condition are usually named as flow-based or flow-dependent algorithm.

In the flow-dependent AID algorithm (Mak and Fan, 2006a), different detection thresholds are adopted under different preincident traffic flow conditions. This is because the response time and magnitudes of incident-induced traffic disturbances vary under different preincident traffic flow conditions. The single detection threshold thus cannot be adapted to capture all incident-induced traffic disturbances under different preincident traffic flow conditions. It is reasonable to adopt different detection thresholds under different preincident traffic flow conditions to improve the incident detection performance.

2.8.2 Rain Condition

Rainfall has effects on the occurrence of incidents. A recent study about the temporal and spatial effects on road traffic accidents in Hong Kong found the number of traffic accidents increases with the rainfall intensity (Li et al., 2012). Traffic accidents occur mostly during the first hour of rain and the first hour after rain. This can be explained by the sudden change of the road environments.

The effects of rainfalls on incident detection performance have not been investigated. However, it has been noted that different degrees of rainfall intensity have different effects on key traffic stream parameters (e.g. free-flow speed and capacity) and traffic speed-flow-density relationship.

It was revealed that jam densities on freeways are not affected by rainfall (Rakha et al., 2008; Billot et al., 2009), but free-flow speeds, speeds at capacity and capacities (or maximum flows) were found to decrease with the increasing rainfall intensity (Unrau et al., 2006; Agarwal et al., 2006; Rakha et al., 2008; Billot et al., 2009). Table 2.4 shows the reductions on key traffic stream parameters for different categories of rainfall intensity in previous studies.

Table 2.4 Reductions of Key Traffic Stream Parameters for Different Categories of Rainfall Intensity

Author and year	Road type	Speed limit (km/h)	Rainfall intensity (mm/h)	Reduction of free-flow speed	Reduction of speed at capacity	Reduction of capacity (maximum flow)	Reduction of jam density
HCM (2000)	Freeway	-	Light	1.9%	-	Minimal	-
			Heavy	4.8%-6.4 %		14%-15%	
Unrau et al. (2006)	Urban expressway	90	(0.1, 2.4)	10%	-	-	-
			(2.4,∞)	-			
Agarwal et al. (2006)	Freeway	90	**(0, 0.26]**	**1%-2%**	-	**1%-3%**	-
			(0.26, 6.35]	**2%-4%**		**5%-10%**	
			(6.35,∞)	4%-7%		10%-17%	
Rakha et al. (2008)	Freeway	140	(0, 0.25]	2%-3.6%	8%-10%	10%-11%	0%
			(0.25, 6.4]	-	-		
			(6.4,∞)	6%-9%	8%-14%		
Billot et al. (2009)	Freeway	110	(0, 2]	8%	-	18.5%	0%
			(2, 3]	12.6%		21%	

Note: '-'represents that such information was not mentioned in the corresponding study. The values in the bracket, e.g., (a, b], denote those are > a and ⩽ b.

As shown in Table 2.4, the free-flow speeds, speeds at capacity and capacities on freeways decreased under rain conditions. For instance, the reduction rate of the free-flow speed increases from 1%-2% to 2%-4% when the rainfall intensity increases from (0, 0.26] to (0.26, 6.35] mm/h. Meanwhile, the reduction rate of the capacity also increases from 1%-3% to 5%-10%. It appears that highway speed limits were related to the reductions of the key traffic stream parameters. The correlation between them, was not significant.

In a recent study by Lam et al. (2013), a generalized speed-flow function and a generalized speed-density function were proposed. The effects of rainfall intensity (mm/h) on free-flow speed were also modeled by taking into account these two generalized functions. Traffic and rainfall intensity data were collected on a study road section in Hong Kong and used to calibrate and validate the two proposed generalized functions. The modeled free-flow speed function with rainfall intensity effects is shown in Eq. (2.29).

$$v_f(r) = \exp(-0.044 \cdot r^{0.296} + 4.260) \tag{2.30}$$

where $v_f(r)$ = the free-flow speed (km/h) with rainfall intensity effects; r =

the rainfall intensity (mm/h).

The generalized speed-flow function and the generalized speed-density function with rainfall intensity effects are shown in Eq. (2.30) and Eq. (2.31), respectively.

$$q = 58.173 \cdot v \cdot \left(4.260 - 0.044 \cdot r^{0.296} - \ln v\right)^{0.626} \tag{2.31}$$

$$v = \exp\left[-0.044 \cdot r^{0.296} + 4.260 + 0.633 \cdot \left(\frac{d}{43.784}\right)^{1.594}\right] \tag{2.32}$$

where v = the space mean speed (km/h); q = the traffic flow (veh/h/lane); d = the traffic density (veh/km/lane); r =the rainfall intensity (mm/h).

Fig. 2.3 illustrates the calibrated traffic speed-flow relationships for various rainfall intensities (Lam et al., 2013).

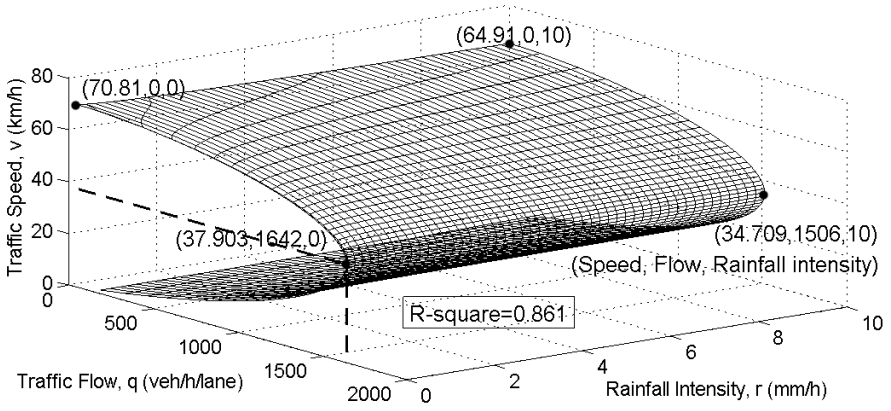

Fig. 2.3 Calibrated generalized traffic speed-flow relationships for various rainfall intensities

As shown in Fig. 2.3, the free-flow speed decreased from 70.81 km/h to 64.91 km/h as the rainfall intensity increased from 0 mm/h to 10 mm/h. Meanwhile, the speed at capacity was also reduced from 37.903 km/h to 34.709 km/h with the increasing rainfall intensity. As the rainfall intensity increased, the capacity (or maximum flow) was reduced from 1642 veh/h/lane to 1506 veh/h/lane.

Fig. 2.4 presents the calibrated traffic speed-density relationships for various rainfall intensities (Lam et al., 2013).

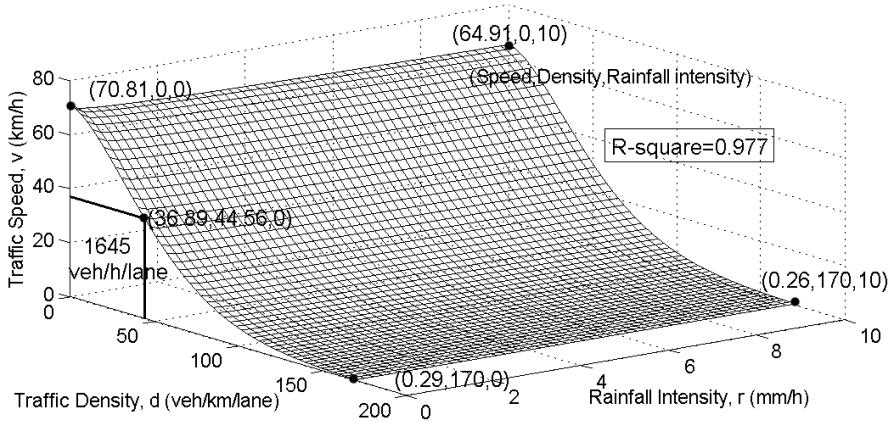

Fig. 2.4 Calibrated generalized traffic speed-density relationships for various rainfall intensities

It is seen in Fig. 2.4 that the free-flow speed decreased from 70.81 km/h to 64.91 km/h when rainfall intensity increased from 0 mm/h to 10 mm/h. The jam density remained 170 veh/km/lane as the rainfall intensity increased.

The key traffic stream parameters and traffic speed-flow-density relationships change with various rainfall intensities. This may result in corresponding changes in traffic conditions, and affect the overall incident detection performance of AID algorithms. The development of new AID algorithms which can adapt to various preincident traffic flow and rain conditions would therefore, be of value.

2.9 The Experience in the Deployments of Existing AID Algorithms

Various AID algorithms have been developed over the last four decades, and some of them have been implemented on freeways and urban roads. Several national wide surveys were conducted in the United States to investigate AID algorithm deployments in practice (Parkany and Xie, 2005; Williams and Guin, 2007). Several studies (Balke, 1993; Hass et al., 2001; Mahmassani et al., 2001; Martin et al., 2001) were also conducted to evaluate the existing AID algorithms based on

either simulated or collected traffic data on specific freeways and urban roads.

Parkany and Xie (2003) conducted a national wide survey on the implementation of AID algorithms across the United States in 2001. Survey data such as implemented data collection technologies and algorithm evaluation results, were collected from 29 transportation management centers and transportation operation centers. The types of data collection technologies, types of traffic stream parameters, and types of data communication mediums were summarized and analyzed. It was found that probe vehicle data collection technologies are less in use compared to fixed-location detectors. Half operators were not satisfied with the implemented data collection technologies due to (1) troublesome installation, (2) frequent malfunction, (3) low accuracy, and (4) high maintenance cost.

Additionally, the implemented AID algorithms were evaluated and their strengths and weaknesses analyzed. Several insightful findings were concluded on the basis of the algorithm evaluation results provided by the responders (Parkany and Xie, 2005):

(1) Manual incident detection methods such as CCTV surveillances and witness calls still remained as the principle means to detect or verify traffic incidents, due to the high FAR, low DR and the long MTTD of AID algorithms.

(2) Most operators prefer AID algorithms specifically developed for local traffic conditions to generalized AID algorithms because of the latter's poor transferability.

(3) AID algorithms are effective mainly for more serious incidents or incidents occurred close to traffic detectors. In general, traffic incidents are usually detected by manual incident detection methods first.

Another national wide survey in the United States was also conducted by Williams and Guin (2007) to investigate the current status of incident detection and reasons for limited AID algorithm implementation. About seventy percent of respondents thought the incident detection capacities to be insufficient. The unacceptably high FAR was also regarded as the main reason for performance dissatisfaction. The findings of this survey also addressed the need to develop more robust and

effective AID algorithms with the use of existing data collection infrastructures.

2.10 Summary

A number of studies in literatures related to automatic incident detection (AID) have been reviewed in this Chapter. The data collection technologies, algorithm categorization, and algorithm development are summarized explicitly. In addition, several typical existing AID algorithms in each category are reviewed in detail.

Evaluative research example results and the findings from the review of relevant literatures are summarized below:

(1) The development of AID algorithms involves data collection and mathematical modeling. Different combinations of the data collection technology used and mathematical model applied result in different types of AID algorithms. These AID algorithms can be categorized according to certain criteria such as types of data collection technology used, mathematical model applied, and number of traffic detectors used.

(2) The incident detection performance of AID algorithms is affected by the quality of input data. Fixed-location traffic detectors and probe vehicle technologies are usually used to collect traffic data. Frequent malfunctions, troublesome installation and high maintenance cost are the negative aspects of traffic detectors encountered in application.

(3) Several AID algorithms have been developed and implemented in past decades. These AID algorithms were developed for their own application and specific conditions such as road type, data collection infrastructure, and available data. It is not feasible to compare incident detection performances of these AID algorithms in a consistent environment.

(4) Every AID algorithm has its own strength and weaknesses. No AID algorithm, however, can be applied to all types of roads and traffic conditions. It is difficult to apply the same AID algorithm to different roads or different traffic conditions, without recalibration or modification.

(5) The detection rate (DR), false alarm rate (FAR) and mean time to detect

(MTTD) are principal performance measurements of AID algorithms. A trade-off between the three primary performance measurements exists. The target for all AID algorithms is to achieve a high DR, a low FAR and a short MTTD. The detection thresholds have to be carefully calibrated to balance the trade-off between the three sub-targets.

(6) The incident detection performances of the existing AID algorithms are not satisfactory when implemented on roads in practice. These AID algorithms have many problems such as high FAR, long detection and verification time, troublesome calibration, large historical database, performance instability, and poor transferability.

(7) Several factors have effects on the detection thresholds which are directly related to incident detection performance. These influencing factors include: preincident traffic flow conditions, weather conditions such as rainfalls, detector spacing, the distance between the incident spot and adjacent traffic detectors. Some of these factors, such as the preincident traffic flow condition, are easily quantified and have been considered for detection threshold determination. Some of the other factors, however, are difficult to be quantified or have insufficient related data for investigation. Rain conditions were found affects the road traffic flow and thus should be considered in the development of AID algorithms.

(8) Generally, fusion methods have been used in the development of more robust and effective AID algorithms. Data fusion and algorithm fusion are two of the typical fusion methods used. Traffic data collected by different technologies, however, have individual strengths and weaknesses. Different traffic stream parameters also respond differently to traffic incidents in both time and magnitude. Therefore, it is reasonable for AID algorithms to adopt multiple traffic stream parameters collected by both fixed-location detectors and probe vehicle technologies. The incident detection results of different AID algorithms can also be fused to determine the incident presence while combining the merits of individual algorithms.

(9) In the previous flow-dependent AID algorithms, different detection thresholds

are specifically adopted under low, medium and heavy preincident traffic flow conditions. In other words, detection thresholds are a step function in preincident traffic flow data. The discrete detection thresholds, however, are sometimes found to be unreasonable in practice. The detection threshold suffers a value jump when the preincident traffic flow value approaches the critical values used to categorize traffic flow conditions (i.e. low, medium and heavy flow conditions). A continuous detection threshold which is also related to the preincident traffic flow, is more reasonable in practice. The AID algorithms with generalized continuous detection thresholds is thus of great value for incident detection. The calibration of the AID algorithm with generalized continuous detection thresholds needs a large traffic and incident database.

Thus, a promising solution for incident detection is to develop AID algorithms in which:

(1) Multiple traffic data from different data sources (e.g. fixed location detector and probe vehicle technology) are used to improve the incident detection performance.

(2) Traffic data collected by the existing data collection infrastructures are used to provide a satisfactory incident detection performance without installing more expensive traffic detectors.

(3) An adaptive detection logic is used to detect incidents under both no-rain and rain conditions.

In Chapter 3, the development of an AID algorithm to detect incidents, is presented. The incident detection under no-rain and rain conditions is likewise investigated and presented in Chapter 4 and Chapter 5, respectively.

Chapter 3. Extended Standard Normal Deviate (ESND) Algorithm

3.1 Introduction

A new extended standard normal deviate (ESND) algorithm is proposed and described in this Chapter. The proposed ESND algorithm is an extension of the widely used standard normal deviate (SND) algorithm (Dudek et al., 1974). The SND algorithm is not difficult to calibrate and also has good transferability. This algorithm is modified by the addition of two extensions. Two new proposed traffic stream parameters together with traditional traffic stream parameters are used to be inputs for the proposed ESND algorithm.

3.2 Extended Standard Normal Deviate (ESND) Algorithm

The previous SND algorithm is modified with two extensions. In the first extension, the weighting method is adopted to enhance the reliability of incident detection results. In the previous SND algorithm, traffic stream parameter values of every time interval within sampling periods are averaged equally for calculating their means and standard deviates. However, the relative importance of traffic stream parameter values in different time intervals varies because they are derived from different numbers of data points.

In the second extension, the variation of input data within sampling periods is restricted. In the previous SND algorithm, the non-incident-induced acute fluctuation of the SND values may cause many false alarms making it difficult to calibrate the detection thresholds. The acute fluctuations of the SND values are often caused by the small standard deviates which are used as the denominators in calculating SND values. Therefore, it is reasonable to avoid a small standard deviate by restricting the variation of input data within sampling periods. The coefficient of variation, which is a statistical measure of the dispersion of data points in a data series around the mean, is used to represent the variation of input

data within sampling periods. Eqs. (3.1) - (3.4) show the calculation process of the modified SND value of a particular traffic stream parameter at every time interval.

$$\bar{\lambda}_t^w = \frac{\sum_{j=t-1}^{t-n} w_j \lambda_j}{\sum_{j=t-1}^{t-n} w_j} \tag{3.1}$$

$$\sigma_t^w = \sqrt{\frac{\sum_{j=t-1}^{t-n} w_j \left(\lambda_j - \bar{\lambda}_t\right)^2}{\frac{\left(n'-1\right)\sum_{j=t-1}^{t-n} w_j}{n'}}} \tag{3.2}$$

$$CV_t = \frac{\sigma_t^w}{\bar{\lambda}_t^w} \tag{3.3}$$

$$SND_t^{'} = \begin{cases} \dfrac{\lambda_t - \bar{\lambda}_t^w}{\sigma_t^w} & \left(CV_t \geq \theta\right) \\ SND_{t-1}^{'} & \left(CV_t < \theta\right) \end{cases} \tag{3.4}$$

where n = the number of time intervals over the sampling period prior to the current time interval t; n' = the number of time intervals in which the traffic data values are not equal to zero over the sampling period; λ_j = the input traffic stream parameter at time j; w_j = the weight of λ_j; $\bar{\lambda}_t^w$, σ_t^w = the respective weighted average and weighted standard deviate of λ_j over the sampling period prior to time t; CV_t = the coefficient of variation of λ_j over the sampling period prior to time t; $SND_t^{'}$, $SND_{t-1}^{'}$ = the modified standard normal deviates of input traffic stream parameter at time t and t-1, respectively; and θ = the predetermined threshold for CV_t.

In the proposed ESND algorithm, the traffic count (q, veh/h/lane) of each time interval is used as the weight when calculating the weighted average and weighted standard deviate of λ_j over the previous sampling period.

In the ESND algorithm, Eqs. (3.1) and (3.2) are used to calculate the weighted average and weighted standard deviate of a particular traffic stream parameter within sampling periods. The coefficient of variation of the traffic stream parameter within sampling periods at each time interval is calculated by Eq. (3.3). If the coefficient of variation of the traffic stream parameter exceeds the predetermined detection threshold, the modified SND value of this traffic stream parameter at the current time interval can be calculated by Eq. (3.4). Otherwise, the modified SND value of the traffic stream parameter at the current time interval is replaced by that at the previous time interval. The modified SND is then compared with the predetermined detection threshold for incident detection.

The SND algorithm is a special case of the proposed ESND algorithm when (1) the weights of input traffic stream parameters are equal, and (2) the variation of the input traffic stream parameters within the comparison window is not restricted.

3.3 An Illustrative Example for Incident Detection with the Proposed Algorithm

An incident which occurred on the Hong Kong road network was selected for analysis to justify the two extensions in the proposed ESND algorithm. Fig. 3.1 presents the location of the selected serious incident and its adjacent video traffic detectors. This incident occurred at 18:25 on 5th Oct, 2010 on Kwun Tong Road in the direction from west to east. The distance between the upstream and downstream video traffic detectors are approximately 2.01 km. The distance between the incident spot and its upstream video traffic detectors is about 1.65 km.

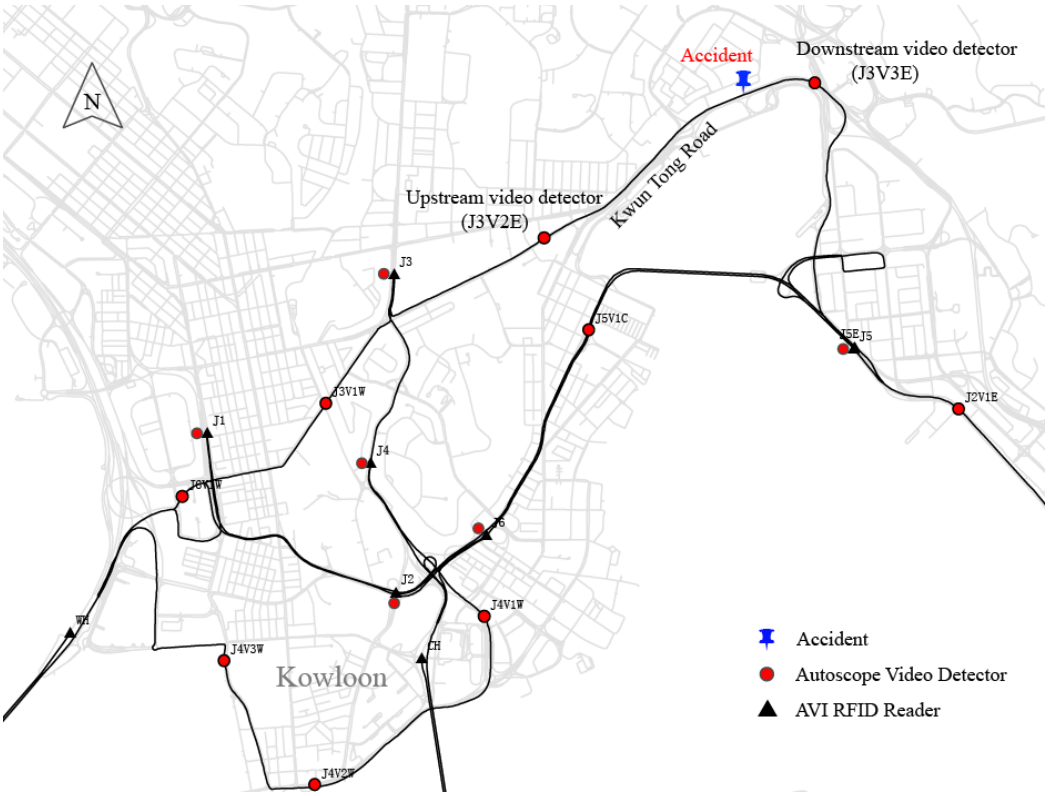

Fig. 3.1 Locations of the selected traffic incidents

The traffic data collected by video traffic detectors include time mean speeds, space mean speeds, variances of time mean speeds, variances of space mean speeds and traffic counts. Occupancy data are not archived in the JTIS database. The space mean speeds in the JTIS database, however, are estimated based on the relationship between time mean speeds and space mean speeds derived by Wardrop (1952). The length of detection zones of Autoscope video traffic detectors was set to be 20 m for various locations. Therefore, the varied length of detection zones would not affect the time mean speed accuracy and hence space mean speeds. Additionally, the vehicle speeds are assumed to be constant along a short road section when converting the time mean speeds to space mean speeds. The instantaneous journey time is estimated by fusing the real-time AVI data, the off-line journey time estimates and the spatial variance-covariance relationships of link journey times (Tam and Lam, 2011).

Traffic data prior to and after 1 hour of the selected incident at its upstream video traffic detector station (i.e. detector J3V2E) were extracted from the Journey Time Indication System (JTIS) database. These traffic data include space mean speeds (v, km/h), traffic counts (q, veh/2-min/lane) and variances of space mean speeds

[*var*, (km/h)^2], averaged across the detected traffic lanes at 2-min intervals. The 2-min traffic counts were transferred to equivalent hourly traffic flow (*q*, veh/h/lane). The time series of traffic speed, prior to and after the occurrence of the selected incident is shown in Fig. 3.2.

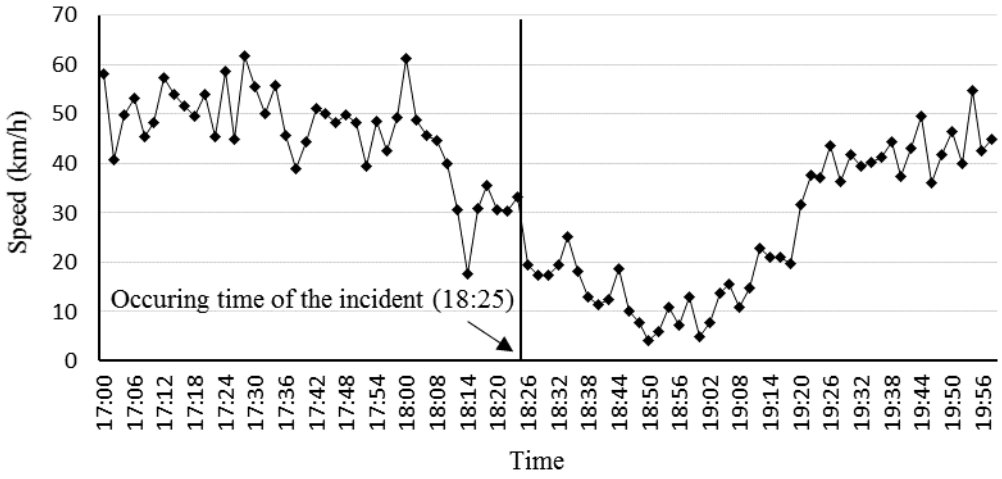

Fig. 3.2 Time series of traffic speeds prior to and after the occurrence of the selected traffic incident

The traffic speed SND values and ESND values were calculated by the SND algorithm and proposed ESND algorithm respectively. In the calculation, the number of time intervals over the sampling period prior to the incident (n) was assumed to be equal to 5. The traffic counts (q_i, veh/2-min/lane) collected by the video traffic detectors are used as the weights of the space mean speeds (v_i) within the sampling period.

Fig. 3.3 shows the time series of calculated SND and ESND values without the restriction of the variation of the input traffic stream parameters within the comparison window.

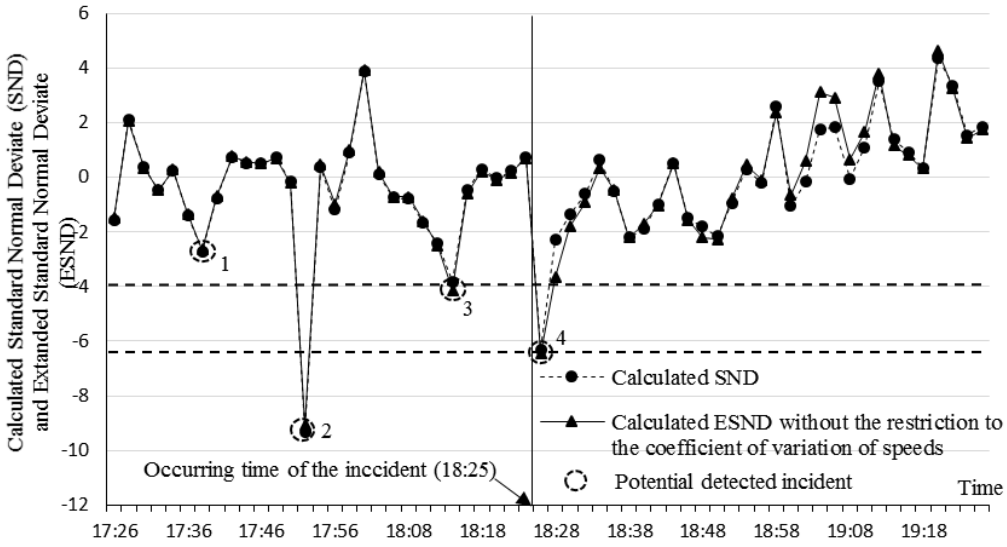

Fig. 3.3 Time series of the calculated SND and ESND values without restriction to the coefficient of variation of speeds within the comparison window

It can be seen from Fig. 3.3 that when the coefficient of variation of speeds within the comparison window is not restricted, the SND and ESND time series are almost the same as those before the incident. Four ESND values (i.e. the data points in circles in Fig. 3.3) are small enough to be used to indicate a potential incident. In order to detect the selected incident and keep false alarms as few as possible, the detection threshold has to be set to values between about -4 and -6.2. A false alarm, however, is likely to be caused by the acute ESND value at around 17:52 (i.e. the data point No. 2 in Fig. 3.3).

The detection threshold for coefficient of variation of input traffic stream parameter (θ) was then set to be 0.1. In other words, the standard deviate of the speeds within the comparison window should not exceed 10% of the mean speed. The time series of the calculated SND and ESND values when θ = 0.1 are presented in Fig. 3.4 for comparison.

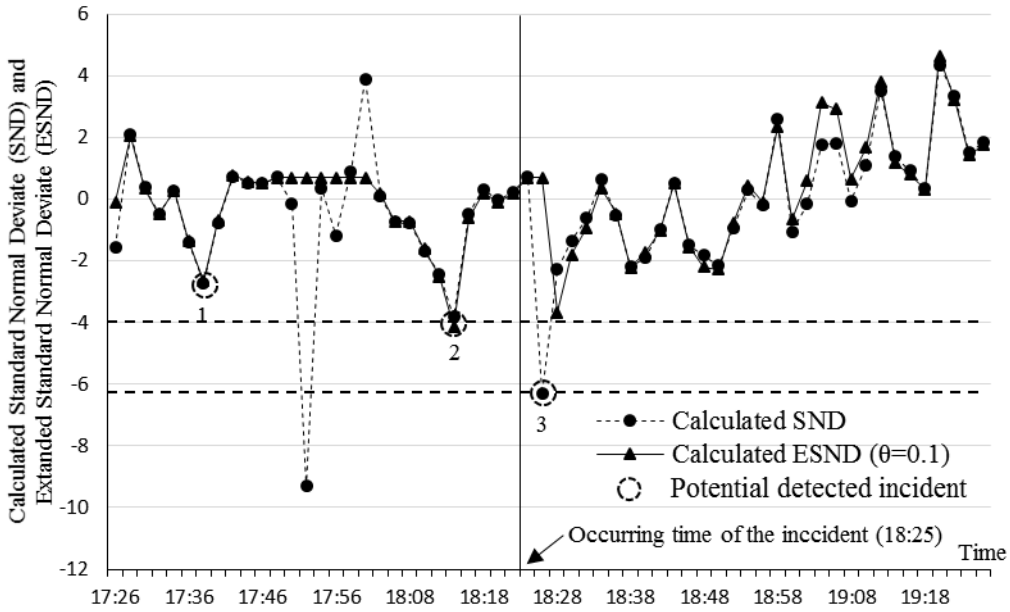

Fig. 3.4 Time series of the calculated SND and ESND values when θ=0.1

Only three ESND values (i.e. the data points in circles in Fig. 3.4) are small enough to be used to indicate the potential incident. Compared to the ESND values when θ=0, the ESND time series values when θ=0.1 are smoother and have fewer acute fluctuations. When the detection threshold is set to be values between about -4 and -6.2, the selected incident can be detected with no false alarms. Thus the restriction of variation of input data within sampling periods reduces the non-incident-induced acute fluctuation of traffic stream parameters, and hence reduces false alarms.

Fig. 3.5 presents the time series of calculated SND and ESND values when θ=0.2.

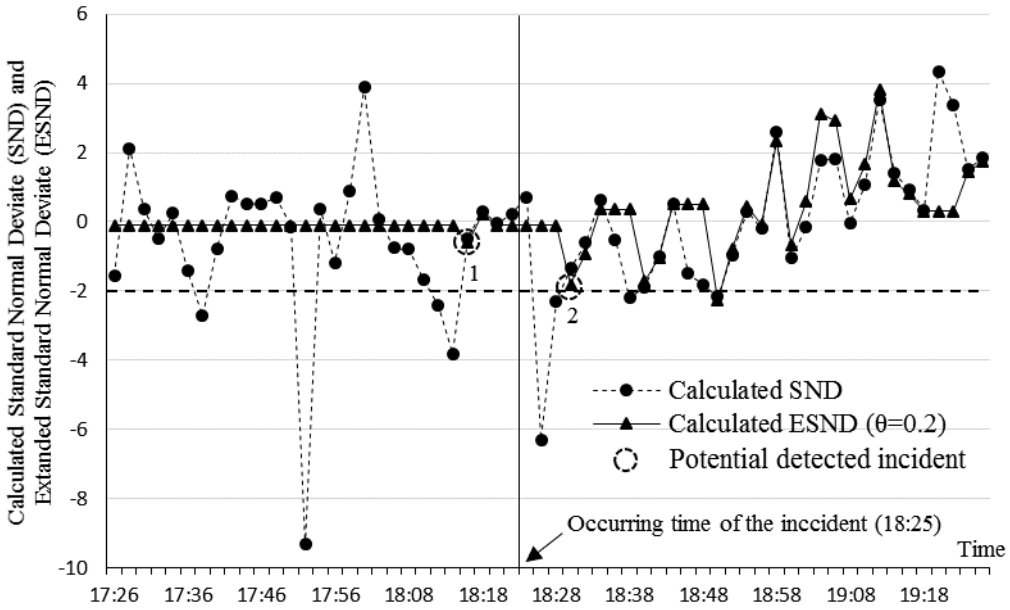

Fig. 3.5 Time series of calculated SND and ESND values when θ=0.2

It can be seen from Fig. 3.5 that only two acute ESND values (i.e. the data points in circles in Fig. 3.5) exist before the incident occurring time when θ=0.2. The selected incident can be detected when the detection threshold is set to be values between -0.5 and 2. There is a delay, however, when the selected incident is detected by the proposed ESND algorithm with a larger θ. In addition, the acute ESND values after the incident occurring time may also increase the number of false alarms.

Both the time series of calculated SND and ESND values when θ=0.3 are presented in Fig. 3.6.

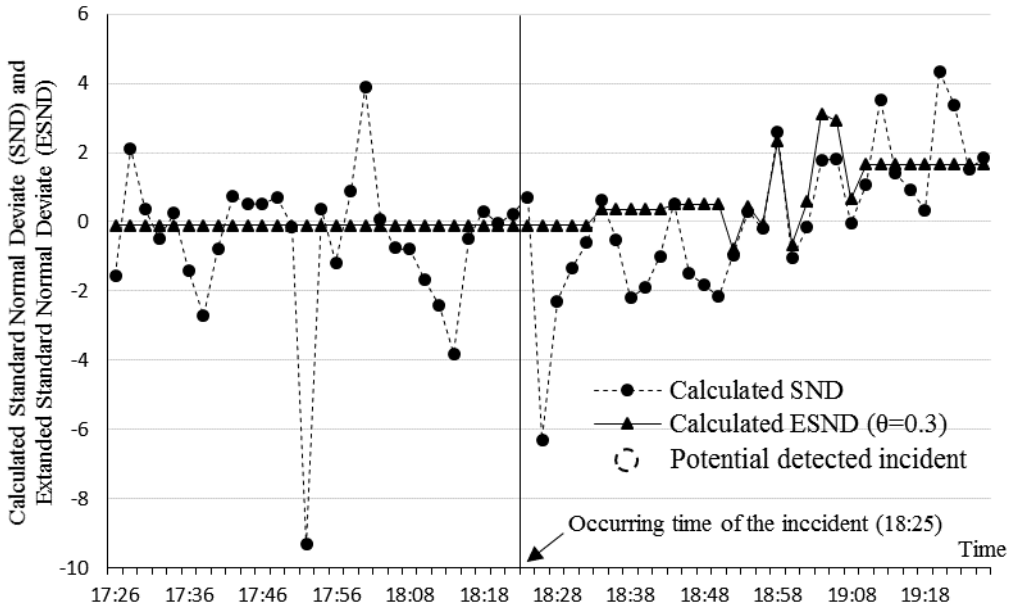

Fig. 3.6 Time series of calculated SND and ESND values when θ=0.3

No significantly small ESND values are found when θ=0.3 (Fig. 3.6). In other words, the selected incidents cannot be detected when θ=0.3, indicating that too large a detection threshold for coefficient of variation of input traffic data (θ) would potentially smooth the time series of ESND value to too great an extent.

3.4 Input Data of the Proposed Algorithms

In addition to commonly used traffic stream parameters such as the speed and occupancy, two new traffic stream parameters are proposed as traffic incident indicators: (1) the coefficient of variation of speed (CVS) at the upstream detector, and (2) the correlation coefficient of speeds (CCS) of two adjacent detectors. The input data of most AID algorithms in previous studies are the means of traffic stream parameters in every aggregate time interval. The proposed CVS at the upstream detector, however, describes the variation of upstream speeds of incidents. The CCS of two adjacent detectors represents the opposite trend of changes of both upstream speeds and downstream speeds over time.

Different traffic stream parameters respond to traffic incidents differently in both time and magnitude (Corby and Saccomanno, 1997). Hence, it is important to select the most appropriate traffic stream parameters as the inputs for the proposed algorithms. An analysis was conducted for the selection of proper input traffic

stream parameters.

3.4.1 New Proposed Traffic Stream Parameter I: Coefficient of Variation of Speed at the Upstream Detector

The coefficient of variation of speed (CVS), which is the quotient of standard deviate of speed and average speed, is used as a crash precursor of the real-time crash prediction model. The CVS has been found to better reflect the variation of traffic speed as opposed to the variance of speed (Lee et al., 2003).

When parts of traffic lanes are blocked by a traffic incident, the vehicles following in the blocked lanes may decelerate or change paths to neighboring unblocked lanes. Meanwhile, other vehicles on the unblocked lanes may also decelerate to pass the incident spot. In other words, the traffic stream at the upstream of a traffic incident may change from the almost homogeneous pattern to stop-and-go pattern. This change may result in an increase in the traffic speed variations at the upstream detector of a traffic incident. Therefore, the CVS at the upstream detector can be used to detect incident-induced traffic disturbances.

The variance of speed obtained from detectors has seldom been used for incident detection in previous studies. However, variance of speed, compared to traffic mean speed, flow and occupancy gives new important information about the traffic stream. The variance of speed can indicate whether the traffic stream is in a homogeneous pattern or stop-and-go pattern. Ignorance of the composite features of variance of speed may affect the incident detection performances. The adoption of the CVS at the upstream detector enables advantage to be taken of the variance of speed in incident detection. The detection of the selected incident described in Section 3.3 is used to justify the use of the CVS at the upstream detector as an incident indicator. Detailed information about this selected incident has been given in Section 3.3. As shown in Fig. 3.7, the CVS at the upstream detector of the selected incident began to increase after the incident occurred, proving that the CVS can be used as an indicator of incident-induced traffic disturbances.

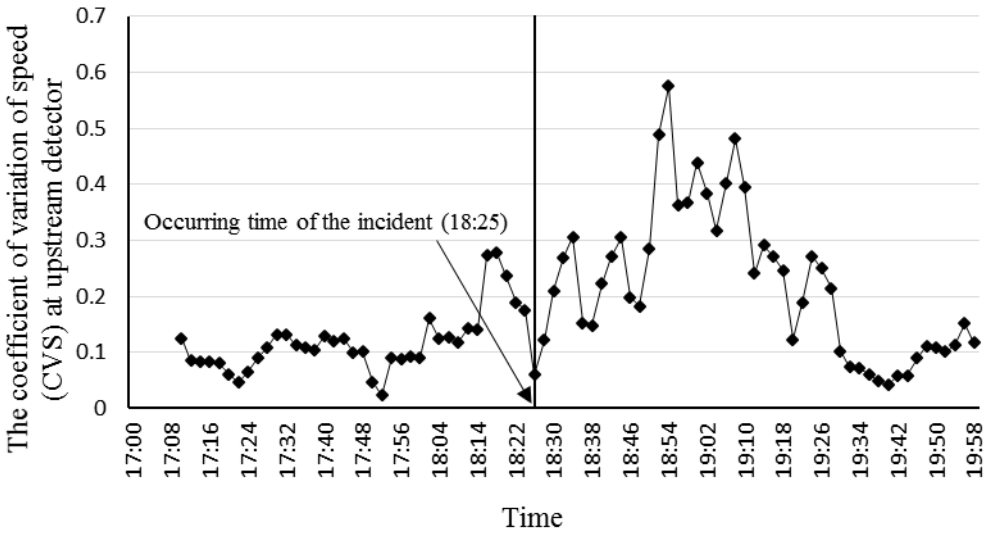

Fig. 3.7 Time series of the coefficient of variation of speed (CVS) at the upstream detector

The availability of the variance of speed data at 2-min time intervals makes it possible to evaluate the feasibility of adopting the CVS at the upstream detector as an AID algorithm input.

3.4.2 New Proposed Traffic Stream Parameter II: Correlation Coefficient of Speeds of Two Adjacent Detectors

The correlation coefficient of speeds (CCS) of two adjacent detectors is a measure of the degree in which the speeds at upstream and downstream detectors simultaneously change. The CCS of two adjacent detectors is defined as the covariance of speeds at both upstream and downstream detectors divided by the product of their standard deviates.

Because the CCS calculation is based on the time series of upstream speeds and downstream speeds in a sampling period, the CCS can capture the opposite trend of changes in both speeds over time. An incident may simultaneously result in a decrease of upstream speed and an increase of downstream speed, causing a decrease in the CCS of two adjacent detectors.

Therefore, the CCS of two adjacent detectors can be used as a traffic incident

indicator. Instead of absolute or relative upstream and downstream speed differences, the CCS of two adjacent detectors is able to simultaneously measure both the magnitude and direction of the upstream and downstream speed changes.

The CCS of two adjacent detectors at a specific time interval is calculated by Eq. (3.5) based on the paired time series of upstream and downstream speeds over a sampling period. The sampling period contains a few time intervals prior to and including the specific time interval.

$$CCS_t = \frac{1}{n\text{-}1}\sum_{j=t}^{t\text{-}n+1}\left(\frac{v_{u,j} - \overline{v}_{u,t}}{\sigma_{u,t}}\right)\left(\frac{v_{d,j} - \overline{v}_{d,t}}{\sigma_{d,t}}\right) \tag{3.5}$$

where CCS_t = the correlation coefficient of speeds of two adjacent detectors at time t; n = the number of time intervals in the sampling period; $v_{u,j}$, $v_{d,j}$ = the respective traffic speeds at upstream and downstream detectors at time j; $\overline{v}_{u,t}$, $\overline{v}_{d,t}$ = the sample average speeds at the respective upstream and downstream detectors, over a sampling period of n intervals prior to and including t; and $\sigma_{u,t}$, $\sigma_{d,t}$ are the sample standard deviates at the respective upstream and downstream detectors, over a sampling period of n intervals prior to and including t.

The selected incident described in Section 3.3 is again used to demonstrate the variation of the CCS of upstream and downstream detectors before and after the incident occurring time (Fig. 3.8).

Fig. 3.8 Time series of the correlation coefficient of speeds (CCS) of upstream and downstream detectors

The CCS of upstream and downstream detectors began to significantly decrease after the incident occurs. The decrease of the CCS of upstream and downstream detectors is due to the decrease of the upstream traffic speed and increase of downstream speed caused by the accident. It is shown in this illustrative example that the CCS of two adjacent detectors can also be used to indicate incident occurrence.

3.5 Summary

In this Chapter, the SND algorithm is extended to be the new extended normal deviate (ESND) algorithm for incident detection. Two extensions were made to the SND algorithm, including (1) adopting the weighting method and (2) restricting the input data variation within sampling periods. An incident detection example was used to illustrate the merits of these two extensions. It is shown in this illustrative example that the proposed two extensions provide more reliable modified SND values and reduce the non-incident-induced acute fluctuation of the SND values. The detection threshold for the coefficient of variation of input traffic stream parameters needs to be carefully calibrated. A too small or too big detection threshold for the coefficient of variation of input traffic stream parameters may lead to more false alarms or low detection rates (DR) and a longer mean time to detect (MTTD).

In addition, two new traffic stream parameters are proposed as incident indicators for incident detection. The coefficient of variation of speed (CVS) at the upstream detector describes the traffic stream changes from the homogeneous pattern to stop-and-go pattern. The correlation coefficient of speeds (CCS) of two adjacent detectors indicates the opposite trend of changes of upstream speed and downstream speed over time.

The ESND algorithm proposed in this Chapter is then used to be extended to new AID algorithms in following Chapter 4 and Chapter 5 with proper input traffic stream parameters and detection logics.

Chapter 4. Flow-Dependent ESND Algorithm for Incident Detection under No-Rain Conditions

4.1 Introduction

In this Chapter, the extended standard normal deviate (ESND) algorithm proposed in Chapter 3 is extended to be flow-dependent ESND algorithm for incident detection under no-rain conditions. A two-step flow-dependent detection logic is adopted in the proposed flow-dependent ESND algorithm to detect traffic incidents. The following sections describe study site and data collection methods, followed by the input traffic data, detection logic, calibration and validation of the proposed flow-dependent ESND algorithm. The proposed flow-dependent ESND algorithm under no-rain conditions is also compared with five existing AID algorithms when applied on the study road section in Hong Kong.

4.2 Study Site

The west bound direction of an urban road section, located in the north of Hong Kong Island, is chosen for this research (Fig. 4.1). This road section is composed of five connected major roads. It is a 5.3 km long busy urban road section with one-way annual average daily traffic of more than 50,000 vehicles (Transport Department, 2011). The majority of this road section has a speed limit of 70 km/h except for the Harcourt Road area (50 km/h). There are no at-grade intersections, only a few on/off ramps.

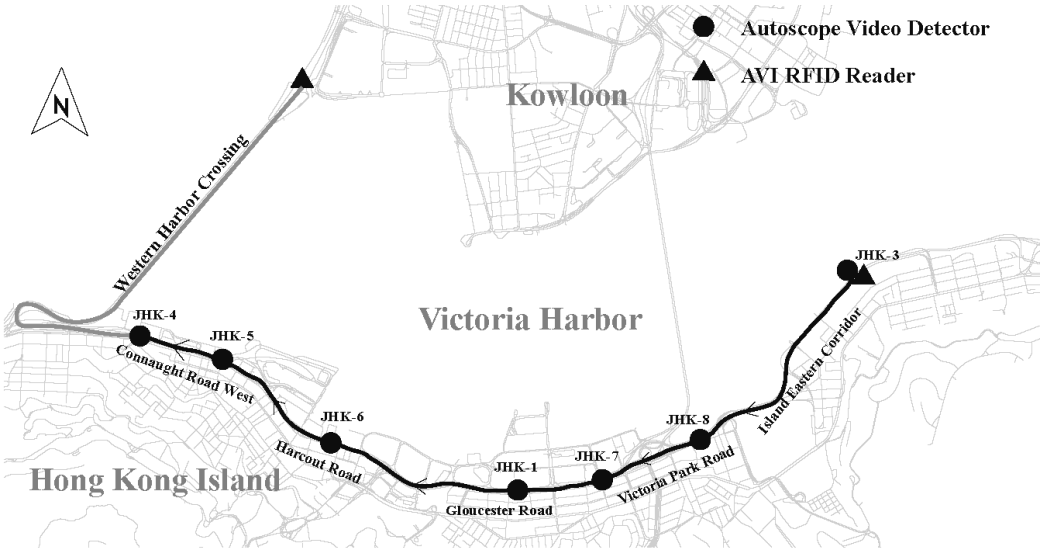

Fig. 4.1 Locations of the selected road section and traffic detectors for the case study

As shown in Fig. 4.1, seven video traffic detectors are installed on the selected road section with detector spacing ranging from 0.5 to 1.52 km. An automatic vehicle identification (AVI) based radio frequency identification device (RFID) reader is installed at the first video traffic detector station (i.e. JHK-3 detector station in Fig.4.1). This RFID reader is paired with another installed for journey time estimation purpose at the Western Harbor Crossing tollgate. The traffic data and incident records from September 1st 2009 to December 31st 2010 are collected on this study road section.

4.3 Data Collection

The 24-h space mean speeds (v, km/h), traffic counts (q, veh/2-min) and variances of space mean speeds [var, $(\text{km/h})^2$], which are averaged across the detected traffic lanes at 2-min intervals, were extracted from the database of the Journey Time Indication System (JTIS) in Hong Kong. The 2-min traffic counts were transferred to equivalent hourly traffic flow (q, veh/h/lane). However, traffic occupancy data were unavailable for use as this data collection system was originally designed only for journey time estimation purpose. Therefore, the traffic density (d, veh/km/lane) is used as the proxy of occupancy for incident detection. The traffic density were calculated by dividing the traffic flows by space mean speeds. The AVI-based instantaneous journey times (τ, s) (Tam and Lam, 2008; Moran, 2011)

between adjacent detectors at 2-min time interval were also extracted.

In this research, only traffic accident records are available for use in Hong Kong. Other incidents such as vehicle breakdowns and spilled loads are not recorded. Thus, the traffic incidents in this research are the recorded traffic accidents in fact. The traffic incident records such as date, time, location, and severity were extracted from the Traffic Accident Database System, which is updated by the Hong Kong Police and the Transport Department. A total of 72 lane-blocking incidents occurred on the selected road section from September 1st 2009 to December 31st 2010. Among the 72 incidents, four incidents were serious incidents, and the others were slight incidents. The reported occurring time of these incidents was adopted as the actual occurring time in this research.

The preincident traffic flow condition at each time interval was measured by aggregating the traffic flow data within 30 minutes prior to the current time interval. In other words, traffic flow data observed within 30 minutes prior to the current time interval was used to calculate the equivalent hourly traffic flow. Because the minimum time period over which traffic conditions are statistically stable, is 15 minutes, the 15-min interval was used as a base period for design and practice (Roess et al., 2004). However, the aggregate time interval of traffic data in this research is 2 minutes. Therefore, two 15-min intervals (i.e. 30 minutes) were used to estimate a stable preincident traffic flow condition.

After investigating the speed-flow relationship under incident-free conditions (Mak and Fan, 2006a), the traffic flow data were classified into three categories: “low” flow (<500 veh/h/lane), “medium” flow (500-1,200 veh/h/lane), and “heavy” flow (>1200 veh/h/lane).

The traffic and incident data were divided into two databases for calibration and validation of the proposed flow-dependent ESND algorithm. The proportions of the numbers of incidents for calibration and validation were determined based on those of previous studies (Mak and Fan, 2006a; Zhang and Taylor, 2006) and the distribution of incidents in the database of this research. The calibration database comprises 40 incidents (3 were serious and 37 were slight) between September 1st 2009 and June 31st 2010. The validation database consists of 32 incidents (1 was

serious and 31 were slight) between July 1st 2010 and December 31st 2010.

4.4 Input Data of the Proposed Algorithm

Different traffic stream parameters in the calibration database were used as inputs for the proposed ESND algorithm in Chapter 3 to form performance curves for comparison (Fig. 4.2). Because the AVI-based traffic flow data are unavailable for use in the JTIS database, the weights of the instantaneous journey time at each time intervals within sampling periods were set to be equal. When using traffic flow data as inputs, the weights of the traffic flow at each time intervals were also set to be equal.

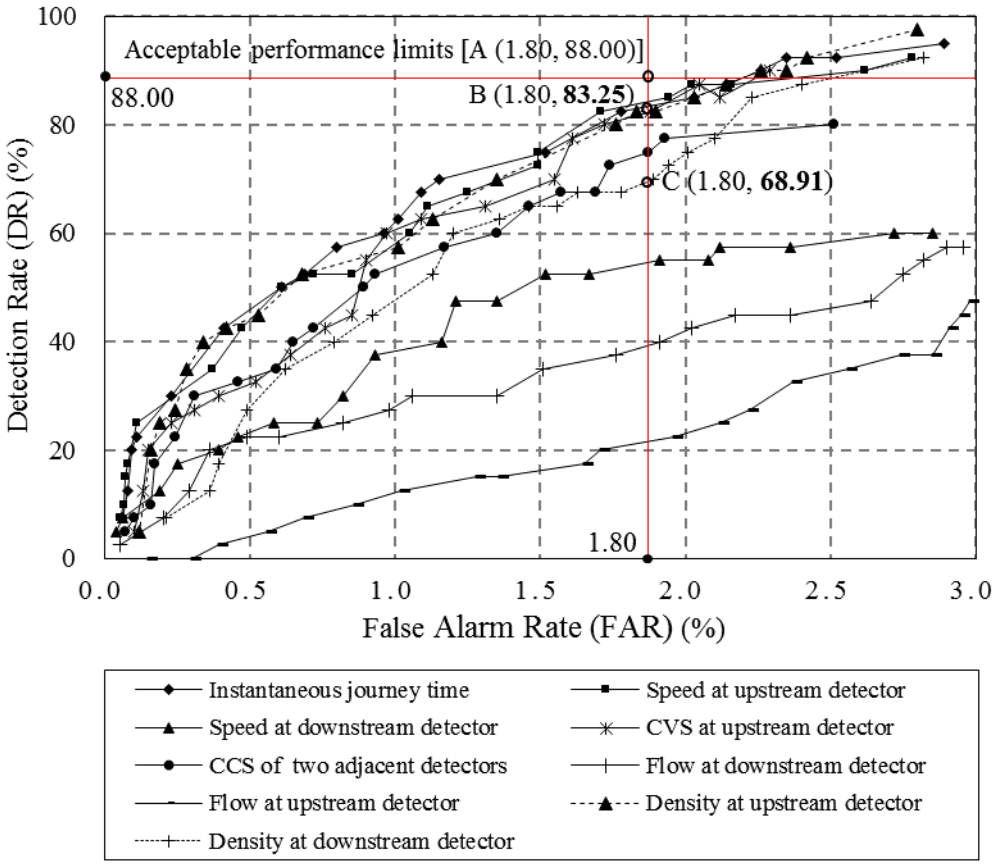

Fig. 4.2 Performances of the proposed ESND algorithm with inputs of different traffic stream parameters

It can be seen from Fig. 4.2 that the performances of the ESND algorithm based on the traffic stream parameters at the upstream detector are better than those based on the traffic stream parameters at the downstream detector. For instance, when the

FAR is fixed to be the acceptable FAR limit of 1.8% (Abdulhai, 1996), the DR for the density at the upstream detector is 83.25% (i.e. point B in Fig. 4.2), larger than the 68.91% for the density at the downstream detector (i.e. point C in Fig. 4.2).

The adoptions of instantaneous journey time and the CCS of two adjacent detectors as input data also result in a good incident detection performance. The ESND algorithm also achieves a good detection performance based on the density at the downstream detector.

Different input traffic stream parameter have different parameter and threshold values at different data point on the performance curves in Fig. 4.2. For instance, Table 4.1 presents the parameter and threshold values of various traffic stream parameters when the FAR is fixed to the acceptable FAR limit of 1.8% (Abdulhai, 1996).

Table 4.1 The Values of Parameters and Thresholds for Different Input Traffic Stream Parameters when the FAR is Fixed to the Acceptable FAR Limit of 1.8% (Abdulhai, 1996)

Input traffic stream parameter	Number of time intervals over the sampling period (n)	Threshold for the coefficient of variation of input data (θ)	Detection threshold (T)
Instantaneous journey time	6	0.2	3
CCS of two adjacent detectors	9	0.15	-3
Speed at upstream detector	6	0.1	-3.5
CVS at upstream detector	7	0.15	**4**
Density at upstream detector	7	0.1	**4**
Density at downstream detector	6	0.15	-3.5

Notes: CCS denotes the correlation coefficient of speeds;
CVS denotes the coefficient of variation of speeds.

It can be seen from Table 4.1 that the detection thresholds for different input traffic stream parameters vary. The absolute values of the CVS and the density at upstream detector are 4, larger than those of the other input traffic stream parameters. This indicating that the CVS and the density at the upstream detector are more sensitive to the incident-induced traffic disturbances than other input traffic stream parameters.

Therefore, only six traffic stream parameters were selected as the inputs for the proposed flow-dependent ESND algorithm: (1) the instantaneous journey time, (2) the CCS of two adjacent detectors, (3) the speed at the upstream detector, (4) the CVS at the upstream detector, (5) the density at the upstream detector, and (6) the density at the downstream detector. The instantaneous journey time and the CCS of two adjacent detectors are dual-station data calculated with the use of traffic data from dual detector stations. The other selected traffic stream parameters are single-station data collected from single detector stations. Traffic flow data were used as the weights and the measurements of preincident traffic flow conditions.

4.5 Detection Logic

The traffic flow condition prior to a traffic incident has a significant influence on the incident detection performance of AID algorithms (Mak and Fan, 2006a). For each preincident traffic flow condition (i.e. low, medium and heavy flow), two detection steps are adopted for incident detection: (1) preliminary detection and (2) persistence test.

First step:

In the first step, a traffic incident will be regarded as preliminarily detected if the following two conditions are met:

Condition 1: $SND_t^{'}(v_u) \le T_v$ or $SND_t^{'}(CVS_u) \ge T_{cvs}$ or $SND_t^{'}(d_u) \ge T_{(q/v)_u}$ or $SND_t^{'}(d_d) \ge T_{(q/v)_d}$ or $SND_t^{'}(CCS) \le T_{CCS}$

Condition 2: $SND_t^{'}(\tau) \ge T_\tau$

Second step:

In the second step, a second-time interval is used to conduct a persistence test to confirm the preliminarily detected traffic incident at the previous time interval. If the following two conditions are still met at the second time interval, an incident alarm will be finally triggered.

Condition 1: $SND'_{t+1}(v_u) \le T_v$ or $SND'_{t+1}(CVS_u) \ge T_{cvs}$ or $SND'_{t+1}(d_u) \ge T_{(q/v)_u}$ or $SND'_{t+1}(d_d) \ge T_{(q/v)_d}$ or $SND'_{t+1}(CCS) \le T_{CCS}$

Condition 2: $SND'_{t+1}(\tau) \ge T_\tau$

where v_u = the traffic speed at the upstream detector; CVS_u = the coefficient of variation of speed at the upstream detector; CCS = the correlation coefficient of speeds of two adjacent detectors; d_u = the density at the upstream detector; d_d = the density at the downstream detector; τ = the instantaneous journey time between two adjacent detectors; $SND'_t(v_u)$, $SND'_t(CVS_u)$, $SND'_t(d_u)$, $SND'_t(d_d)$, $SND'_t(CCS)$, and $SND'_t(\tau)$ = the modified SND values of corresponding traffic stream parameters at time *t*; $SND'_{t+1}(v_u)$, $SND'_{t+1}(CVS_u)$, $SND'_{t+1}(d_u)$, $SND'_{t+1}(d_d)$, $SND'_{t+1}(CCS)$, and $SND'_{t+1}(\tau)$ = the modified SND values of corresponding traffic stream parameters at time *t+1*; T_v, T_{cvs}, T_{d_u}, T_{d_d}, T_τ and T_{CCS} = the corresponding detection thresholds of corresponding traffic stream parameters; the T_v, T_{d_d}, and T_{CCS} are negative because they tend to decrease after incidents; T_{cvs}, T_{d_u}, and T_τ are positive because they tend to increase after incidents. These parameters and thresholds are different under various preincident traffic flow conditions.

Traffic incidents have different effects on different traffic stream parameters in both time and magnitude (Corby and Saccomanno, 1997). This may be caused by the detector spacing, prevailing traffic flow condition, incident severity and distance between the incident spot and its adjacent traffic detectors. A single traffic stream parameter may be inadequate for incident detection under different conditions.

To achieve a robust incident detection performance, five video traffic detector based traffic stream parameter data together with the AVI-based instantaneous journey time data are used as parallel inputs for the proposed flow-dependent ESND algorithm. These five video traffic detector based traffic stream parameters

are: (1) the traffic speed at the upstream detector, (2) the CVS at the upstream detector, (3) the density at the upstream detector, (4) the density at the downstream detector, and (5) the CCS of two adjacent detectors. The modified SND values of these traffic stream parameters are calculated for comparison with their corresponding predetermined detection thresholds.

The traffic incident occurred between two adjacent traffic detectors may result in a longer journey time. Therefore, the AVI-based instantaneous journey time is adopted as additional information to the video traffic detector based data for incident detection.

The persistence test is used to reduce false alarms of incident detection. If the two conditions are met in two successive time intervals, an incident alarm will be triggered.

4.6 Algorithm Calibration

The 40 incidents from September 1st 2009 to June 31st 2010 were used in the calibration of the parameter values and threshold values of the proposed flow-dependent ESND algorithm. Among the 40 incidents for calibration, 18 occurred under heavy flow conditions and 21 under medium flow conditions. Only one incident occurred under low flow conditions. In this research, only heavy and medium flow conditions are investigated because the only incident under low flow conditions is inadequate for calibration of the proposed flow-dependent ESND algorithm.

A range of possible parameter values and threshold values were analyzed for each traffic flow condition (Mak and Fan, 2006a). A number of detection performances (DR-FAR pairs and the corresponding MTTDs) were obtained by varying the detection threshold values for each parameter combination. The performance curve was then used to present the overall incident detection performance. Each data point on the performance curve in Fig. 4.3 is related to a parameter combination and the corresponding detection threshold values.

The incident detection performance of the calibrated flow-dependent ESND algorithm is shown in Fig. 4.3. The DR and the FAR together with the MTTD are

plotted to illustrate their interrelationship. Additionally, the performance of the proposed flow-independent ESND algorithm is drawn on, as seen in Fig. 4.3, for comparison with the proposed flow-dependent ESND algorithm.

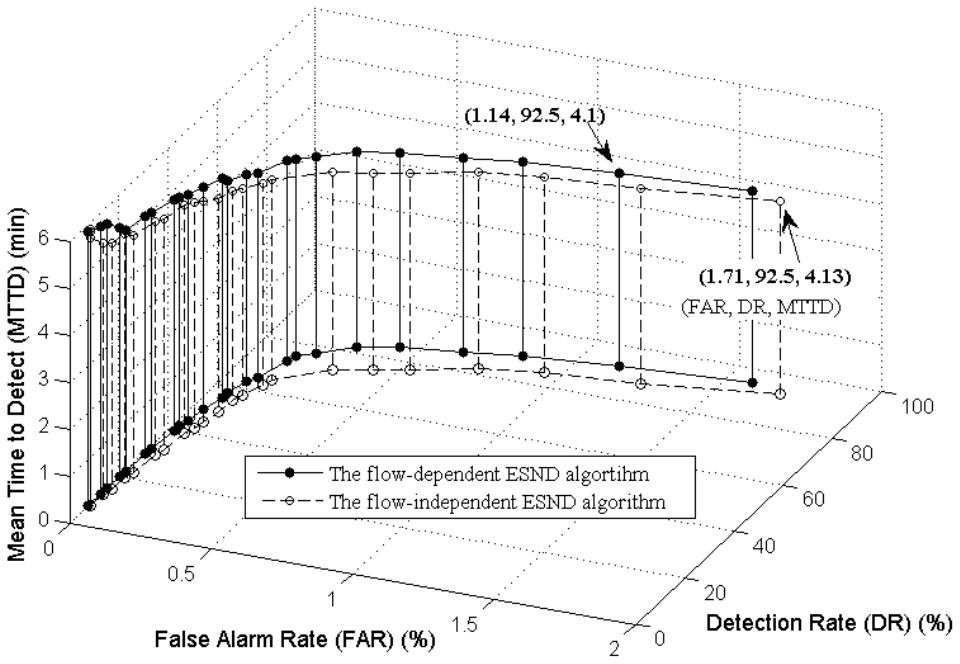

Fig. 4.3 Performances of the flow-dependent flow-independent ESND algorithm

The overall incident detection performance of the proposed flow-dependent ESND algorithm is better than that of the flow-independent ESND algorithm. When the DR is 92.5%, the FAR of the proposed flow-dependent ESND algorithm is 1.14%, lower than the 1.71% of the flow-independent ESND algorithm. When converting the FAR to the daily false alarms, the proposed flow-dependent ESND algorithm produces about 8 false alarms per day, which is less than the 12 false alarms of flow-independent ESND algorithm. In other words, the traffic operators may have to deal with about 8 false alarms every day. The MTTDs of the proposed flow-dependent ESND algorithm are slightly longer than those of the flow-independent ESND algorithm.

It is worth noting that the minimum MTTD in the calibration is 4.10 minutes, a value which is longer than those of most existing AID algorithms (Parkany and Xie, 2005). This difference exists because the aggregate time interval of the traffic data in this research is 2 minutes, and the proposed flow-dependent ESND

algorithm needs two successive time intervals for incident detection. The MTTDs of the existing AID algorithms (Mak and Fan, 2006a; Mak and Fan, 2007), which also adopt persistence tests, are also about twice the aggregate time interval of the traffic data used. In their studies, MTTDs are about 2 minutes and the data aggregate time interval is only 1 minute. Therefore, the large MTTD of the flow-dependent ESND algorithm proposed in this Chapter is acceptable in view of the large aggregate time interval of the traffic data used.

Therefore, the inclusion of the preincident traffic flow condition in the detection logic of the proposed flow-dependent ESND algorithm can effectively improve the incident detection performance.

The values of parameters and thresholds of the flow-dependent ESND algorithm vary under different traffic flow condition for different traffic stream parameters. Table 4.2 shows the calibrated parameter and threshold values of the flow-dependent ESND algorithm when the DR is 92.5%, the FAR is 1.14% and the MTTD is 4.1 minutes.

Table 4.2 The Values of Parameters and Thresholds of the Flow-dependent ESND Algorithm under Different Traffic Flow Condition when the DR is 92.5%, the FAR is 1.14% and the MTTD is 4.1 Minutes

Traffic flow condition	Input traffic stream parameter	Number of time intervals over the sampling period (n)	Threshold for the coefficient of variation of input data (θ)	Detection threshold (T)
Low flow condition	τ	8	0.2	3
	CCS	8	0.15	-3
	v_u	6	0.1	-4.5
	CVS_u	8	0.15	4
	d_u	7	0.1	**4.5**
	d_d	6	0.15	-4
Medium flow condition	τ	7	0.2	2.5
	CCS	8	0.15	-2.5
	v_u	5	0.1	-3
	CVS_u	8	0.15	3.5
	d_u	6	0.1	**3.5**
	d_d	6	0.15	-3
Heavy flow condition	τ	5	0.2	2
	CCS	7	0.15	-2.5
	v_u	5	0.1	-2.5
	CVS_u	6	0.15	3
	d_u	5	0.05	**3**
	d_d	5	0.1	-2.5

Notes: τ denotes the instantaneous journey time between two adjacent detectors;

d_u denotes the density at the upstream detector;

d_d denotes the density at the downstream detector;

v_u denotes the traffic speed at the upstream detector;

CVS_u denotes the coefficient of variation of speed at the upstream detector;

CCS denotes the correlation coefficient of speeds of two adjacent detectors.

That the detection threshold values are found to decrease when the traffic condition changes from low flow condition to heavy flow condition in Table 4.2. For instance, the detection threshold for density at upstream detector is 4.5 under low flow conditions. However, the detection threshold decreases to 3.5 under

medium flow conditions and 3 under heavy flow conditions. This can be explained by the different magnitudes of incident-induced traffic disturbances under different traffic flow conditions. When the traffic becomes more congested, the vehicle maneuverability is reduced. The incident may cause more significant effects on the magnitudes of the traffic disturbances under heavy traffic conditions. Even a slight incident may block the road and significantly reduce the road capacity. Therefore, the incident-induced traffic disturbances under heavier conditions can be detected with a smaller detection threshold.

4.7 Algorithm Validation

The 32 incidents recorded in the validation database were used to evaluate the calibrated flow-dependent ESND algorithm when applied to an independent database. For each DR level, the lowest FAR and the corresponding MTTD were chosen as the final performance measurements. Referring to the acceptable incident detection performance limits obtained from a survey by Abdulhai (1996), only those results, the DR of which is higher than 88% and the FAR lower than 1.8%, were selected.

An analysis was also conducted to justify the adoption of the persistence test. The proposed flow-dependent ESND algorithm without a persistence test was recalibrated and then applied to the validation database. The acceptable incident detection performances of the proposed flow-dependent ESND algorithm with and without persistence tests are shown in Table 4.3.

Table 4.3 Validation Results of the Proposed Flow-Dependent ESND Algorithm with and without Persistence Tests

	Detection rate (DR) (%)	False alarm rate (FAR) (%)	Mean time to detect (MTTD) (min)
Detection without the persistence test	96.88	2.161	2.13
	93.75	1.945	2.16
	90.63	1.753	2.23
Average	**93.75**	**1.953**	**2.17**
Detection with the persistence test	96.88	1.564	4.11
	93.75	1.043	4.13
	90.63	0.795	4.21
Average	**93.75**	**1.134**	**4.15**

The proposed flow-dependent ESND algorithm with a persistence test detects about 93.75% of traffic incidents. The average FAR is 1.134%, meaning that about 0.34 false alarms are triggered in one hour. In other words, a false alarm may be triggered about every three hours. The average MTTD is 4.15 minutes. The average MTTD of the proposed flow-dependent ESND algorithm without a persistence test is reduced from 4.15 minutes to 2.17 minutes. The average FAR, however, increases from 1.134% to 1.953%. In other words, the adoption of the persistence test reduces 42% of false alarms at the cost of one more time interval, 2 minutes in this case. There is a trade-off between the FAR and the MTTD when adopting the persistence test. Because the high FAR is intolerable in operation, it is worth adopting the persistence test at the cost of a longer MTTD.

4.8 Comparison with Existing AID Algorithms

Five existing AID algorithms were compared with the proposed flow-dependent ESND algorithm based on the database in Hong Kong. These five AID algorithms compose the standard normal deviate (SND) algorithm (Dudek et al., 1974), California #7 algorithm (Payne et al., 1976), double exponential smoothing (DES) algorithm (Cook and Cleveland, 1974), Minnesota algorithm (Stephanedes and Chassiakos, 1993) and flow-dependent combined detector evaluation (CODE) algorithm (Mak and Fan, 2007). The SND algorithm, California #7 algorithm, DES algorithm and Minnesota algorithm originally adopted traffic occupancy obtained from inductive loop detectors as inputs. The flow-dependent CODE algorithm adopted both the traffic speed and occupancy obtained from the video traffic detectors as inputs. In general, these five existing AID algorithms can be classified into single-station or dual-station algorithms as shown in Table 4.4.

Table 4.4 Classification of the Five Existing AID Algorithms for Comparison

Classification	Algorithm
Single-station AID algorithm	(S1) SND algorithm (S2) DES algorithm
Dual-station AID algorithm	(D1) California #7 algorithm (D2) Minnesota algorithm (D3) Flow-dependent CODE algorithm

The calibrations of the five existing AID algorithms are similar to those found in

previous studies (Mak and Fan, 2005; Mak and Fan, 2007) based on the calibration database in this research. During the calibrations of these five AID algorithms, only combinations of parameter and threshold values corresponding to the lowest FAR at each DR were selected.

Based on the combinations of calibrated parameter and threshold values, the five existing AID algorithms together with the proposed flow-dependent ESND algorithm were applied to the validation database. The incident detection performances of these five existing AID algorithms and the proposed flow-dependent ESND algorithm were compared and shown in Fig. 4.4. The average MTTDs were calculated based on only those results, the DR of which is higher than 88% and the FAR lower than 1.8% (Abdulhai, 1996).

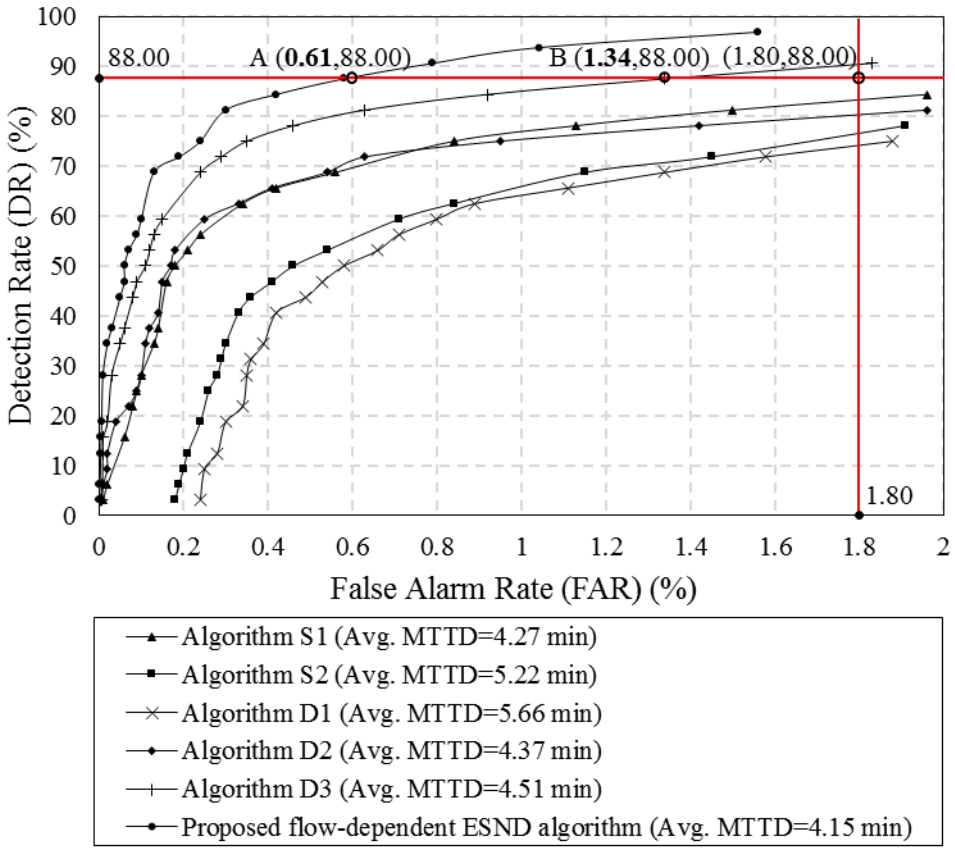

Fig. 4.4 Performances of the proposed flow-dependent ESND algorithm and the other five existing AID algorithms

It is seen in Fig. 4.4 that the proposed flow-dependent ESND algorithm outperforms the five existing AID algorithms. The performances of only the

flow-dependent CODE algorithm (D3) and the proposed flow-dependent ESND algorithm reaches the acceptable performance limits in which the minimum DR is 88% and the maximum FAR is 1.8% (Abdulhai, 1996). When the DR is fixed to be the acceptable limit of 88%, the FAR of the proposed flow-dependent ESND is 0.61%, much lower than the 1.34% of the flow-dependent CODE algorithm. This can be explained by the two extensions made to the SND algorithm described in Chapter 3. The incident detection performances of the SND algorithm (S1), Minnesota algorithm (D2) and DES algorithm (S2) perform better than the California #7 algorithm (D1). This is because the statistical algorithm (S1) and the time series algorithms (D2 and S2) can better capture the dynamic changes of the traffic stream on urban roads than the pattern recognition algorithms (D1).

At the same DR level, the FAR of the proposed flow-dependent ESND algorithm is lower than those of the five existing AID algorithms. This is because the flow-dependent ESND algorithm proposed in this Chapter restricts the variation of input data within sampling periods. At the same FAR level, the DR of the proposed flow-dependent ESND algorithm is higher than those of the five existing AID algorithms. This can be explained by the adoption of hybrid traffic stream parameters as inputs for the proposed flow-dependent ESND algorithm. The single-station data (speed, the CVS, density at the upstream and downstream detector) and dual-station data (instantaneous journey time and the CCS) both contribute to the overall incident detection performance of the proposed algorithm. The proposed flow-dependent ESND algorithm with both single-station and dual-station data as inputs is more adaptive to various conditions. This makes the incident detection performance of the proposed algorithm more effective and robust. In addition, the MTTD of the proposed algorithm is 4.15 minutes, a value shorter than those of the five existing AID algorithms. Because of the adoption of hybrid traffic stream parameters as inputs, the proposed flow-dependent ESND algorithm can detect traffic incidents as soon as any one of the selected traffic stream parameters has a significant variation when the journey time also increases.

4.9 Summary

A flow-dependent ESND algorithm is proposed for incident detection under

no-rain conditions in this Chapter. The proposed flow-dependent ESND algorithm is an extension to the ESND algorithm proposed in Chapter 3. Based on the validation database, the calibrated flow-dependent ESND algorithm detected about 93.75% of the traffic incidents. The FAR was about 1.134% which is equivalent to about 8.02 false alarm per day in this research. The MTTD was 4.15 minutes which is about twice the data aggregate time interval (i.e. 2 minutes) because the proposed AID algorithm needs two successive time intervals to detect potential incidents and conduct persistence tests. The adoption of the persistence test reduced false alarms by 42% at the cost of a longer average MTTD. The false alarm was reduced from once every two hours to once every three hours. Although the MTTD of the proposed algorithm is greater than those of previous studies (Parkany and Xie, 2005; Mak and Fan, 2006a), it is still reasonable because the aggregate time interval of traffic data in Hong Kong is greater than that of the more widely used 20 to 60 seconds (Mak and Fan, 2006a).

The interrelationship of the DR, FAR and MTTD is illustrated in a three-dimensional figure. A trade-off exists between these three performance measurements. The increase in the detection thresholds of the AID algorithm parallels a decrease in both the DR and FAR and an increase in the MTTD.

Incident detection performance was more successfully achieved after the adoption of the proposed two extensions to the previous Standard Normal Deviate (SND) algorithm: (1) the adoption of the weighting method and (2) the restriction of the input data variation within sampling periods. Compared with the five existing AID algorithms, the proposed flow-dependent ESND algorithm has proved capable of reducing the FAR while maintaining a high DR.

The two new proposed traffic stream parameters, CVS at upstream detector and CCS of two adjacent detectors, proved feasible indicators of traffic incidents. The hybrid traffic data obtained from both the video traffic detectors and AVI readers, makes clear that the proposed flow-dependent ESND algorithm achieved good results even though individual traffic stream parameters respond differently to traffic incidents, in both time and magnitude. The adoption of hybrid input data effectively increased the DR and reduced the MTTD. The instantaneous journey time and the CCS of two adjacent detectors are dual-station data calculated with

the use of traffic data from dual detector stations. The traffic speed at the upstream detector, density at the upstream detector, density at the downstream detector and the CVS at the upstream detector are single-station data collected from single detector stations. The adoption of both the single-station and dual-station input data enhanced the ability of the proposed algorithm to possess the strengths of both single-station algorithms and dual-station algorithms. The proposed flow-dependent ESND algorithm performed well on the selected road section with impacts from variations in road geometry, detector spacing, the presence of on/off ramps and the prevailing traffic condition.

The consideration of the preincident traffic flow condition in the detection logic of the proposed flow-dependent ESND algorithm proved effective in improving the incident detection performances. Although the difference between the MTTDs of the proposed flow-dependent and flow-independent ESND algorithm was small, the FAR was significantly reduced when the preincident traffic flow condition was incorporated into the detection logic.

The proposed flow-dependent ESND algorithm, however, was calibrated and validated with traffic and incident data on only one road section. Further investigation is of interest in terms of the algorithm's robustness and overall value. Hence the incident detection performance of the proposed flow-dependent ESND algorithm needs to be further examined on the basis of the available data collected on the urban road network under the JTIS.

As stated in Chapter 2, rainfall has been found to affect traffic stream parameters, in particular the traffic flow and capacity. Thus, it is of value for such effects to be considered in attempts to improve the incident detection performance of AID algorithms.

The following Chapter focuses on incident detection under both no-rain and rain conditions on a territory-wide basis. The flow-dependent ESND algorithm is further extended to be the flow-rain-dependent ESND algorithm. Continuous detection thresholds generated by generalized detection threshold functions are adopted under various preincident traffic and rain conditions to improve the incident detection performance. The incident detection performance of the

proposed flow-rain-dependent ESND algorithm is additionally examined with the use of the data collected on the urban road network under the JTIS in order to investigate its potential for territory-wide application.

Chapter 5. Flow-Rain-Dependent ESND Algorithm for Incident Detection under No-Rain and Rain Conditions

5.1 Introduction

Pisano and Goodwin (2004) addressed the research needs for weather-responsive traffic management. Automatic incident detection (AID), an important component of traffic management, should adapt to different weather conditions such as rain conditions.

Rainfall has been found to affect traffic stream parameters and speed-flow-density relationships (Lam et al., 2013). Both the time and magnitude of incident-induced traffic disturbances are affected by the rainfall. Consideration of the preincident rain condition together with the traffic condition may further improve the detection performances of AID algorithms.

The traffic flow has been used to indicate the preincident traffic condition in previous flow-dependent AID algorithms such as the flow-dependent combined detector evaluation (CODE) algorithm (Mak and Fan, 2007). In these flow-dependent AID algorithms, different discrete detection thresholds are calibrated and adopted under different preincident traffic flow conditions. The preincident traffic flow conditions are usually categorized into low, medium and heavy flow conditions according to the values of the preincident traffic flow.

The discrete detection thresholds under different preincident traffic flow conditions, however, are sometimes found to be unreasonable in practice. For instance, if the respective detection thresholds under low flow (<500 veh/h/lane) and medium flow conditions (500-1200 veh/h/lane) are set to be 3.5 and 4 when the incremental value is 0.5, it is unreasonable to adopt 3.5 when the traffic flow is 499 veh/h/lane and 4 when the traffic flow is 501 veh/h/lane. There should not be such a large difference in the detection threshold values between the traffic flow conditions of 499 and 501 veh/h/lane. Thus, continuous detection thresholds may

be more appropriate in practice.

The preincident traffic flow condition also cannot fully reflect the actual traffic condition on roads with different speed limits, road configurations and weather conditions. Instead of the traffic flow, the volume/capacity (V/C) ratio is proposed to represent the preincident traffic condition in this Chapter. The preincident V/C ratio is better in describing the level of service or the congestion level on roads.

In this Chapter, the flow-dependent extended standard normal deviate (ESND) algorithm proposed in Chapter 4 is further extended to be a more generalized flow-rain-dependent ESND algorithm for incident detection under both no-rain and rain conditions. Instead of the traffic flow, the V/C ratio is adopted to indicate the preincident traffic condition. Additionally, the proposed flow-rain-dependent ESND algorithm adopts continuous detection thresholds instead of discrete ones. The continuous detection thresholds are obtained by generalized detection threshold functions in which both the preincident traffic and rain conditions are considered explicitly.

The parameters and the generalized detection threshold functions of the proposed flow-rain-dependent ESND algorithm are calibrated and validated on the basis of the historical traffic, incident and rainfall intensity data. These data are collected on the urban road network under the Journey Time Indication System (JTIS) in Hong Kong.

A method is also proposed to estimate the generalized detection threshold functions for roads with various speed limits. When data on the road with a certain speed limit is not available, the generalized detection threshold function of this road can be estimated based on the data collected on roads with the other speed limits.

The incident detection performance of the proposed flow-rain-dependent ESND algorithm proposed in this Chapter is also compared with the flow-dependent ESND algorithm presented in Chapter 4 and other existing AID algorithms.

5.2 Study Site

Instead of the selected road section in Chapter 4, the urban road network under the JTIS, described in Chapter 1 and shown in Fig. 5.1, is selected for study in this Chapter. The study road network, on which more incidents occurred, could be used to develop an AID algorithm for use under rain conditions and enable an investigation of its potential for territory-wide use.

The study road network comprises expressways, trunk roads and primary distributors with speed limits ranging from 50 to 80 km/h (Transport Department, 2011). Several video traffic detectors and radio frequency identification device (RFID) readers are installed at strategic locations on the study road network for data collection as described in Chapter 4 (Fig. 5.1). The video traffic detector spacing ranges from 0.53 to 3.90 km and the average is 1.05 km. The AVI reader spacing ranges from 0.28 to 9.85 km and the average is 4.45 km.

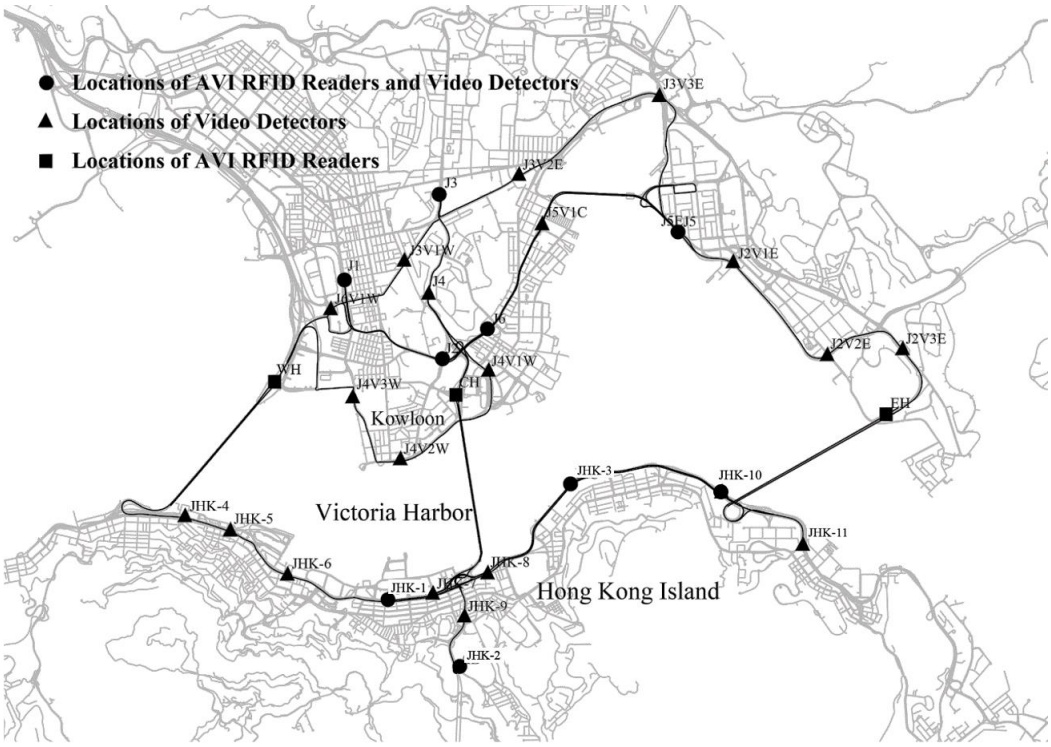

Fig. 5.1 Study road network under the Journey Time Indication System (JTIS) and locations of traffic detectors

5.3 Data Collection

In this Chapter, two years' traffic data from January 1st 2010 to December 31st 2011 were used for study. The 24-h space mean speed (v, km/h), traffic count (q, veh/2-min/lane) and variance of space mean speed [var, $(km/h)^2$] at 2-min time interval, collected by video traffic detectors, were extracted from the JTIS database. The 2-min traffic counts were transferred to equivalent hourly traffic flow (q, veh/h/lane). The traffic density (d, veh/km/lane) was again calculated and adopted as the proxy of occupancy, as in Chapter 4. The estimated instantaneous journey time (τ, s) between adjacent video traffic detectors at 2-min time interval (Tam and Lam, 2008; Moran, 2011) were also obtained from the JTIS database.

The preincident traffic flow at each time interval was also measured by aggregating the traffic flow data within 30 minutes prior to the current time interval, as described in Section 4.3. Instead of the traffic flow, the volume/capacity ratio was adopted to represent the preincident traffic condition. It is worth noting that the "volume" in this research is actually the traffic flow indeed. Therefore, the volume/capacity ratio is always no more than 1 in this research.

Incident data on the study road network were also extracted from the Hong Kong Traffic Accident Database System. It is worth noting that the selected incidents should meet three conditions: (1) occurred on the study road network, (2) occurred between two adjacent video traffic detectors, and (3) the traffic data of their adjacent traffic detectors are available for use.

A total of 943 lane-blocking incidents were finally found to have occurred on the study road network in 2010 and 2011. These 943 incidents were only 61.67% of the total incidents on the study road network. Among the 943 incidents, 45 occurred under rain conditions, and the others occurred under no-rain conditions.

Table 5.1 Selected Incidents on the Study Road Network from January 1st 2010 to December 31st 2011

Year	Incidents **under rain conditions**				Incidents **under no-rain conditions**				Total
	Fatal	Serious	Slight	Subtotal	Fatal	Serious	Slight	Subtotal	
2010	0	2	17	**19 (4.02%)**	2	17	413	**432 (95.80%)**	**451**
2011	0	3	23	**26 (5.28%)**	4	35	427	**466 (94.72%)**	**492**

Among the 451 incidents in 2010, 19 (i.e. 4.02%) occurred under rain conditions. In 2011, 26 out of 492 (i.e. 5.28%) incidents occurred under rain conditions. Most incidents are slight incidents. It can be seen from Table 5.1 that more numbers of fatal and serious incidents occurred under rain conditions than under no-rain conditions. Although the number of available incidents under rain conditions is limited, a framework can still be developed for further investigation when more incidents under rain conditions are available for study.

Rainfall intensity (r, mm/h) represents the rainfall precipitation over a certain time period. Hourly rainfall intensity around Hong Kong is recorded by 18 rainfall stations which are operated by the Hong Kong Observatory. A Geography Information System platform (Li et al., 2012) was used to obtain the hourly rainfall intensity on the occasion of every incident based on data collected from its nearest weather station. The hourly rainfall intensity data were used to indicate the preincident rain condition.

Traffic data, incident data and rainfall intensity data were finally matched into a database to be used to calibrate and validate the proposed flow-rain-based ESND algorithm. The 451 incidents in 2010 were used for calibration. The 492 incidents in 2011 were used for validation.

5.4 Detection Logic

The detection logic of the proposed flow-rain-dependent ESND algorithm in this Chapter is the same as that of the flow-dependent ESND algorithm in Chapter 4. The detection thresholds, however, are determined by the generalized detection threshold functions in which both the preincident volume/capacity ratio and rainfall intensity are modeled explicitly.

It is worth noting that the volume/capacity (V/C) ratio is relevant to traffic speed. When the traffic speed is higher than the speed at capacity, the V/C ratio is a decreasing function of the traffic speed. When the traffic speed is lower than the speed at capacity, the V/C ratio is an increasing function of traffic speed. Therefore, the generalized detection threshold function [$T(v,q,r)$] is written as follows:

$$T(v,q,r)=\begin{cases} f_1\left(\dfrac{q}{C(r)}\right), v > v_c(r) \\ f_2\left(\dfrac{q}{C(r)}\right), v \le v_c(r) \end{cases} \tag{5.1}$$

where v = the traffic speed (km/h); q = the traffic flow (or traffic volume) (veh/h/lane); $C(r)$ = the capacity function with rainfall intensity effects (veh/h/lane); r = the rainfall intensity (mm/h); $v_c(r)$ = the speed at capacity function with rainfall intensity effects (km/h).

The speed at capacity function with rainfall intensity effects [Eq. (5.3)] can be derived from the generalized speed-density function with rainfall intensity effects [Eq. (5.2)] (Lam et al., 2013). Both the speed at capacity function with rainfall intensity effects [Eq. (5.3)] and the capacity with rainfall intensity effects [Eq. (5.4)] can be obtained from Eq. (5.2).

$$v = v_f(r)\cdot\exp\cdot\left[-\psi\ln\left(\frac{d}{d_m}\right)^{\eta}\right], (\psi\cdot\eta=1) \tag{5.2}$$

$$v_c(r)=\exp\left(\frac{-1}{\eta}\right)\cdot v_f(r) \tag{5.3}$$

$$C(r)=\exp\left(\frac{-1}{\eta}\right)\cdot v_f(r)\cdot d_m \tag{5.4}$$

where v = the traffic speed (km/h); d = the traffic density (veh/km/lane); d_m = the density at capacity (veh/km/lane) ; $v_f(r)$ = the free-flow speed function with

rainfall intensity effects (km/h); $C(r)$ = the capacity with rainfall intensity effects; ψ, η = the parameters to be calibrated.

With the use of the detection thresholds generated by the generalized detection threshold function [Eq. (5.1)], incidents are detected with the following steps:

First step:

In the first step, an incident is preliminarily detected when the following two conditions are met:

Condition 1: $SND_t^{'}(v_u) \le T_v(v,q,r)$ or $SND_t^{'}(CVS_u) \ge T_{cvs}(v,q,r)$ or $SND_t^{'}(d_u) \ge T_{d_u}(v,q,r)$ or $SND_t^{'}(d_d) \ge T_{d_d}(v,q,r)$ or $SND_t^{'}(CCS) \le T_{CCS}(v,q,r)$

Condition 2: $SND_t^{'}(\tau) \ge T_{\tau}(v,q,r)$

Second step:

In the second step, a second-time interval is used to conduct a persistence test to confirm the preliminarily detected traffic incident at the previous time interval. If the following two conditions are still met at the second time interval, an alarm is finally triggered.

Condition 1: $SND_{t+1}^{'}(v_u) \le T_v(v,q,r)$ or $SND_{t+1}^{'}(CVS_u) \ge T_{cvs}(v,q,r)$ or $SND_{t+1}^{'}(d_u) \ge T_{d_u}(v,q,r)$ or $SND_{t+1}^{'}(d_d) \ge T_{d_d}(v,q,r)$ or $SND_{t+1}^{'}(CCS) \le T_{CCS}(v,q,r)$

Condition 2: $SND_{t+1}^{'}(\tau) \ge T_{\tau}(v,q,r)$

where v_u = the traffic speed at the upstream detector (km/h); CVS_u = the coefficient of variation of speed at the upstream detector; CCS = the correlation coefficient of speeds of two adjacent detectors; d_u = the density at the upstream detector (veh/km/lane); d_d = the density at the downstream detector

(veh/km/lane); τ = the instantaneous journey time between two adjacent detectors (s); r = the rainfall intensity (mm/h); $SND_t^{'}(v_u)$, $SND_t^{'}(CVS_u)$, $SND_t^{'}(d_u)$, $SND_t^{'}(d_d)$, $SND_t^{'}(CCS)$, and $SND_t^{'}(\tau)$ = the modified SND values of corresponding traffic stream parameters at time *t*; $SND_{t+1}^{'}(v_u)$, $SND_{t+1}^{'}(CVS_u)$, $SND_{t+1}^{'}(d_u)$, $SND_{t+1}^{'}(d_d)$, $SND_{t+1}^{'}(CCS)$, and $SND_{t+1}^{'}(\tau)$ = the modified SND values of corresponding traffic stream parameters at time *t+1*; $T_v(v,q,r)$, $T_{cvs}(v,q,r)$, $T_{d_u}(v,q,r)$, $T_{d_d}(v,q,r)$, $T_\tau(v,q,r)$ and $T_{CCS}(v,q,r)$ = the generalized detection threshold function of corresponding traffic stream parameters; the $T_v(v,q,r)$, $T_{d_d}(v,q,r)$, and $T_{CCS}(v,q,r)$ are negative; $T_{cvs}(v,q,r)$, $T_{d_u}(v,q,r)$, and $T_\tau(v,q,r)$ are positive. These parameter and threshold values are different under various preincident traffic flow and rain conditions.

Compared to the discrete detection thresholds adopted in previous flow-dependent AID algorithms, the detection thresholds of the proposed flow-rain-dependent ESND algorithm are continuous. Instead of the traffic flow, the V/C ratio is adopted to better describe the congestion level or level of service on roads. Rainfall intensity is found to have effects on road capacity (Lam et al, 2013), thus affecting the V/C ratio. Therefore, the use of the preincident V/C ratio incorporate both the effects of traffic flow and rainfall intensity into the incident detection.

The capacity function and the free-flow speed function with rainfall intensity effects are firstly calibrated in Section 5.5. The generalized detection threshold functions for each input traffic stream parameter on roads with different speed limits are then derived. The continuous detection thresholds, in which both the preincident traffic and rain conditions are considered, would make the proposed flow-rain-dependent ESND algorithm more adaptive and effective.

5.5 Algorithm Calibration

The traffic data, incident data and rainfall intensity data in 2010 were used to calibrate the proposed flow-rain-dependent ESND algorithm. The capacity

functions and free-flow speed functions with rainfall intensity effects for roads with different speed limits were firstly calibrated. The generalized detection threshold functions for various input traffic stream parameters were also calibrated on the basis of the collected data. Finally, the generalized detection threshold functions for various input traffic stream parameter on roads with different speed limits were determined.

5.5.1 Calibration of the Capacity Function with Rainfall Intensity Effects

The traffic data were firstly divided into groups according to the speed limits of roads on which they are collected. Each group of traffic data was then used to calibrate the capacity function with rainfall intensity effects $[C(r)]$ for roads with the corresponding speed limit.

For each speed limit, the corresponding traffic data was firstly divided into several sub-groups according to the rainfall intensity values. The rainfall intensities were grouped into no rain (0 mm/h), light rain (0-0.5 mm/h), medium rain (0.5-2.5 mm/h) and heavy rain (>2.5 mm/h) (Lam et al., 2013).

For each rainfall intensity group, the relationship between the traffic speed and density was fitted by the generalized speed-density function [Eq. (5.2)]. The speed at capacity and the capacity for each rainfall intensity group were then calculated by Eq. (5.3) and Eq. (5.4). Finally, the relationship between the capacity and the rainfall intensity was modeled and calibrated for each speed limits by the non-linear regression method (Fox, 2008). Several function forms such as polynomial, exponential and power functions were tried. The exponential function was found to fit best. The calibrated capacity functions with rainfall intensity effects on roads with various speed limits are given in Table 5.2.

Table 5.2 Capacity Function with Rainfall Intensity Effects for Roads with Various Speed Limits

Road Type	Speed limit (km/h)	Capacity function with rainfall intensity effects
Expressway/ Urban trunk road	80	$C(r) = \exp\left(-0.06951 \cdot r^{0.2347} + \mathbf{7.470}\right)$
Primary distributor	70	$C(r) = \exp\left(-0.08841 \cdot r^{0.2216} + \mathbf{7.338}\right)$
	60	$C(r) = \exp\left(-0.10301 \cdot r^{0.2037} + \mathbf{7.248}\right)$
	50	$C(r) = \exp\left(-0.12170 \cdot r^{0.1638} + \mathbf{7.182}\right)$

The relationships between the capacity and rainfall intensity on roads with various speed limits are further illustrated in Fig. 5.2.

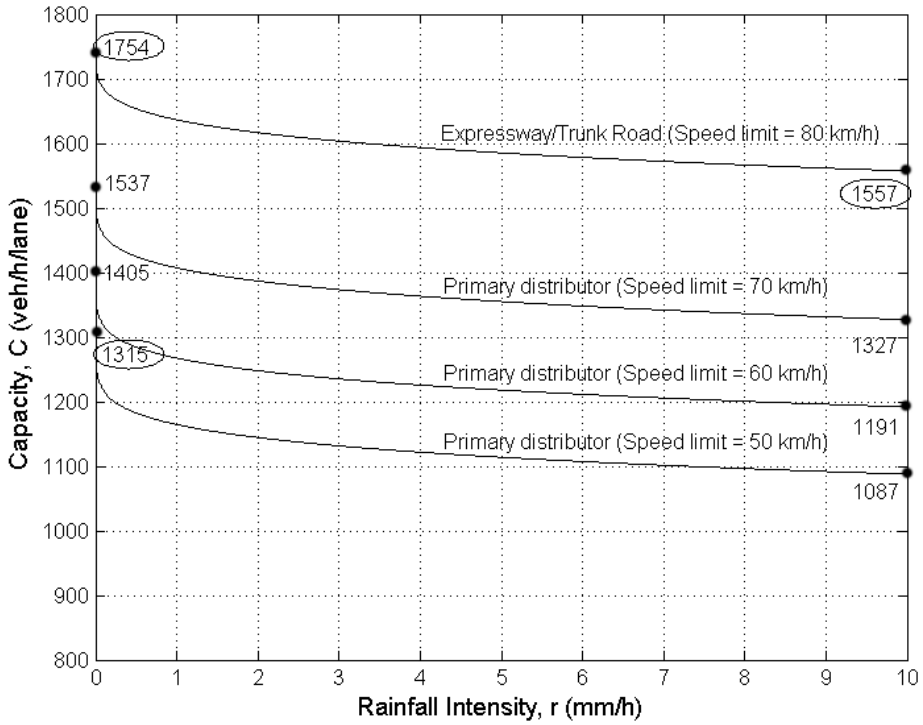

Fig. 5.2 Relationships between the capacity and rainfall intensity on roads with various speed limits

It can be seen in Fig. 5.2 that the capacity is reduced when the rainfall intensity increases because the capacity is a decreasing function of the rainfall intensity as shown in Table 5.2. For instance, the capacity of expressway/urban trunk roads with a speed limit of 80 km/h decreases from 1754 to 1557 veh/h/lane (i.e. a 11.23% decrease) when the rainfall intensity increases from 0 to 10 mm/h. The reduction rate of the capacity in Fig. 5.2 is found to decrease with the increasing

rainfall intensity. This can be explained by the power parameter of the rainfall intensity (r) in the capacity functions with rainfall intensity effects in Table 5.2.

Additionally, Fig. 5.2 shows that the capacity decreases with decreasing speed limit, as in HCM (2000). The decreasing coefficient and power parameter of the rainfall intensity (r) in the capacity function with rainfall intensity effects [$C(r)$] in Table 5.2 also reflect the decreasing trend of the capacity when the speed limit decreases. For instance, under no-rain condition, the capacity decreases from 1754 to 1315 veh/h/lane when the speed limit decreases from 80 to 50 km/h. This can be explained by the capacity function [Eq. (5.4)] in which the free-flow speed and the density at capacity are modelled. Under a certain rainfall condition, the variations of the calibrated density at capacity (d_m) and the parameter η in Eq. (5.4) for different speed limits are not significant. Therefore, the capacity is mainly affected by the free-flow speed (v_f) which is determined by the speed limit. Roads with a higher speed limit usually have a higher capacity under the same rainfall condition.

The calibrated capacity function with rainfall intensity effects [$C(r)$] will be used to be plugged into the generalized detection threshold function in which capacity is considered explicitly in Section 5.5.3.

5.5.2 Calibration of the Free-flow Speed Function with Rainfall Intensity Effects

The free-flow speed function with rainfall intensity effects [$v_f(r)$] is modeled and calibrated with similar methods in the related study by Lam et al. (2013).

As in Section 5.5.1, for each speed limit, the collected traffic data were also divided into several groups according to the rainfall intensity values (i.e. no-rain, light rain, medium rain and heavy rain). The generalized speed-density function [Eq. (5.2)] were again used to fit the speed-density relationship for each rainfall intensity group. The free-flow speed for each rainfall intensity group was obtained from the fitted generalized speed-density function. Finally, the

relationship between the free-flow speed and the rainfall intensity was modeled for each speed limit by the non-linear regression method (Fox, 2008). Similar to the capacity function with rainfall intensity effects, the exponential function was found to fit best. The calibrated free-flow speed functions with rainfall intensity effects [$v_f(r)$] for roads with various speed limits are given in Table 5.3.

Table 5.3 Relationship between the Free-Flow Speed and Rainfall Intensity for Roads with Different Speed Limits

Road type	Speed limit (km/h)	Free-flow speed function with rainfall intensity effects
Expressway/ Urban trunk road	80	$v_f(r) = \exp\left(-0.045 \cdot r^{0.315} + \mathbf{4.390}\right)$
Primary distributor	70	$v_f(r) = \exp\left(-0.044 \cdot r^{0.296} + \mathbf{4.260}\right)$
	60	$v_f(r) = \exp\left(-0.044 \cdot r^{0.278} + \mathbf{4.103}\right)$
	50	$v_f(r) = \exp\left(-0.042 \cdot r^{0.263} + \mathbf{3.920}\right)$

The relationships between the free-flow speed and rainfall intensity on roads with various speed limits are further illustrated in Fig. 5.3.

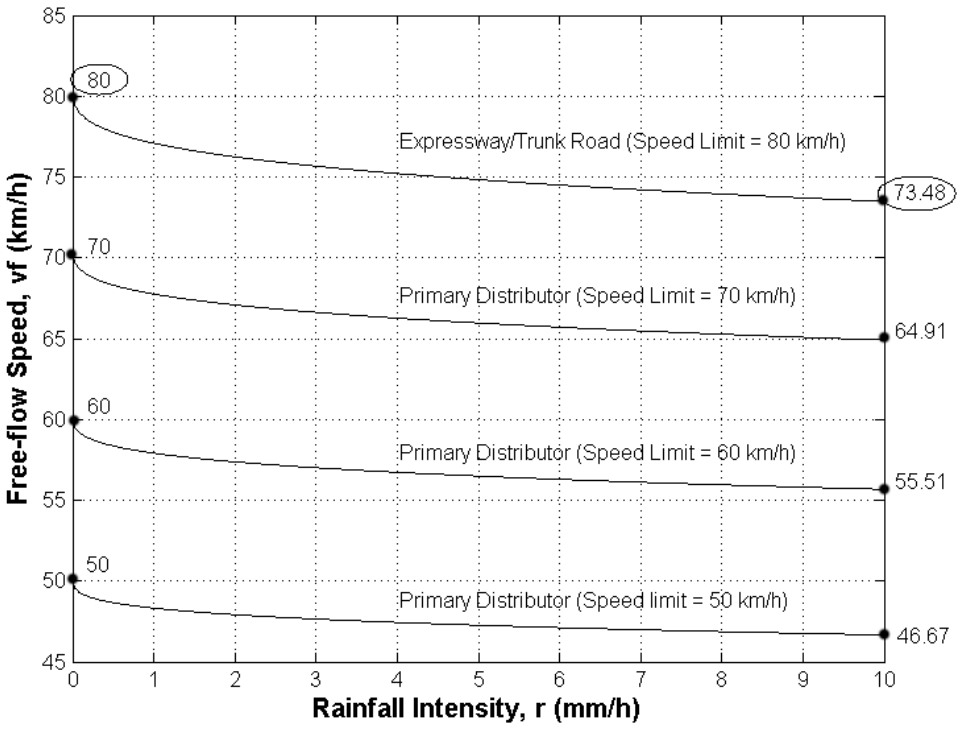

Fig. 5.3 Relationships between the free-flow speed and rainfall intensity on roads with various speed limits

The free-flow speeds, as shown in Fig. 5.3, decrease with the increasing rainfall intensity. For instance, the free-flow speed of expressway/urban trunk roads with a speed limit of 80 km/h decreases from 80 to 73.48 km/h (i.e. a decrease of 8.15%) when rainfall intensity increases from 0 to 10 mm/h. The negative

coefficients of the rainfall intensity (r) in the free-flow functions in Table 5.3 indicate the decreasing trend of the free-flow speed when the rainfall intensity increases.

The reduction rate of the free-flow speed also decreases with the increasing rainfall intensity. The power parameter of the rainfall intensity (r) and the constant in the free-flow speed function [$v_f(r)$] in Table 5.4 also decrease when the speed limit decreases. This indicates that the free-flow speed decreases with the decreasing speed limit.

5.5.3 Calibration of the Generalized Detection Threshold Function

In this Section, the generalized detection threshold function [Eq. (5.1)] for each input traffic stream parameter is individually calibrated.

The preincident V/C ratio of each incident was firstly calculated by dividing the preincident traffic flow by the capacity which is generated from the capacity function with rainfall intensity effects [$C(r)$]. The speed at capacity were calculated with Eq. (5.3) in which the free-flow speed function with rainfall intensity effects [$v_f(r)$] and parameter η are calibrated explicitly.

For each input traffic stream parameter, the incidents in the calibration database were divided into several groups according to their preincident V/C ratio interval. These V/C ratio intervals were as follows: (0, 0.1], (0.1, 0.2] … (0.9, 1]. Incidents in each preincident V/C ratio interval were used to calibrate the corresponding detection threshold. The calibrated detection thresholds together with their corresponding upper bounds of V/C ratio intervals were finally used to calibrate the generalized detection threshold function (Eq. 5.1) for each input traffic stream parameter.

For the sake of simplicity, the traffic density at the upstream detector is taken as an example to demonstrate the calibration of the generalized detection threshold function.

For each V/C ratio interval, corresponding incidents were used to calibrate the detection thresholds with the same method described in Chapter 4. A range of possible parameter and detection threshold values were analyzed to generate detection performance measurements (DR-FAR pairs and the corresponding MTTD). For consistency, the parameters and detection thresholds were determined when the FAR reaches the acceptable FAR limit of 1.8% (Abdulhai, 1996).

The calibrated detection thresholds and their corresponding V/C ratios were then used to fit the generalized detection threshold function [Eq. (5.1)]. Fig. 5.4 shows the fitted generalized detection threshold function for the traffic density at the upstream detector.

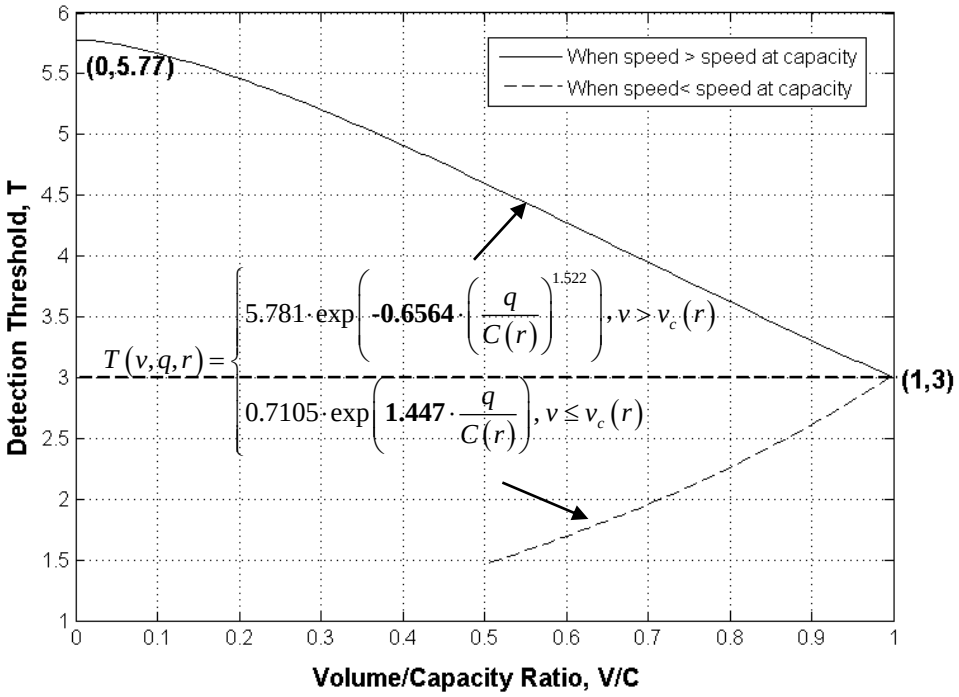

Fig. 5.4 Calibrated generalized detection threshold function for traffic density at the upstream detector

It is shown in Fig. 5.4 that the detection threshold for traffic density at the upstream detector decreases as the V/C ratio increases when traffic speed is higher than the speed at capacity (i.e. $v > v_c$). For instance, the detection threshold decreases from 5.77 to 3 when the V/C ratio increases from 0 to 1. This

is also reflected by the negative coefficient of the V/C ratio (i.e. -0.6564) in the generalized detection threshold function in Fig. 5.4. When the traffic becomes more congested (i.e. $v < v_c$), the detection threshold decreases when the V/C ratio inversely decreases from 1 to 0. The positive coefficient of the V/C ratio (i.e. 1.447) also reflects the increasing trend of the detection threshold under congested conditions (i.e. $v < v_c$). Under congested traffic conditions, the incident tends to cause more significant effects on the magnitudes of the traffic disturbances. A slight incident may block the road and significantly reduce the traffic speed at upstream of the incident spot. Therefore, the traffic disturbances under congested conditions can be detected with a relatively small detection threshold.

The increase of the preincident traffic flow and the decrease of the capacity can both increase the V/C ratio, and thus increasing the congestion level. When the rainfall intensity increases, the capacity decreases and thus the V/C ratio increases at a given preincident traffic flow. Therefore, both the preincident traffic flow and rain intensity are considered explicitly for threshold determination. The generalized detection threshold function can also generate more reasonable continuous detection thresholds instead of discrete ones.

Similar to the calibration of the generalized detection threshold function for the density at the upstream detector, the generalized detection threshold functions for the other input traffic stream parameters were calibrated with the same method. These generalized detection threshold functions are shown in Table 5.4.

Table 5.4 Generalized Detection Threshold Functions for Various Input Traffic Stream Parameters

Input traffic stream parameter	Generalized detection threshold function
Density at the upstream detector	$T(v,q,r)=\begin{cases}5.781\cdot\exp\left(-0.6564\cdot\left(\frac{q}{C(r)}\right)^{1.522}\right), v>v_c(r)\\ 0.7105\cdot\exp\left(1.447\cdot\frac{q}{C(r)}\right), v\le v_c(r)\end{cases}$
Density at the downstream detector	$T(v,q,r)=\begin{cases}-5.843\cdot\exp\left(-0.6193\cdot\left(\frac{q}{C(r)}\right)^{1.874}\right), v>v_c(r)\\ -0.6178\cdot\exp\left(1.6094\cdot\frac{q}{C(r)}\right), v\le v_c(r)\end{cases}$
Coefficient of variation of speed (CVS) at the upstream detector	$T(v,q,r)=\begin{cases}4.543\cdot\exp\left(-0.7432\cdot\left(\frac{q}{C(r)}\right)^{1.813}\right), v>v_c(r)\\ 0.3898\cdot\exp\left(1.8202\cdot\frac{q}{C(r)}\right), v\le v_c(r)\end{cases}$
Speed at the upstream detector	$T(v,q,r)=\begin{cases}-5.093\cdot\exp\left(-0.6892\cdot\left(\frac{q}{C(r)}\right)^{2.17}\right), v>v_c(r)\\ -0.2976\cdot\exp\left(2.1203\cdot\frac{q}{C(r)}\right), v\le v_c(r)\end{cases}$
Correlation coefficient of speeds (CCS) of two adjacent detectors	$T(v,q,r)=\begin{cases}-4.178\cdot\exp\left(-0.7751\cdot\left(\frac{q}{C(r)}\right)^{1.422}\right), v>v_c(r)\\ -0.4524\cdot\exp\left(1.4384\cdot\frac{q}{C(r)}\right), v\le v_c(r)\end{cases}$
Instantaneous journey time between two adjacent detectors	$T(v,q,r)=\begin{cases}3.698\cdot\exp\left(-1.024\cdot\left(\frac{q}{C(r)}\right)^{1.914}\right), v>v_c(r)\\ 0.4524\cdot\exp\left(1.4384\cdot\frac{q}{C(r)}\right), v\le v_c(r)\end{cases}$

Note: T denotes detection threshold; q denotes traffic flow; v denotes traffic speed; r denotes rainfall intensity; v_c denotes speed at capacity; $C(r)$ denotes capacity function with rainfall intensity effects.

The relationships between the detection threshold and the V/C ratio for various input traffic stream parameters are further shown in Fig. 5.5. The detection threshold values for T_v, T_{d_d}, and T_{CCS} are negative because they tend to decrease

after incidents. The detection threshold values for T_{cvs}, T_{d_u}, and T_{τ} are positive because they tend to increase after incidents.

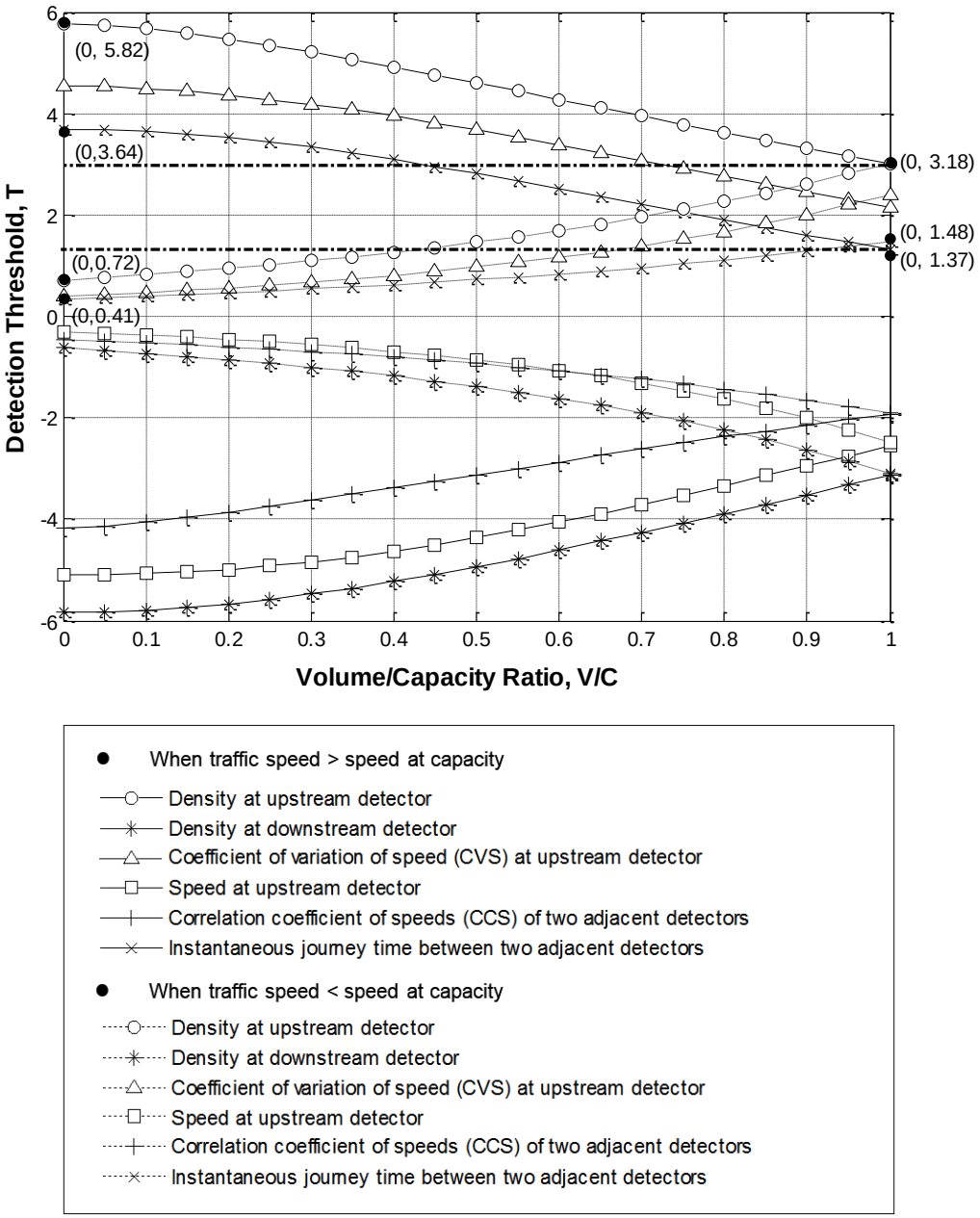

Fig. 5.5 Relationships between the detection thresholds and volume/capacity ratios for various input traffic stream parameters

It is shown in Fig. 5.5 that the absolute values of the detection thresholds for all input data decrease with the increasing V/C ratio when the traffic speed (v) is greater than the speed at capacity (v_c). For instance, the detection threshold for the density at upstream detectors decreases from 5.82 to 3.18 when the V/C ratio

increases from 0 to 1 when $v > v_c$. When $v > v_c$, the increase of traffic flow results in increasing V/C ratio and more congested traffic conditions. When the traffic condition is more congested, the incidents tend to cause more significant effects on the magnitudes of the traffic disturbances. For instance, a slight incident may block the road and significantly reduce the traffic speed at the upstream of the incident. Therefore, the incident-induced traffic disturbances under more congested conditions can be detected with a smaller detection threshold.

When the traffic speed decreases to be smaller than the speed at capacity (i.e. $v < v_c$), the absolute values of detection thresholds inversely decrease with the decreasing V/C ratio. For instance, the detection threshold for instantaneous journey time decreases from 3.18 to 0.72 when the V/C ratio inversely decreases from 1 to 0 when $v < v_c$. Based on the traffic flow theory, when $v < v_c$, the ever-increasing vehicles would not further increase the traffic flow beyond capacity. The ever-increasing vehicles when $v < v_c$ results in a decreasing traffic flow and hence a decreasing V/C ratio. In other words, the traffic becomes more congested with the decreasing V/C ratio when $v < v_c$. Therefore, the detection thresholds tend to decrease with the decreasing V/C ratio when $v < v_c$. When the traffic becomes more congested with the decreasing V/C ratio when $v < v_c$, the slight incident-induced traffic disturbances can be detected by a relatively small detection threshold.

The absolute values of the detection thresholds for density at upstream and downstream detectors are found to be larger than those of the other input traffic parameters in Fig. 5.5. For instance, the detection threshold for the density at the upstream detector is 5.82 when the V/C ratio is 0, greater than the 3.64 for the instantaneous journey time. This indicates that the upstream occupancy is more sensitive to the incident-induced traffic disturbances than other traffic stream parameters. When the absolute value of the detection threshold is large, only those traffic parameters with high sensitivity can be detected. The sensitivities of the selected input traffic stream parameters to incident-induced traffic disturbances are listed in descending order as follows: (1) the density at the

downstream detector, (2) the density at the upstream detector, (3) speed at the upstream detector, (4) the CVS at the upstream detector, (5) the CCS of two adjacent detectors, and (6) the instantaneous journey time between adjacent two detectors.

It is worth noting that a slight difference exists between the detection thresholds when V/C=1 which are respectively calibrated when $v < v_c$ and $v > v_c$. For instance, the detection threshold when V/C=1 for the instantaneous journey time, which is calibrated based on the data when $v > v_c$, is 1.37. However, the detection threshold when V/C=1 which is estimated based on the data when $v < v_c$, is 1.48.

The capacity function and speed at capacity function with rainfall intensity effects (i.e. $C(r)$ and $v_c(r)$) for roads with each speed limit were then plugged into the calibrated generalized detection threshold functions as shown in Table 5.5. For instance, the generalized detection threshold function for the density at the upstream detector on the expressways/trunk roads with a speed limit of 80 km/h [Eq. (5.9)] can be derived with Eqs. (5.5) - (5.8).

$$C(r) = \exp\left(-0.06951 \cdot r^{0.2347} + 7.470\right) \tag{5.5}$$

$$v_f(r) = \exp\left(-0.045 \cdot r^{0.315} + 4.390\right) \tag{5.6}$$

$$v_c(r) = \exp(-0.673) \cdot v_f(r) \tag{5.7}$$

$$T(v,q,r) = \begin{cases} 5.781 \cdot \exp\left(-0.6564 \cdot \left(\dfrac{q}{C(r)}\right)^{1.522}\right), v > v_c(r) \\ 0.7105 \cdot \exp\left(1.447 \cdot \dfrac{q}{C(r)}\right), v \le v_c(r) \end{cases} \tag{5.8}$$

$$T(v,q,r) = \begin{cases} 5.781 \cdot \exp\left(-0.6564 \cdot \left(\dfrac{q}{\exp\left(-0.06951 \cdot r^{0.2347} + 7.470\right)}\right)^{1.522}\right), v > \exp\left(-0.045 \cdot r^{0.315} + 3.717\right) \\ 0.7105 \cdot \exp\left(1.447 \cdot \dfrac{q}{\exp\left(-0.06951 \cdot r^{0.2347} + 7.470\right)}\right), v \le \exp\left(-0.045 \cdot r^{0.315} + 3.717\right) \end{cases} \tag{5.9}$$

where $C(r)$ = the capacity function with rainfall effects (veh/h/lane); r = the rainfall intensity (mm/h); q = the traffic flow (or traffic volume) (veh/h/lane); $v_c(r)$ = the speed at capacity with rainfall intensity effects (veh/h/lane); $v_f(r)$ = the free-flow speed function with rainfall intensity effects (km/h).

In application, the detection threshold for upstream traffic density on expressway/trunk roads with a speed limit of 80 km/h can be calculated with Eq. (5.9) given the preincident traffic speed, flow and rainfall intensity.

For other input traffic stream parameters, the corresponding generalized detection threshold functions on roads with various speed limits can also be obtained with the same method as described above.

5.6 Algorithm Validations

The proposed flow-rain-dependent ESND algorithm was applied to the validation database in order to examine its incident detection performance. The traffic incidents in 2011 together with their corresponding traffic and rainfall intensity data were used for validation.

Similar to the validation of the flow-dependent ESND algorithm in Chapter 4, the lowest FAR and the corresponding MTTD for each DR were chosen as the final performance of the proposed flow-dependent ESND algorithm.

The DR and the FAR together with the MTTD were plotted to illustrate the incident detection performance of the proposed flow-rain-dependent ESND algorithm. The flow-dependent ESND algorithm was also recalibrated on the basis of the collected data on study road network and applied to the same validation database. Calibration details are similar to those given in Chapter 4. The incident detection performances of the proposed flow-dependent and flow-rain-dependent ESND algorithms were compared and are shown in Fig. 5.6.

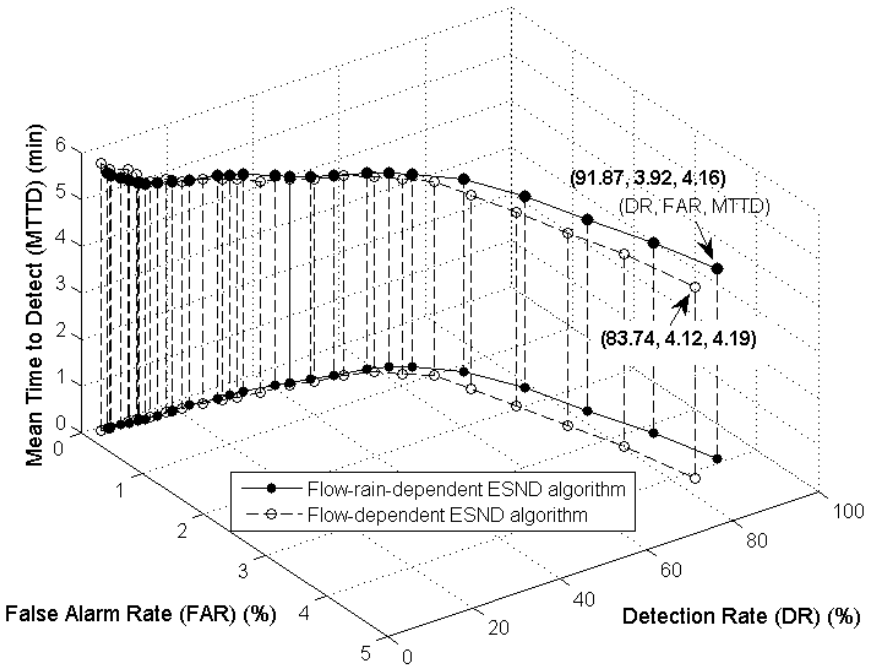

Fig. 5.6 Incident detection performance of flow-rain-dependent ESND algorithm and flow-dependent ESND algorithm

It is shown in Fig. 5.6 that the proposed flow-rain-dependent ESND algorithm outperforms the flow-dependent ESND algorithm. The proposed flow-rain-dependent ESND algorithm detected about 91.87% of incidents when the FAR was 3.92%, higher than the highest 83.74% of the flow-dependent ESND algorithm with a higher FAR of 4.12%. The MTTD of the flow-rain-dependent ESND algorithm is 4.16 minutes, shorter than the 4.19 minutes of the flow-dependent ESND algorithm. In other words, the proposed flow-rain-dependent ESND algorithm detected more incidents with fewer false alarms and a shorter MTTD. This can be explained by the continuous detection thresholds in which both preincident traffic and rain conditions are considered explicitly.

The largest FAR of the proposed flow-rain-dependent ESND algorithm was 3.92%, which is equivalent to about 28 false alarms per day. In other words, the traffic operator may have to dispose about 28 false alarms per day.

A trade-off between DR, FAR and MTTD is also found in Fig. 5.6. The DR decreases with the increasing FAR, while the MTTD increases.

The data points on the performance curve in Fig. 5.6 correspond to combinations of parameters and detection thresholds for different traffic incidents. For each traffic incident, the parameters and detection thresholds for different input traffic stream parameters are different. For instance, Table 5.5 shows the values of parameters and thresholds for the selected traffic incident in Chapter 3 when the DR is 91.87%, the FAR is 3.92% and the MTTD is 4.16 minutes.

Table 5.5 The Values of Parameters and Thresholds for the Selected Incident in Chapter 3 when the DR is 91.87%, the FAR is 3.92% and the MTTD is 4.16 Minutes

Input traffic stream parameter	Number of time intervals over the sampling period (n)	Threshold for the coefficient of variation of input data (θ)	Detection threshold (T)
Instantaneous journey time	5	0.2	2.72
CCS of two adjacent detectors	8	0.15	-2.61
Speed at upstream detector	6	0.1	-3.85
CVS at upstream detector	6	0.15	3.83
Density at upstream detector	5	0.1	3.98
Density at downstream detector	5	0.15	-3.35

Notes: CCS denotes the correlation coefficient of speeds;
CVS denotes the coefficient of variation of speeds.

It can be seen from Table 5.5 that the detection threshold values are different from the discrete ones whose incremental values is 0.5 in Table 4.1. These continuous detection threshold values are calculated by the generalized detection threshold functions for each traffic incident. Different input traffic stream parameters have different detection thresholds. The continuous detection thresholds are more reasonable in application.

It is worth noting that the detection performance of the proposed flow-rain-dependent ESND algorithm did not meet the acceptable limits with a minimum DR of 88% and a maximum FAR of 1.8% (Abdulhai, 1996). The incident detection performance of the proposed flow-dependent ESND algorithm on the study road network was also not as good as that on the selected road section in Chapter 4. This is because of: (1) more road segments with traffic detectors at the ends, and (2) some larger detector spacing on the study road network as shown

in Table 5.6.

Table 5.6 Comparison between the Features of the Study Road Section presented in Chapter 4 and the Study Road Network presented in Chapter 5

Feature	Selected road section in Hong Kong island	Urban road network under the Journey Time Indication System (JTIS)
Number of road segments with traffic detectors at the ends	**6**	**29**
Mean of detector spacing (km)	0.94	1.34
Standard deviate of detector spacing (km)	0. 42	0.48

It can be seen in Table 5.6 that the mean and standard deviate of detector spacing on the study road network are larger than those on the selected road section in Chapter 4. The relatively longer detector spacing on the study road network degrades the detection performance of the proposed flow-dependent ESND algorithm. In addition, the 28 road segments with traffic detectors installed at the ends, are also more than the only 6 road segments in Chapter 4. When traffic data from more road segments are used to calibrate and validate the AID algorithms, the factors such as road configuration and sight distance on different road segments would certainly influence the incident-induced traffic disturbances and thus the detection performance of AID algorithms.

5.7 Comparison with Existing AID Algorithms

The proposed flow-rain-dependent ESND algorithm was also compared with the five selected existing AID algorithms as indicated in Chapter 4. These AID algorithms are standard normal deviate (SND) algorithm (Dudek et al., 1974), California #7 algorithm (Payne et al., 1976), double exponential smoothing (DES) algorithm (Cook and Cleveland, 1974), Minnesota algorithm (Stephanedes and Chassiakos, 1993) and flow-dependent combined detector evaluation (CODE) algorithm (Mak and Fan, 2007).

These five existing AID algorithms were again calibrated through methods in previous studies (Mak and Fan, 2005) with the collected traffic data on the study road network. As indicated in Chapter 4, only combinations of the parameter and threshold values corresponding to the lowest FAR at each DR were selected.

The detection performances of these five existing AID algorithms and the proposed flow-rain-dependent ESND algorithm were compared and are shown in Fig. 5.7. As described in Section 4.8, the five existing AID algorithms are also numbered and classified into single-station or dual-station algorithms as shown in Table 4.2.

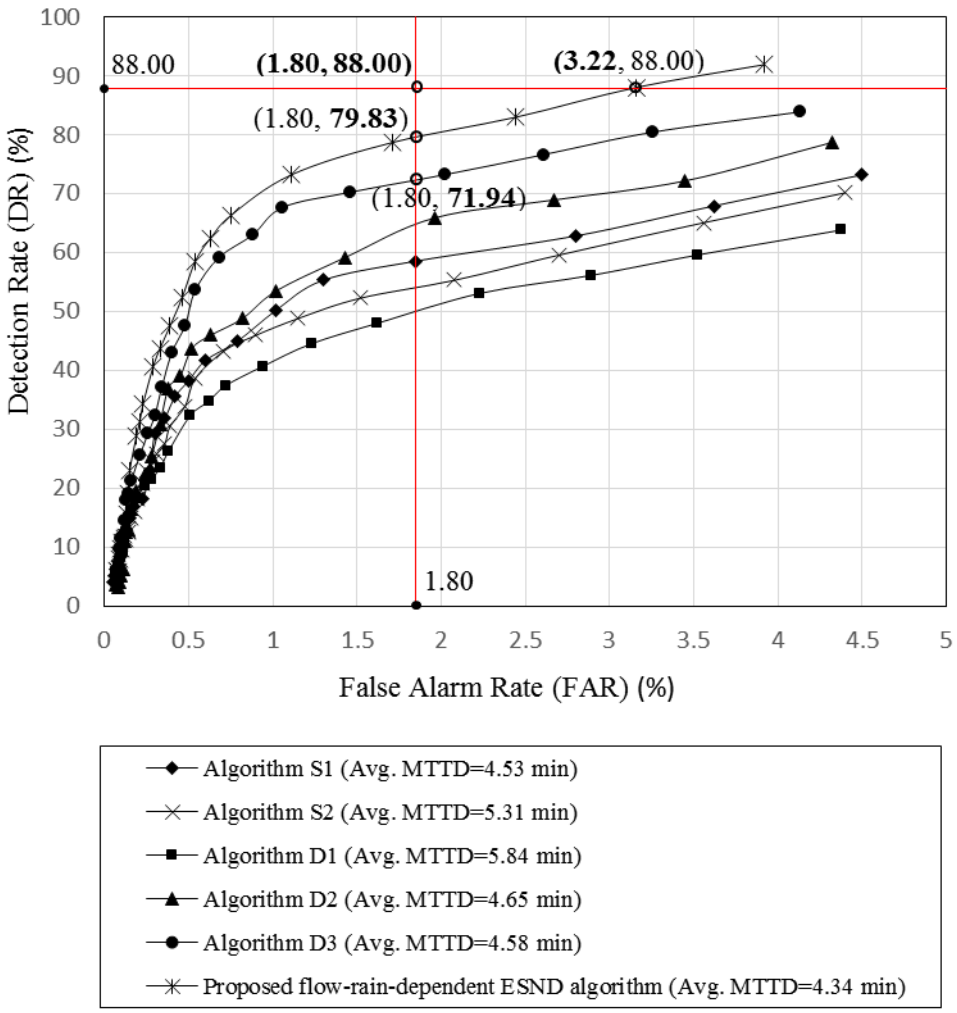

Fig. 5.7 Comparison of the performances of the proposed flow-rain-dependent ESND algorithm and existing AID algorithms

As shown in Fig. 5.7, the proposed flow-rain-dependent ESND algorithm also outperforms the five selected AID algorithms on the basis of the available data collected on the study road network. For instance, when the FAR is fixed to be the acceptable limit of 1.8% (Abdulhai, 1996), the DR of the proposed flow-rain-dependent ESND algorithm is 79.83%, higher than the 71.94% of the

flow-dependent CODE algorithm (D3). Additionally, the average MTTD (i.e. 4.34) of the proposed flow-rain-dependent ESND algorithm is shorter than those of the five selected AID algorithms.

However, the acceptable minimum DR limit (88%) and the maximum FAR limit (1.8%) (Abdulhai, 1996) cannot be obtained simultaneously by all these AID algorithms when applied to the study road network. When the DR of the proposed flow-rain-dependent ESND algorithm is 88%, the corresponding FAR is 3.22%, higher than the acceptable limit of 1.8%. This indicates that the performance of the proposed flow-rain-dependent ESND algorithm on the territory-wide basis is inferior to that on the study road section in Chapter 4. This is mainly because of the relative larger detector spacing, more complex road configuration and more varying sight distances on the study road network. However, the proposed flow-rain-dependent ESND algorithm is still feasible for use in detecting incidents under both no-rain and rain conditions on a territory-wide basis.

5.8 Estimation of the Generalized Detection Threshold Functions for Various Speed Limits

The generalized detection threshold functions for roads with different speed limits (i.e. 50, 60, 70 and 80 km/h) are calibrated with corresponding collected data in Section 5.5. In practice, it is of value to estimate the generalized detection threshold function for a road with a certain speed limit such as 90 km/h, especially when the data on this road are not available for calibration. The generalized detection threshold function for roads with a certain speed limit can be estimated on the basis of the collected data on roads with the other speed limits.

As shown in Table 5.5, the generalized detection threshold functions [$T(q,v,r)$] for various input traffic stream parameters are functions of the traffic flow (q), capacity function with rainfall intensity effects [$C(r)$], traffic speed (v), and speed at capacity function with rainfall intensity effects [$v_c(r)$]. For instance, the generalized detection threshold function for the speed/flow at the upstream detector is shown as Eq. (5.10). The relationship between the speed at capacity

and free-flow speed [Eq. (5.11)] can be obtained from Eq. (5.3) in Section 5.4.

$$T(q,v,r)=\begin{cases}5.781\cdot\exp\left(-0.6564\cdot\left(\dfrac{q}{C(r)}\right)^{1.522}\right), v>v_c(r)\\ 0.7105\cdot\exp\left(1.447\cdot\dfrac{q}{C(r)}\right), v\le v_c(r)\end{cases} \tag{5.10}$$

$$\eta=\frac{-1}{\ln\left(\dfrac{v_c}{v_f}\right)} \tag{5.11}$$

where *C(r)* = the capacity function with rainfall intensity effects (veh/h/lane); *r* = the rainfall intensity (mm/h); *q* = the traffic flow (or traffic volume) (veh/h/lane); *v* = the traffic speed (km/h); $v_c(r)$ = the speed at capacity function with rainfall intensity effects (km/h); η = the parameter to be calibrated; $v_f(r)$ = the free-flow speed function with rainfall intensity effects (km/h).

In order to estimate the generalized detection threshold function for a road with a certain speed limit, the capacity function with rainfall intensity effects [$C(r)$], free-flow speed function with rainfall intensity effects [$v_f(r)$] and parameter η on this road need to be firstly estimated.

In this Section, the data collected on roads with speed limits of 50, 70 and 80 km/h were used to estimate the generalized detection threshold function for roads with a speed limit of 60 km/h. The data collected on roads with a speed limit of 60 km/h were used for validation.

The capacity function with rainfall intensity effects [$C(r)$] for roads with a speed limit of 60 km/h was firstly interpolated on the basis of functions for speed limits of 50, 70 and 80 km/h with the following steps:

Step 1: Generate rainfall intensity values from 0 to 10 mm/h with an incremental value of 0.1 mm/h.

Step 2: For each rainfall intensity value, the capacities for roads with speed limits of 50, 70 and 80 km/h were individually calculated by the corresponding capacity functions with rainfall intensity effects in Table 5.2. The calculated capacity values for roads with speed limits of 50, 70 and 80 km/h were the used to estimate the capacity for roads with the speed limit of 60 km/h. Several function forms such as linear, polynomial and exponential functions were tried to fit the relationship between the speed limit and capacity. Finally, the exponential function fitted best. The fitted exponential function was then used to calculate the capacity for roads with the speed limit of 60 km/h. For other rainfall intensity values, the corresponding capacities for roads with the speed limit of 60 km/h were calculated with the same method.

Step 3: With the calculated capacities for each rainfall intensity value, the exponential function form was again used to fit the relationship between the capacity and rainfall intensity. Finally, the capacity function with rainfall intensity effects for roads with the speed limit of 60 km/h was estimated as shown in Eq. (5.12).

$$C'(r) = \exp(-0.10313 \cdot r^{0.2039} + 7.242) \tag{5.12}$$

where r = the rainfall intensity (mm/h).

The free-flow speed function [$v_f(r)$] for roads with the speed limit of 60 km/h was also interpolated with the same method as indicated above. The estimated free-flow speed function with rainfall intensity effects is shown as follows:

$$v'_f(r) = \exp\left(-0.043 \cdot r^{0.280} + 4.095\right) \tag{5.13}$$

where r = the rainfall intensity (mm/h).

The parameter η for roads with the speed limit of 60 km/h was also interpolated on the basis of the values of η on roads with the other speed limits. The values of η on roads with speed limits of 50, 70 and 80 km/h were calibrated on the basis of the collected data. The exponential function form was again found to best fit the relationship between the speed limit (L) and parameter η. The relationship

between the parameter η and speed limit (L) is modelled as follows:

$$\eta' = 2.096 \cdot \exp(-0.004431 \cdot L) \tag{5.14}$$

where L = the speed limit (km/h).

When the speed limit is 60 km/h, the estimated parameter η' is 1.61. The estimated speed at capacity function for the speed limit of 60 km/h [Eq. (5.15)] can be derived from Eq. (5.3) with the estimated parameter η and free-flow speed function with rainfall intensity effects [Eq. (5.13)].

$$v'_c(r) = \exp\left(-0.043 \cdot r^{0.280} + 3.474\right) \tag{5.15}$$

where r = the rainfall intensity (mm/h).

With the estimated capacity function with rainfall intensity effects [Eq. (5.11)] and the speed at capacity function with rainfall intensity effects [Eq. (5.14)], the estimated generalized detection threshold function [$T'(v,q,r)$] for the speed/flow at the upstream detector on roads with a speed limit of 60 km/h can be derived from Eq. (5.9) as follows:

$$T'(v,q,r) = \begin{cases} 5.781 \cdot \exp\left(-0.6564 \cdot \left(\dfrac{q}{\exp(-0.10313 \cdot r^{0.2039} + 7.242)}\right)^{1.522}\right), v > \exp\left(-0.043 \cdot r^{0.280} + 3.474\right) \\ 0.7105 \cdot \exp\left(1.447 \cdot \dfrac{q}{\exp(-0.10313 \cdot r^{0.2039} + 7.242)}\right), v \le \exp\left(-0.043 \cdot r^{0.280} + 3.474\right) \end{cases} \tag{5.15}$$

where v = the traffic speed (km/h); q = the traffic flow (or traffic volume) (veh/h/lane); r = the rainfall intensity (mm/h).

The real generalized detection threshold function [$T(v,q,r)$] for the speed/flow at the upstream detector on roads with a speed limit of 60 km/h, which has been calibrated in Section 5.5, are shown as follows:

$$T(v,q,r) = \begin{cases} 5.781 \cdot \exp\left(-0.6564 \cdot \left(\dfrac{q}{\exp(-0.10301 \cdot r^{0.2037} + 7.248)}\right)^{1.522}\right), v > \exp\left(-0.044 \cdot r^{0.278} + 3.476\right) \\ 0.7105 \cdot \exp\left(1.447 \cdot \dfrac{q}{\exp(-0.10301 \cdot r^{0.2037} + 7.248)}\right), v \le \exp\left(-0.044 \cdot r^{0.278} + 3.476\right) \end{cases} \tag{5.16}$$

where v = the traffic speed (km/h); q = the traffic flow (or traffic volume) (veh/h/lane); r = the rainfall intensity (mm/h).

The detection thresholds, generated by the estimated generalized detection threshold function, were compared with those generated by the real generalized detection threshold function. The detection thresholds were calculated by varying the rainfall intensity from 0 to 10 mm/h with an incremental value of 0.5 and varying the traffic flow from 0 to 1200 veh/h/lane with an incremental value of 1. For each pair of rainfall intensity and traffic flow values, the corresponding detection threshold values was calculated by both the real and estimated generalized detection threshold functions.

The mean absolute error (MAE) and the mean absolute percentage error (MAPE) which reflect the predictability accuracy of the estimated generalized detection threshold function were calculated. The MAE and MAPE of the speed at capacity were 0.600 and 1.858%. When the traffic speed is higher than the speed at capacity, the MAE and MAPE of the detection threshold were 0.002 and 0.028%. The MAE and MAPE of the detection threshold were 0.046 and 5.920% when the traffic speed is lower than the speed at capacity. The results indicate that the accuracy of the estimated generalized detection threshold function is better when applied under uncongested conditions than congested conditions. However, the overall accuracy of the estimated generalized detection threshold function is satisfactory.

The method in this Section can be used to estimate the generalized detection threshold functions for roads with various speed limits. For instance, when the data on roads with speed limits of only 60, 70, 90 and 110 km/h are available for use, the generalized detection threshold function for roads with speed limits of 80 and 100 km/h can be estimated.

5.9 Summary

A flow-rain-dependent ESND algorithm for incident detection under both no-rain and rain conditions was proposed in this Chapter. Continuous detection thresholds were determined by the generalized detection threshold functions in which both preincident traffic and rainfall conditions are considered explicitly. Traffic data,

incident data and rainfall intensity data collected on the urban road network under the JTIS in Hong Kong were used to calibrate and validate the proposed algorithm. The largest DR of the proposed flow-rain-dependent ESND algorithm was 91.87% when applied to the validation database. Its corresponding FAR is 3.92%, meaning that about one false alarm will be triggered every 50 minutes. On average, the proposed flow-rain-dependent ESND algorithm took 4.16 minutes to detect incidents.

The detection performance of the proposed flow-rain-dependent ESND algorithm on the territory-wide basis was found to be not as good as that on only one road section in Chapter 4. This is mainly attributed to the relative larger detector spacing, more complex road configuration and more varying sight distances on the study road network. However, the proposed flow-rain-dependent ESND algorithm is indeed promising as regards its use in detecting incidents on a territory-wide basis.

The interrelationship of the DR, FAR and MTTD of the proposed flow-rain-dependent ESND algorithm was plotted in a three-dimensional figure to show the trade-off between these three performance measurements. The proposed flow-rain-dependent ESND algorithm in this Chapter was also compared with the flow-dependent ESND algorithm in which only preincident traffic flow is considered. It is found that the inclusion of the impact of the rain condition in detection threshold determination could improve the overall detection performance.

The proposed flow-rain-dependent ESND algorithm was also compared with the five selected existing AID algorithms described in Chapter 4. The comparison results showed that, on a territory-wide basis, the proposed flow-rain-dependent ESND algorithm still outperforms the other five existing AID algorithms.

Instead of the traffic flow, the volume/capacity (V/C) ratio was used to indicate the preincident traffic condition in the proposed flow-rain-dependent ESND algorithm. The V/C ratio better describes the congestion level or level of service on roads. To overcome the shortcomings of discrete detection thresholds in previous flow-dependent AID algorithms, continuous detection thresholds were adopted.

These continuous detection thresholds were generated by the calibrated generalized detection threshold functions in which both preincident traffic and rain conditions are modeled explicitly.

Given the same preincident traffic flow, the detection threshold was found to decrease with the increasing rainfall intensity. This is because, given the same traffic flow, the capacity is reduced under rain conditions. Thus, the V/C ratio which describes the road congestion level increases. In other words, the traffic becomes more congested when rainfall intensity increases at a given traffic flow. Under more congested traffic conditions, incident-induced traffic disturbances are more easily detected by relatively small detection thresholds.

A method was also proposed in this Chapter to estimate the generalized detection threshold functions for roads with various specific speed limits. With the use of the available data collected on roads with certain speed limits, the generalized detection threshold function on roads with other speed limits can be estimated. The detection threshold values, generated by the estimated and the real generalized detection threshold function for the density at the upstream detector on roads with a speed limit of 60 km/h, are compared. The small mean absolute error and mean absolute percentage error of the estimation results indicated a satisfactory predictability accuracy of this estimation method.

The flow-rain-dependent ESND algorithm proposed in this Chapter needs to be further calibrated and validated with more traffic and incident data particularly under rain conditions.

Chapter 6. Conclusions and Recommendations for Further Research

6.1 Conclusions

Incident detection has been one of the critical components for making incident management effectively. Incident detection problems such as high false alarm rates, strict traffic detector installation and data quality requirements have reduced the effectiveness of the existing automatic incident detection (AID) algorithms, particularly under adverse weather conditions. Additionally, the existing AID algorithms are usually developed on the basis of specific-designed detector data for different road types under a certain environment. In general, the traffic data collected on urban roads, which were originally used for journey time estimation purpose, may not be suitable for the development of AID algorithms using conventional methods and traffic stream parameters.

Additionally, these conventional methods and the associated traffic stream parameters for incident detection may not be appropriate to Hong Kong local conditions as the necessary rainfall data have not been considered. The substantial rainfall throughout the year in Hong Kong would certainly affect the effectiveness of existing AID algorithms. In view of the above, it is essential to develop reliable AID algorithms on the basis of the readily available traffic data, collected from infrastructures relevant to the targeted area in Hong Kong, by considering the substantial rain conditions.

The study presented in this thesis has demonstrated the development of AID algorithms under both no-rain and rain conditions on the basis of the available traffic data collected in Hong Kong for journey time estimation purpose only. The previous standard normal deviate (SND) algorithm was firstly extended to be an extended standard normal deviate (ESND) algorithm by (1) adopting the weighting method and (2) restricting the input data variation within sampling periods.

With consideration of the preincident traffic flow condition, a flow-dependent

ESND algorithm was proposed for incident detection under no-rain conditions. A more generalized flow-rain-dependent ESND algorithm was then proposed for incident detection under both no-rain and rain conditions. Both preincident traffic and rain condition were considered in the proposed flow-rain-dependent ESND algorithm for the detection threshold determination. The proposed flow-rain-dependent ESND algorithm adopted continuous detection thresholds which are generated by a generalized detection threshold function. Traffic data, incident data and rainfall data collected on the study road network under the Hong Kong Journey Time Indication System (JTIS) were used to calibrate and validate the two proposed algorithms.

The proposed flow-dependent ESND algorithm was calibrated and applied to a selected road section in Hong Kong Island. The proposed algorithm detected about 93.75% of the traffic incidents on the basis of the validation database. The false alarm rate (FAR) was about 1.134%, which means that about 8 false alarms per day. The mean time to detect (MTTD) was 4.15 min, which is about twice the data aggregate time interval (i.e., 2 min) because the proposed flow-dependent ESND algorithm needs a second-time interval to conduct persistence tests. With the persistence test, the false alarm rate was reduced from 1.953% to 1.134% at the cost of a longer average MTTD. In other words, the persistence test reduced the daily false alarms from 14 to 8 by about 42%. Although the MTTD of the proposed flow-dependent ESND algorithm is greater than those of previous studies (Parkany and Xie, 2005; Mak and Fan, 2006a), it is still reasonable because the aggregate time interval of traffic data in Hong Kong is greater than the more widely used 20-60 seconds (Mak and Fan, 2006a).

It was shown in this research that the consideration of the preincident traffic flow condition would improve the detection performance of the proposed flow-dependent ESND algorithm. It was found in the case study that the difference between the MTTDs of the flow-dependent and flow-independent ESND algorithm was relatively small. The FAR, however, was significantly reduced when the preincident traffic flow condition was considered in the proposed flow-dependent ESND algorithm.

Incident detection performance was further improved after adopting two

proposed extensions to the previous SND algorithm: (1) the adoption of the weighting method and (2) the restriction of the input data variation within sampling periods. Compared with the five selected existing AID algorithms, the proposed flow-dependent ESND algorithm has proven capable of reducing the FAR while maintaining a high DR and a shorter MTTD.

In this research, two new traffic stream parameters were also proposed as indicators for detecting incidents. They are: (1) the coefficient of variation of speed (CVS) at the upstream detector and (2) the correlation coefficient of speeds (CCS) of two adjacent detectors. These two new traffic stream parameters have proved feasible indicators of traffic incidents. The CVS at the upstream detector describes the traffic stream changes from the homogeneous pattern to the stop-and-go pattern. The CCS of two adjacent detectors indicates the opposite trend of changes of upstream speed and downstream speed over time.

On the basis of the hybrid traffic data obtained from both the video traffic detectors and automatic vehicle identification (AVI) readers under the JTIS in Hong Kong, the proposed AID algorithms achieved good results in terms of a higher DR, a lower FAR and a shorter MTTD. Different traffic stream parameters respond differently to traffic incidents in both time and magnitude. The adoption of hybrid input data may make use of the strengths of different traffic stream parameters and effectively increase the DR and reduced the MTTD.

The instantaneous journey time and the CCS of two adjacent detectors are dual-station data which are calculated on the basis of traffic data collected from dual detector stations. The traffic speeds at the upstream detector, density at the upstream detector, density at the downstream detector, and the CVS at the upstream detector are single-station data which are collected from single detector stations. The adoption of both the single-station and dual-station input data enhanced the ability of the proposed algorithms to possess the strengths of both single-station and dual-station algorithms. With single-station input data, AID algorithms are more adaptive with fewer impacts from variations in road geometry, detector spacing, the presence of on/off ramps and the prevailing traffic condition. The use of dual-station input data (e.g. the CCS of two adjacent detectors) provides additional information other than single-station input data.

The proposed flow-rain-dependent ESND algorithm was calibrated and applied to the study road network under the JTIS in Hong Kong. The accident data in 2010 with corresponding traffic and rainfall intensity data were used for calibration. When applied to the database in 2011, the calibrated proposed flow-rain-dependent ESND algorithm detected 91.91% of incidents with a false alarm rate (FAR) of 3.92%. The MTTD is 4.16 minutes.

The proposed flow-rain-dependent ESND algorithm was also compared with the flow-dependent ESND algorithm in which only the preincident traffic flow condition is considered for the detection threshold determination. The flow-rain-dependent ESND algorithm outperformed the flow-dependent ESND algorithm, indicating that the consideration of both rainfall intensity and traffic flow in the detection threshold determination could improve the overall detection performance. The proposed flow-rain-dependent ESND algorithm has proved effective in incident detection on the territory-wide basis.

The flow-rain-dependent ESND algorithm with consideration of both traffic and rain conditions outperformed the flow-dependent ESND algorithm. The adoption of the continuous detection thresholds, generated by a generalized detection threshold function, are more sensible and reasonable in practice.

In the proposed flow-rain-dependent ESND algorithms, the preincident volume/capacity (V/C) ratio is adopted to describe the traffic conditions. The V/C ratio can better describe the road congestion level. The generalized detection threshold is a function of the V/C ratio in which the effects of the rainfall intensity on the capacity, free-flow speed and speed at capacity can be modeled explicitly.

In this research, the interrelationship of the detection rate (DR), FAR, and MTTD of the flow-dependent and flow-rain-dependent ESND algorithms are illustrated in three-dimensional figures. A trade-off exists between these three performance measurements. When the increasing detection threshold, both the DR and FAR of the AID algorithms decrease and the MTTD increases.

6.2 Recommendations for Further Research

Although the proposed AID algorithms in this research performed well in the case study, some limitations of this research need to be addressed. There also remains a few interesting questions and improvements that should be investigated in future studies.

AID algorithms were usually developed and calibrated on the basis of either observed or simulated traffic data. The performances of AID algorithms largely depend on the size of the calibration database. In this research, only one year of traffic and incident data were used to calibrate the proposed AID algorithms. Another year of traffic and incident data were used for validation. The number of incidents, especially under rain conditions, is limited. The limited number of incidents under rain conditions in this research restricts the calibration and validation of the generalized detection threshold function, particularly under rain conditions. In addition, the calibrated parameters and detection thresholds based on limited data may be biased or improper for use in applications. Therefore, the AID algorithms proposed in this research need to be further calibrated and validated using more observed traffic and incident data, particularly under rain conditions in future studies.

The accuracy of the MTTD is largely affected by the actual occurring time of traffic incidents. This is because the MTTD is defined as the average difference between the actual occurring time of incidents and the detection time by AID algorithms. However, the available occurring time of incidents in the database for calibration is usually the incident occurring time reported either by police or drivers. The reported occurring time is sometimes not the actual occurring time of incidents. A time delay may exist between these two occurring times. In this research, the reported time of incidents were used as the actual occurring time. The difference between the actual and reported time of incidents may result in an inaccurate MTTD, and thus an unreliable detection performance. Hence, it is of value to accurately estimate the actual occurring time of traffic incidents, especially when the actual occurring time is not recorded in the database.

The proposed AID algorithms in this research were only applied on the Hong

Kong road network. However, it is of value to implement the proposed AID algorithms on road networks in other cities. Hence, the transferability of the proposed AID algorithms needs to be assessed before its implementation in new cities in practice. The assessment of the transferability of the proposed AID algorithms needs to be based on the observed traffic and incident data collected from the targeted cities. When applied on the database of other cities, the performances of the proposed AID algorithms can be obtained and further assessed. Additionally, the input data and detection logic can be adjusted to increase the transferability of the proposed algorithms, enhancing their feasibility for application in cities with a data collection system originally installed for journey time estimation purpose only.

Many factors may affect the detection performance of AID algorithms. These factors include: (1) operating traffic conditions such as the preincident traffic flow condition, (2) road configurations such as on/off ramps, (3) environmental factors such as the rainfall, (4) incident duration, (5) incident severity, (6) detector spacing, (7) incident location, and (8) topography features such as the gradient and turning radius. In this research, only the preincident traffic flow and rainfall intensity are considered in the determination of detection thresholds.

As indicated in Section 2.8, the influencing factors cannot be all considered in the development of one single AID algorithm. This is usually because the impact mechanism of some factors on detection thresholds has not been clearly investigated. The lack of related data may also limits the investigation to some influencing factors. Additionally, some factors are too complex to be directly included in the generalized detection threshold function.

However, through investigating the speed changes at a given gradient and turning radius, the effects of topography features can be considered in the detection threshold determination. For instance, the vehicles may decelerate when making a turn or climbing. The decrease of traffic speeds caused by vehicle turning or climbing may be mistaken for incident-induced speed decrease by AID algorithms. Therefore, a mechanism or an adjustment should be included in the AID algorithms to correctly detect incidents at the turning or climbing. In addition, the decrease of speeds at the turning or climbing can be quantified by investigating the

relationships between the prevailing traffic speed, gradient and turning radius. The numerical results can be used in the generalized detection threshold function to generate detection thresholds at a given gradient or turning radius. In further studies, more influencing factors needs to be considered in detection logic design and detection threshold determination to enhance the algorithm performance.

The MTTD of the proposed AID algorithms in this research is about 4 minutes, longer than those of most existing AID algorithms (Parkany and Xie, 2005). This is mainly because the aggregate time interval of the observed data is 2 minutes and a persistence test is adopted. Although the large MTTD of the proposed algorithms is acceptable in view of the large data aggregate time interval, the incidents may be rapidly reported by the drivers or viewed on the video monitor. This may lead to the AID less useful, especially in cities with busy traffic and high mobile phone penetration like Hong Kong. However, the proposed AID still can be used to verify the reported incidents by the drivers. For cities with similar data collection infrastructure, less busy traffic and low mobile phone penetration, the proposed AID algorithms can still provide an effective and timely incident detection.

Another potential benefit for the proposed AID algorithms is that they can detect the incidents occurred along the roads (either within or outside the camera vision). However, the video surveillance method detects only the incidents occurred within the camera vision. Video surveillance also needs continuous monitoring by traffic operators. In this sense, AID algorithms are less labour-intensive.

This research only focuses on the incident detection, which is the first step of incident management. The following steps (i.e. incident verification, response and clearance) are not investigated. In Hong Kong, most incidents are reported by drivers or patrol police. These incidents are usually recorded and disposed by the police. However, the real-time incident information cannot be timely shared with the Transport Department and released to the travellers. Thus, it is difficult for the Transport Department to take appropriate actions to alleviate the incident-induced congestions. In further studies, it is of value to investigate the timely sharing of incident information between the police and Transport Department.

It is also promising to form a framework of the incident management system in which both the police and the Transport Department involve. The incident information obtained by AID algorithms, calls from drivers and video surveillance can be integrated to provide more reliable and timely detection results. The detection results of each method can be used to verify each other. The incident information can be used by both Transport Department and the police to assist traffic operators in (1) releasing incident information to the public, (2) implementing emergency responses, (3) clearing the incident and (4) alleviate the incident-induced congestions. The released incident information by the Transport Department can help the travellers in route choice to avoid the road sections impeded by the incidents.

Appendices

Appendix A. Raw Traffic Data under No-rain Condition for the Illustrative Example in Chapter 3

Detector	Date	Time interval	Space mean speed (km/h)	Variance of space mean speed (km/h)	Traffic flow (veh/2-min/lane)
J3V2E	2010/10/5	17:26-17:27	44.96	125.67	28
J3V2E	2010/10/5	17:28-17:29	61.74	276.40	31
J3V2E	2010/10/5	17:30-17:31	55.58	306.86	24
J3V2E	2010/10/5	17:32-17:33	50.00	136.50	37
J3V2E	2010/10/5	17:34-17:35	55.75	62.98	24
J3V2E	2010/10/5	17:36-17:37	45.67	35.69	27
J3V2E	2010/10/5	17:38-17:39	38.87	24.58	31
J3V2E	2010/10/5	17:40-17:41	44.27	38.49	22
J3V2E	2010/10/5	17:42-17:43	51.14	55.19	29
J3V2E	2010/10/5	17:44-17:45	50.22	129.49	27
J3V2E	2010/10/5	17:46-17:47	48.29	141.92	28
J3V2E	2010/10/5	17:48-17:49	49.77	68.66	22
J3V2E	2010/10/5	17:50-17:51	48.41	68.17	27
J3V2E	2010/10/5	17:52-17:53	39.42	123.06	33
J3V2E	2010/10/5	17:54-17:55	48.68	129.48	25
J3V2E	2010/10/5	17:56-17:57	42.46	207.44	28
J3V2E	2010/10/5	17:58-17:59	49.43	40.46	21
J3V2E	2010/10/5	18:00-18:01	61.24	51.36	25
J3V2E	2010/10/5	18:02-18:03	48.93	53.99	28
J3V2E	2010/10/5	18:04-18:05	45.57	161.90	35
J3V2E	2010/10/5	18:08-18:09	44.55	80.38	33
J3V2E	2010/10/5	18:10-18:11	40.00	196.64	29
J3V2E	2010/10/5	18:12-18:13	30.60	273.33	25
J3V2E	2010/10/5	18:14-18:15	17.76	20.11	25
J3V2E	2010/10/5	18:16-18:17	30.83	131.06	23
J3V2E	2010/10/5	18:18-18:19	35.61	196.78	31
J3V2E	2010/10/5	18:20-18:21	30.66	125.49	47
J3V2E	2010/10/5	18:22-18:23	30.48	117.97	50
J3V2E	2010/10/5	18:24-18:25	33.32	155.41	38
J3V2E	2010/10/5	18:26-18:27	19.54	37.27	13
J3V2E	2010/10/5	18:28-18:29	17.29	113.15	31
J3V2E	2010/10/5	18:30-18:31	17.45	24.16	20
J3V2E	2010/10/5	18:32-18:33	19.42	16.43	24
J3V2E	2010/10/5	18:34-18:35	25.25	60.72	24
J3V2E	2010/10/5	18:36-18:37	18.30	60.77	30
J3V2E	2010/10/5	18:38-18:39	13.06	52.91	36
J3V2E	2010/10/5	18:40-18:41	11.29	55.97	17
J3V2E	2010/10/5	18:42-18:43	12.58	28.59	19

J3V2E	2010/10/5	18:44-18:45	18.82	14.76	11
J3V2E	2010/10/5	18:46-18:47	10.15	32.81	13
J3V2E	2010/10/5	18:48-18:49	7.75	21.80	16
J3V2E	2010/10/5	18:50-18:51	4.13	12.21	23
J3V2E	2010/10/5	18:52-18:53	6.00	33.33	4
J3V2E	2010/10/5	18:54-18:55	10.93	31.15	14
J3V2E	2010/10/5	18:56-18:57	7.29	26.24	7
J3V2E	2010/10/5	18:58-18:59	13.00	0.00	1
J3V2E	2010/10/5	19:00-19:01	4.87	21.72	46
J3V2E	2010/10/5	19:02-19:03	7.91	30.09	32
J3V2E	2010/10/5	19:04-19:05	13.83	18.33	12
J3V2E	2010/10/5	19:06-19:07	15.69	21.23	13
J3V2E	2010/10/5	19:08-19:09	10.88	19.57	42
J3V2E	2010/10/5	19:10-19:11	14.91	10.86	32
J3V2E	2010/10/5	19:12-19:13	22.78	44.52	36
J3V2E	2010/10/5	19:14-19:15	21.09	83.04	45
J3V2E	2010/10/5	19:16-19:17	21.08	122.38	48
J3V2E	2010/10/5	19:18-19:19	19.71	52.81	38
J3V2E	2010/10/5	19:20-19:21	31.59	180.47	46
J3V2E	2010/10/5	19:22-19:23	37.63	89.65	52
J3V2E	2010/10/5	19:24-19:25	37.15	98.47	60

Appendix B. Samples of Traffic Data Under both No-rain and Rain Conditions

Date		2010/09/21 (Tuesday), **under rain condition**				2010/09/28 (Tuesday), **under no rain condition**			
Detector	Time interval	Space mean speed (km/h)	Variance of space mean speed (km/h)	Traffic flow (veh/2-min/lane)	Rainfall intensity (mm/h)	Space mean speed (km/h)	Variance of space mean speed (km/h)	Traffic flow (veh/2-min/lane)	Rainfall intensity (mm/h)
J3V2E	18:00-18:01	37.833332	177.936783	30	5.0	53.153847	26	76.615387	0
J3V2E	18:02-18:03	49.111111	159.564102	27	5.0	46.258064	31	107.064514	0
J3V2E	18:04-18:05	47.411766	85.461678	34	5.0	45.4375	32	28.576612	0
J3V2E	18:06-18:07	54.772728	111.89827	22	5.0	55.028572	35	103.20504	0
J3V2E	18:08-18:09	49.032257	122.765594	31	5.0	48.617645	34	66.970589	0
J3V2E	18:10-18:11	47.878788	105.547348	33	5.0	49.483871	31	114.191399	0
J3V2E	18:12-18:13	40.1875	41.963711	32	5.0	53.583332	24	96.166664	0
J3V2E	18:14-18:15	43.620689	31.458128	29	5.0	55.115383	26	117.066154	0
J3V2E	18:16-18:17	46.68182	98.798698	22	5.0	42.444443	27	80.717949	0
J3V2E	18:18-18:19	47.620689	126.029556	29	5.0	47.296295	27	107.447296	0
J3V2E	18:20-18:21	48.416668	59.907143	36	5.0	46.67857	28	69.115082	0
J3V2E	18:22-18:23	35.590908	43.317123	44	5.0	52.433334	30	36.805748	0
J3V2E	18:24-18:25	28.174999	99.378845	40	5.0	57.794117	34	171.501785	0
J3V2E	18:26-18:27	24.527779	113.856346	36	5.0	54.3125	48	262.94281	0
J3V2E	18:28-18:29	54.545456	89.116882	22	5.0	44.862068	29	131.480301	0
J3V2E	18:30-18:31	54.342857	181.93782	35	5.0	45	42	97.024391	0
J3V2E	18:32-18:33	49.914288	212.315964	35	5.0	42.938774	49	157.642014	0
J3V2E	18:34-18:35	53.392857	195.062164	28	5.0	43.710526	38	149.778809	0
J3V2E	18:36-18:37	62.967743	102.765594	31	5.0	44.906979	43	58.848282	0

J3V2E	18:38-18:39	57.5625	87.028229	32	5.0	42.32	50	84.834282	0
J3V2E	18:40-18:41	58.137932	66.766006	29	5.0	42.684212	38	54.275959	0
J3V2E	18:42-18:43	57.75	96.935715	36	5.0	40.023254	43	48.499447	0
J3V2E	18:44-18:45	62.576923	90.413849	26	5.0	46.416668	36	44.82143	0
J3V2E	18:46-18:47	58.303032	80.467804	33	5.0	44.589745	39	95.985153	0
J3V2E	18:48-18:49	59.75	160.066666	16	5.0	41.75	40	61.987179	0
J3V2E	18:50-18:51	63.291668	163.780792	24	5.0	44.222221	45	45.767677	0
J3V2E	18:52-18:53	51.058823	67.754013	34	5.0	46.767441	43	118.658913	0
J3V2E	18:56-18:57	42.439999	59.067757	50	5.0	41.465115	43	40.540421	0
J3V2E	18:58-18:59	43.489361	101.124886	47	5.0	44.295456	44	90.631607	0

Appendix C. Samples of Estimated Instantaneous Journey Time under No-rain Condition in the Journey Time Indication System Database

Time interval	Road link ID	Instantaneous journey time (s)
2010-01-01 07:00-07:01	781-50098	60.46224562
2010-01-01 07:02-07:03	781-50098	48.85117718
2010-01-01 07:04-07:05	781-50098	54.24091998
2010-01-01 07:06-07:07	781-50098	58.27712543
2010-01-01 07:08-07:09	781-50098	51.79827246
2010-01-01 07:10-07:11	781-50098	54.4197244
2010-01-01 07:12-07:13	781-50098	50.09504693
2010-01-01 07:14-07:15	781-50098	50.74846587
2010-01-01 07:16-07:17	781-50098	56.29509389
2010-01-01 07:18-07:19	781-50098	56.59970133
2010-01-01 07:20-07:21	781-50098	50.88173098
2010-01-01 07:22-07:23	781-50098	63.10784271
2010-01-01 07:24-07:25	781-50098	65.63343123
2010-01-01 07:26-07:27	781-50098	56.98621687
2010-01-01 07:28-07:29	781-50098	58.65271687
2010-01-01 07:30-07:31	781-50098	54.72979794
2010-01-01 07:32-07:33	781-50098	61.20669531
2010-01-01 07:34-07:35	781-50098	61.75227106
2010-01-01 07:36-07:37	781-50098	56.86766108
2010-01-01 07:38-07:39	781-50098	60.86085831
2010-01-01 07:40-07:41	781-50098	61.88055397
2010-01-01 07:42-07:43	781-50098	53.86564588
2010-01-01 07:44-07:45	781-50098	59.22368533
2010-01-01 07:46-07:47	781-50098	58.33661667
2010-01-01 07:48-07:49	781-50098	54.14500161
2010-01-01 07:50-07:51	781-50098	59.24578861
2010-01-01 07:52-07:53	781-50098	51.29212494
2010-01-01 07:54-07:55	781-50098	57.10926083
2010-01-01 07:56-07:57	781-50098	56.05557652
2010-01-01 07:58-07:59	781-50098	53.86564588

Appendix D. Information of Traffic Accidents in the Hong Kong Traffic Accident Database System

Attribute	Description
Severity	1=Fatal, 2= Serious, 3= Slight
Police Division	-
District Board Area	-
Hit and run	1= Yes, 2= No
Date of accident	DD/MM/YY
Time	HH/MM
Day of week	1= Mon, 2= Tue, 3= Wed, 4= Thu, 5= Fri, 6= Sat, 7= Sun
Street Name	-
Within 70m of junction	1= Yes, 2= No
Second Street name	-
Within 20m of junction	1= Yes, 2= No
Identifying feature	-
Easting Grid	-
Northing Grid	-
Precise location	-
How accident happened	-
Number of vehicles	-
Number of casualties	-
Weather	1= Clear, 2= Dull, 3= Fog/mist, 4= Strong Wind, 9= Not known
Rain	1= Not raining, 2= Light rain, 3= Heavy rain, 9= Not known
Natural Light	1= Daylight, 2= Dawn/ Dusk, 3= Dark, 9= Not known
Street Lighting	1= Good, 2= Poor, 3= Obscured, 4= Not lit, 5= None, 6= Daylight, 9= Not known
Speed Limit	-
Condition of Traffic Aids	1= Poor markings, 2= Other poor aids, 3= No significant deficiencies, 9= Not known
Traffic Congestion	1= Severe, 2= Moderate, 3= None, 9= Not known
Road Surface	1= Wet, 2= Dry, 9= Not known
At or Near	A= Roadwork (Govt), B= roadwork (Utilities), C= Construction materials, D= Landslip/ fallen tree, E= Flooding, F=Timber walkway, G= Others, H= None, Z= Not known
On a crossing controlled by	1= Zebra, 2= Traffic signal, 3= Police, 4= Crossing patrol, 5= Cautionary Crossing, 8= None
Within 15m of crossing controlled by	1= Zebra, 2= Traffic signal, 3= Police, 4= Crossing patrol, 5= Cautionary Crossing, 6= Footbridge/ subway, 8= None
Junction control	1= No, 2= Stop, 3= Give way, 4= Traffic signal, 5= Police, 6= Not junction
Junction type	1= Roundabout, 2= T-junction, 3= Staggered, 4= Y-junction, 5= Slip road, 6= Cross-roads, 7= Multiple, 8= Private access, 9= Other, 10= Not within 20M
Road type	1= One way, 2= Two way, 3= Dual Carriageway, 4= More than 2 carriageway

Carriage Width	-
Number of Lanes	1= One lane, 2= Two lanes, 3= More than two lanes
Road Classification	1= Primary Distributor, 2= Private Road, 3= Other
Vehicle Movements	1= One moving veh, 2= 2 in same direction, 3= 2 from opposite direction, 4= 2 from different roads, 5= >2 from same direction, 6= >2 from opposite direction, 7= >2 from different roads
Overtaking	1= One vehicle overtaking, 2= 2+ vehicle overtaking, 3= No overtaking
Contributory Factor	-

Appendix E. Samples of the Traffic Accident Data in the Hong Kong Traffic Accident Database System

Serial	Severity	Date	Time	Grid_E	Grid_N	Precise Location	Rain
1	3	2010/1/1	00:10	12491	11186	Near Lamppost BC0548 Tung Chung Road LT New Territories	1
2	3	2010/1/1	00:19	35115	22266	Tai Po Road at the junction of Cornwall Street SSPO Kowloon	1
3	3	2010/1/1	01:22	15617	29093	Lamppost H1686 San Wo Lane East	1
4	2	2010/1/1	01:29	35284	20957	Outside No. 50 Tai Po Road South SSPO Kowloon	1
5	3	2010/1/1	01:48	35667	19104	Nathan Road near junction of Wing Sing Lane YT Kowloon	1
6	3	2010/1/1	01:53	36014	15317	Johnston Road at the junction of Triangle Street Hong Kong	1
7	2	2010/1/1	02:14	35529	19495	Hamilton Street near junction of Portland Street YT Kowloon	1
8	3	2010/1/1	02:45	35936	17783	Carnarvon Road near Cameron Road YT Kowloon	1
9	3	2010/1/1	04:15	42846	14028	Yue Wan Market No. 33 - 33 Yee Fung Street Hong Kong Loading area	2
10	3	2010/1/1	06:15	35464	20215	MK Kowloon Somewhere in Mongkok area	1
11	3	2010/1/1	06:45	35951	17576	Mody Road near junction of Minden Row YT Kowloon	1
12	3	2010/1/1	07:35	31227	24257	Near Lamppost DC 0118 Kwai Chung Plaza Kwai Foo Road KWC New Territories	1
13	3	2010/1/1	08:45	37206	15457	Leighton Road Yun Ping Road Hong Kong	1
14	3	2010/1/1	10:15	39431	19998	Near Mega Box Kwun Tong Bypass	1

Notes: In the “Rain” column, 11= Not raining, 2= Light rain, 3= Heavy rain, 9= Not known;

In the “Severity” column, 1= Fatal, 2= Serious, 3= Slight.

Appendix F. Samples of Rainfall Intensity Data Collected by the Hong Kong Observatory Weather Stations

Date	Time interval	r (mm/h)
2010/9/11	00:00-00:59	27
2010/9/11	01:00-01:59	2.1
2010/9/11	02:00-02:59	1.2
2010/9/11	03:00-03:59	0.7
2010/9/11	04:00-04:59	1.3
2010/9/11	05:00-05:59	7.5
2010/9/11	06:00-06:59	11
2010/9/11	07:00-07:59	4.4
2010/9/11	08:00-08:59	4.7
2010/9/11	09:00-09:59	3.7
2010/9/11	10:00-10:59	1.6
2010/9/11	11:00-11:59	2.7
2010/9/11	12:00-12:59	0.7
2010/9/11	13:00-13:59	0.1
2010/9/11	14:00-14:59	0.9
2010/9/11	15:00-15:59	1.3
2010/9/11	16:00-16:59	1
2010/9/11	17:00-17:59	0
2010/9/11	18:00-18:59	0
2010/9/11	19:00-19:59	0
2010/9/11	20:00-20:59	0.4
2010/9/11	21:00-21:59	0
2010/9/11	22:00-22:59	0.5

Appendix G. The Distance between Adjacent Video Traffic Detectors under the Journey Time Indication System in Hong Kong

Pair of video traffic detectors	Distance between adjacent video traffic detectors (m)
JHK5-JHK4	564.60
JHK7-JHK1	566.80
JHK2-JHK9	674.96
J6-J2	691.51
JHK9-JHK7	718.53
JHK6-JHK5	924.14
JHK9-JHK8	930.89
J3-J3V1W	943.55
JEV2E-JEV3E	1,102.43
J4V2W-J4V3W	1,155.75
J3V1W-J6V1W	1,163.01
J4-J4V1W	1,231.46
J3-J4	1,298.23
JHK1-JHK6	1,306.63
JHK10-JHK11	1,315.35
J5E-J2V1E	1,325.54
J3-J3VE2	1,334.61
J5V1C-J6	1,505.86
JHK8-JHK3	1,566.57
J2V1E-JEV2E	1,676.27
J2-J6V1W	1,716.03
J4V1W-J4V2W	1,759.80
J1-J2	1,845.26
JHK3-JHK10	1,933.07
J5-J5V1C	2,032.29
J3V2E-J3V3E	2,061.29
J5V1C-J5E	2,129.75
J2-J5V1C	2,139.93

Notes: J1, J2… denote video traffic detectors installed in Kowloon;

JHK1, JHK2…denote video traffic detectors installed in Hong Kong Island.

Appendix H. The Distances between Adjacent Automatic Vehicle Identification Readers under the Journey Time Indication System in Hong Kong

Pair of AVI readers	Distance between AVI readers (m)
J4-WH	282.44
J1-J2	453.66
J6-CH	966.60
J2-CH	1,136.51
JHK1-CH	1,263.22
J3-J4	1,298.23
J4-CH	1,416.40
J1-WH	2,185.18
J3-WH	3,316.57
JHK11-JHK3	3,327.91
J5-J6	3,538.15
J6-WH	3,617.55
JHK2-CH	3,683.59
JHK11-EH	3,873.43
J2-J5E	4,269.68
J5E-EH	4,526.25
JHK3-CH	4,728.36
JHK1-EH	8,100.84
JHK2-WH	8,275.51
JHK2-EH	8,422.39
JHK3-WH	9,134.82
J3-EH	9,846.41

Notes: AVI denotes Automatic Vehicle Identification;

J1, J2… denote AVI readers in Kowloon;

JHK1, JHK2…denote AVI readers in Hong Kong;

WH denotes AVI reader installed at Western Harbor Tunnel;

EH denotes AVI reader installed at Eastern Harbor Tunnel;

CH denotes AVI reader installed at Central Harbor Tunnel.

References

Abdulhai, B., 1996, A neuro-genetic-based universally transferable freeway incident detection framework. Ph.D. thesis, University of California, Irvine.

Abdulhai, B. and Ritchie, S. G., 1999, Enhancing the universality and transferability of freeway incident detection using a Bayesian-based neural network. *Transportation Research Part C - Emergency Technologies*, 7(5), pp. 261-280.

Adeli, H. and Samant, A., 2000, An adaptive conjugate gradient neural network-wavelet model for traffic incident detection. *Computer-Aided Civil and Infrastructure Engineering*, 15(4), pp. 251-260.

Ahmed, S. A. and Cook, A. R., 1982, Application of time-series analysis techniques to freeway incident detection. *Transportation Research Record*, 841, pp. 19-21.

Agarwal, M., Maze, T. H., and Souleyette, R., 2006, The weather and its impact on urban freeway traffic operations. *Proceeding of the 85th Annual Meeting of the Transportation Research Board*, Washington, DC.

Balke, K. N., 1993, An evaluation of existing incident detection algorithms. *Research Report FHWA/TX-93/1232-20*, Texas Transportation Institute, the Texas A&M University System, College Station, TX.

Balke, K. N., Dudek, C. L., and Mountain, C., 1996, Using probe-measured travel times to detect major freeway incidents in Houston, Texas. *Transportation Research Record*, 1554, pp. 213-220.

Billot, R., El Faouzi, N. E., and De Vuyst, F., 2009, A multi-level assessment of the rain impact on drivers' behaviors: standardized methodology and empirical analysis. *Transportation Research Record*, 2107, pp. 134-142.

Black, J. 1997, Automatic Incident Detection Algorithms. http://www.path.berkeley.edu/~leap/TTM/Incident_Manage/Detection/aida.html.

Box, G. P. and Jenkins, G. M., 1976, Time Series Analysis: Forecasting and Control. Holden-Day, Inc., San Francisco, CA.

Chang, E. C-P. and Wang, S-H., 1994, Improved freeway incident detection using fuzzy set theory. *Transportation Research Record*, 1453, pp. 75-82.

Cheu, R. L. and Ritchie, S. G., 1995, Automated detection of lane-blocking freeway incidents using artificial neural networks. *Transportation Research Part C - Emergency Technologies*, 3(6), pp. 371-388.

Cheu, R. L. and Tay, G. C. W., 2004, Sampling strategies for probe-vehicle-based freeway incident detection algorithms. *Transportation Research Record,* 1867, 80-88.

Cheu, R. L., Qi, H., and Lee, D.-H., 2002, Mobile Sensor and Sample-Based Algorithm for Freeway Incident Detection. *Transportation Research Record,* 1811, 12–20.

Chung, E., and Rosalion, N., 1999, Effective incident detection and management on freeways. *Research Report ARR 327*, ARRB Transport Research, Victoria, Australia.

Cook, A. R. and Cleveland, D. E., 1974, Detection of freeway capacity-reducing incidents by traffic-stream measurements. *Transportation Research Record*, 495, pp. 1-11.

Corby, M. J. and Saccomanno, D. E., 1997, Analysis of freeway accident detection. *Transportation Research Record*, 1603, pp. 80-89.

Dia, H. and Rose, G., 1997, Development and evaluation of neural network freeway incident detection models using field data. *Transportation Research Part C - Emergency Technologies*, 5(5), pp. 313-331.

Dia, H. and Thomas, K., 2011, Development and evaluation of arterial incident detection models using fusion of simulated probe vehicle and loop detector data. *Information Fusion*, 12(1), pp. 20-27.

Dinh-Zarr, T. B., 2008, United Nations debates road safety this spring. *ITE Journal-Institution of Transport Engineers*, 78(4), pp. 42-44.

Dudek, C. L., Messer, C. J., and Dutt, A. K., 1974, Study of detector reliability for a motorist information system on the gulf freeway. *Transportation Research Record*, 495, pp. 35-43.

Fox, J., 2008, Applied regression analysis and generalized linear models. Sage, Los Angeles.

Haas, C. T., Mahmassani, H. S., Khoury, J., Haynes, M., Rioux, T., and Logman, H., 2001, Evaluation of automatic vehicle identification for San Antonio's TransGuide for incident detection and advanced traveler information

systems. *Report FHWA/TX-7-4957-1*, Center for Transportation Research, Bureau of Engineering Research, the University of Texas, Austin.

Hellinga, B. and Knapp, G., 2000, Automatic vehicle identification technology based freeway incident detection. *Transportation Research Record*, 1727, pp. 142-153.

Highway Capacity Manual (HCM), 2000, Special Rep. No. 209, 4th Ed., Transportation Research Board, National Research Council, Washington, D.C.

Ishak, S. and Al-Deek, H., 1999, Performance of automatic ANN-based incident detection on freeways. *ASCE Journal Transportation Engineering*, 125(4), pp. 281-290.

Ivan, J. N. and Sethi, V., 1998, Data fusion of fixed detector and probe vehicle data for incident detection. *Computer-Aided Civil and Infrastructure Engineering*, 13(5), pp. 329-337.

Jin, J. and Ran, B., 2009, Automatic freeway incident detection based on fundamental diagrams of traffic flow. *Transportation Research Record*, 2099, pp. 65-75.

Karlaftis, M. G. and Vlahogianni, E. I., 2011, Statistical methods versus neural networks in transportation research: Differences, similarities and some insights. *Transportation Research Part C - Emergency Technologies*, 19(3), pp. 387-399.

Karim, A. and Adeli, H., 2002, Incident detection algorithm using wavelet energy representation of traffic patterns. *ASCE Journal of Transportation Engineering*, 128(3), pp. 232-242.

Khoury, J. A., Haas, C. T., Mahmassani, H., Logman, H., and Rioux, T., 2003, Performance comparison of automatic vehicle identification and inductive loop traffic detectors for incident detection. *ASCE Journal of Transportation Engineering*, 129(6), pp. 600-607.

Klein, L. A., 2001, Sensor technologies and data requirement for ITS. Artech House, Norwood, MA.

Lam, W. H. K., Tam, M. L., Cao, X. and Li, X., 2013, Modeling the effects of rainfall intensity on traffic speed, flow, and density relationships for urban roads. *ASCE Journal of Transportation Engineering*, 139(7), pp. 758-770.

Lee, C., Hellinga, B., and Saccomanno, F., 2003, Proactive freeway crash prevention using real-time traffic control. *Canadian Journal of Civil Engineering*, 30(6), pp. 1034-1041.

Levin, M. and Krause, G. M., 1978, Incident detection: a Bayesian approach. *Transportation Research Record*, 682, pp. 52-58.

Li, D. P., Li, X. M., and Lam, W. H. K., 2012, Temporal and spatial impacts of rainfall intensity on traffic accidents in Hong Kong. *Proceeding of the 17th International Conference of Hong Kong Society for Transportation Studies*, Hong Kong, pp. 333-340.

Li, X., Lam, W. H. K., and Tam, M. L., 2013, Automatic Incident Detection under Various Rain Conditions. Proceeding of Asia Symposium on Engineering and Information, Asia-Pacific Education & Research Association Bangkok, Thailand, pp.125-135.

Lin, C. K. and Chang, G. L., 1998, Development of a fuzzy-expert system for incident detection and classification. *Mathematical and Computer Modeling*, 27(9-11), pp. 9-25.

Lindley, J. A., 1987, Urban freeway congestion: quantification of the problem and effectiveness of potential solutions. *ITE Journal-Institution of Transport Engineers*, 57(1), pp. 27-32.

Luk, J. Y. K., Chung, E. C. S., and Sin, F. Y. C., 2001, Characterization of incidents on an urban arterial road. *Journal of Advanced Transportation*, 35(1), pp. 67-92.

Mahmassani, H. S., Haas, C. T., Zhou, S., and Peterman, J., 1999, Evaluation of incident detection methodologies. *Report FHWA/TX-00/1795-1*, Center for Transportation Research, Bureau of Engineering Research, the University of Texas, Austin.

Mak, C. L. and Fan, H. S. L., 2005, Transferability of expressway incident detection algorithms to Singapore and Melbourne. *ASCE Journal of Transportation Engineering*, 131(2), pp. 101-111.

Mak, C. L. and Fan, H. S. L., 2006a, Single-station algorithm using video-based data for detecting expressway incidents. *Computer-Aided Civil and Infrastructure Engineering*, 21(2), pp. 120-135.

Mak, C. L. and Fan, H. S. L., 2006b, Algorithm fusion for detecting incidents on

Singapore's Central Expressway. *ASCE Journal of Transportation Engineering*, 132(4), pp. 321-330.

Mak, C. L. and Fan, H. S. L., 2007, Development of dual-station automated expressway incident detection algorithms. *IEEE Transactions on Intelligent Transportation Systems*, 8(3), pp. 480-490.

Martin, P., Perrin, J., and Blake, H., 2001, Incident detection algorithm evaluation. Utah Department of Transportation.

Masters, P. H., Lam, J. K., and Kam, W., 1991, Incident detection algorithms for COMPASS - An advanced traffic management system. *Proceeding of the Conference of Vehicle Navigation and Information Systems*, 2, pp. 295-310.

Moran, C. A., 2011, Relevance of congestion performance measures: A study on the dynamics of congestion in road area networks. *Proceeding of the 16th International Conference of Hong Kong Society for Transportation Studies*, Hong Kong Society for Transportation Studies, Hong Kong, pp. 53-60.

Mussa, R. N. and Upchurch, J. E., 2000, Simulator evaluation of incident detection using wireless communications. *Proceeding of the 79th Transportation Research Board Annual Meeting* (CD-ROM), Transportation Research Board, Washington, DC.

Parkany, E. and Xie, C., 2005, A complete review of incident detection algorithms and their deployment: What works and what doesn't. *Report NETCR 37, Project No. 00-7*, New England Transportation Consortium, Storrs, CT.

Payne, H. J., Hwelfenbein, E. D., and Knobel, H. C., 1976, Development and testing of incident detection algorithms, Volume 2: Research methodology and results. *Report No. FHWA-RD-76-20*, Federal Highway Administration, Washington, DC.

Payne, H. J. and Tignor, S. C., 1978, Freeway incident detection algorithms based on decision trees with states. *Transportation Research Record*, 682, pp. 30-37.

Persaud, B. N., Hall, F. L., Hall, L. M., 1990, Congestion identification aspects of the McMaster incident detection algorithm. *Transportation Research Record*, 1287, pp. 167-175.

Pisano, P. A. and Goodwin, L. C., 2004, Research needs for weather-responsive

traffic management. *Transportation Research Record*, 1867, pp. 127-131.

Rakha, H., Farzaneh, M., Arafeh, M., and Sterzin, E., 2008, Inclement weather impacts on freeway traffic steam behavior. *Transportation Research Record*, 2071, pp. 8-18.

Ritchie, S. G. and Cheu, R. L., 1993, Simulation of freeway incident detection using artificial neural networks. *Transportation Research Part C - Emergency Technologies*, 1(3), pp. 203-217.

Rosses, R. P., Prassas, E. S., and McShane, W. R., 2004, Traffic engineering third edition. Pearson Education Inc.

Stephanedes, Y. J. and Chassiakos, A. P., 1993, Freeway incident detection through filtering. Transp. *Transportation Research Part C - Emergency Technologies*, 1(3), pp. 219-233.

Stephanedes, Y. J. and Liu, X., 1995, Artificial neural networks for freeway incident detection. *Transportation Research Record*, 1494, pp. 91-97.

Tam, M. L. and Lam, W. H. K., 2008, Using automatic vehicle identification data for travel time estimation in Hong Kong. *Transportmetrica*, 4(3), pp. 179-194.

Tam, M. L. and Lam, W. H. K., 2011, Validation of instantaneous journey time estimation: A Journey Time Indication System in Hong Kong. *Proceeding of the 9th International Conference of the Eastern Asia Society for Transportation Studies*, 8, Eastern Asia Society for Transportation Studies, Tokyo, pp. 336-346.

Transport Department, 2011, The annual traffic census 2010. Government of the Hong Kong Special Administrative Region.

Unrau, D. and Andrey, J., 2006, Driver response to rainfall on urban expressways. *Transportation Research Record*, 1980, pp. 24-30.

Wardrop, J. G., 1952, Some theoretical aspects of road traffic research. *Proceeding of the Institution of Civil Engineers*, 1-2, pp. 325-378.

Weil, R., Wootton, J., and Garcia-Ortiz, A., 1998, Traffic incident detection: sensors and algorithms. *Mathematical and Computer Modeling*, 27(9-11), pp. 257-291.

Westman, M., Litjens, R., and Garcia-Ortiz, A., 1996, Integration of probe vehicle and induction loop data: estimation of travel times and automatic

incident detection. *PATH Research Report UCB-ITS-PRR-96-13*, Institute of Transportation Studies, University of California, Berkeley, CA.

Williams, B. M. and Guin, A., 2007, Traffic management center use of incident detection algorithms: Findings of a nationwide survey. *IEEE Transactions on Intelligent Transportation Systems*, 8(2), pp. 351-358.

Zhang, K. and Taylor, M. A. P., 2006, Effective arterial road incident detection: A Bayesian network based algorithm. *Transportation Research Part C - Emergency Technologies*, 14(6), pp. 403-417.